Dissertation

submitted to the
Combined Faculties for the Natural Sciences and for Mathematics
of the Ruperto-Carola University of Heidelberg, Germany
for the degree of
Doctor of Natural Sciences

presented by
Sebastian Sorge, Master of Science
born in Apolda, Germany
Oral examination: 19.10.2018

A mitochondrial PERK mediates mitonuclear communication through induction of an ATF4-dependent transcriptional response

Referees:

Prof. Dr. Ingrid Lohmann

Prof. Dr. Joachim Wittbrodt

The work presented in this thesis was performed in the laboratory of Prof. Dr. Ingrid Lohmann at the University of Heidelberg, Germany.

Table of Contents

Summary IX
Zusammenfassung X
Acknowledgements XII
Frequently used Abbreviations XIV
Publications and Contributions 1
I – Introduction 1
Part One: Control of organ growth during development 1
Organ-intrinsic regulation of growth in *Drosophila* imaginal discs *2*
Inter-organ growth coordination in the *Drosophila* larva *5*
Growth regulation in the eye-antenna disc *7*
Part Two: Cellular stress signalling and metabolic adaptation 12
The Unfolded Protein Response of the Endoplasmic Reticulum *14*
The Integrated Stress Response through ATF4 *15*
The Unfolded Protein Response of Mitochondria *17*
Aims of this thesis 19
II – Results 21
Chapter One: A genetic screen for modifiers of eye growth 21
The RNAi screen *21*
The over-expression screen *24*
Chapter Two: COX7a is required for eye development 25
COX7a knockdown induces apoptosis and affects proliferation *26*
COX7a knockdown causes differentiation defects *29*
Chapter Three: A genetic characterisation of COX7a knockdown phenotypes 31
Chapter Four: COX7a knockdown phenotypes and over-proliferation with Notch signalling follow different genetic requirements 33
Delta, COX7a induces similar cellular phenotypes as COX7a or Delta alone *33*
Delta, COX7a phenotypes are driven by different genetic determinants than COX7a phenotypes *35*
Chapter Five: Transcriptomic analysis reveals a nuclear response to COX7a knockdown 36
Distinct transcriptional responses *36*
COX7a knockdown transcriptional signature *38*
No transcriptional cooperation *42*
Chapter Six: ATF4 mediates the transcriptional response to COX7a knockdown 43

Target gene and motif analysis suggest ATF4 as a potential regulator 43
ATF4 is required for Delta, COX7a-induced over-proliferation 44
ATF4 becomes translated upon COX7a knockdown 44
ATF4 is the main transcription factor downstream of COX7a knockdown 46
Chapter Seven: A mitochondrial PERK isoform mediates ATF4 activation 48
PERK is required for Delta, COX7a-induced over-proliferation 48
PERK isoform B localises to mitochondria 50
Chapter Eight: Internal and external dependencies of Delta, COX7a over-proliferation 53
Impact of ATF4 target genes on Delta, COX7a-induced over-proliferation 53
COX7a phenotypes are nutrient dependent 55
The transcriptional signature of amino acid limitation 57
Chapter Nine: Mitochondrial defects of COX7a loss of function 59
COX7a-depleted S2R+ cells show metabolic alterations consistent with reduced ETC function 59
Mitochondrial morphology and function are not altered in vivo 61
Chapter Ten: A generalisation of COX7a-induced phenotypes in the *Drosophila* eye disc 63
COX7a phenotypes represent a common ETC knockdown effect 63
ETC phenotypes are not a consequence of general metabolic interference 65
Interactions between the ATF4 response and oncogenic EGFR/Ras signalling 66
Appendix 67
III – Discussion 71
Part One: A mitochondrial PERK connects ETC defects with the ATF4-induced integrative stress response (ISR) and mitochondrial unfolded protein response (UPR^{mt}) 71
The ATF4-induced transcriptomic response 72
Mitochondrial PERK activates ATF4 in response to mitochondrial stress 74
ETC defects trigger the PERK-ATF4 response 76
A unified picture of the Drosophila mitochondrial stress response 77
Part Two: General implications for ETC-knockdown and/or ATF4-dependent phenotypes 78
ETC knockdown phenotypes in the eye disc 78
The ATF4-response and its involvement in ETC-knockdown phenotypes 79
The ATF4-response in cancer 81
Part Three: An assessment of experimental conditions 83
Effects of larval density on development and phenotypes 84
RNAi phenotypes in the larval eye-antenna disc 85
The metabolic status of imaginal discs 86

IV – Conclusions 88
V – Materials and Methods 89
1. Fly husbandry *89*
2. Immunofluorescence *93*
3. Microscopy and image analysis *94*
4. RNA-isolation, RT, qPCR and Microarray *94*
5. Cell culture *96*
6. Metabolomics analysis *96*
7. Transmission electron microscopy (TEM) *98*
8. Molecular biology *98*
9. Media and Solutions *98*
10. Consumables *101*
VI – References 102

Summary

Intracellular homeostasis depends on a multitude of enzymatic networks that control all basic cellular processes. To respond to stress – in the sense of disturbed homeostasis – cells have evolved adaptive responses, many of which involve nuclear transcription of proteins intended to counteract the stress and re-establish homeostasis. A particular stress, known to induce transcriptional responses, is protein aggregation or misfolding. Different, specific responses have been well characterised in response to protein folding stress within the cytosol or the endoplasmic reticulum. Protein folding stress within mitochondria has also been described to induce a nuclear transcriptional response. However, how folding stress within mitochondria is sensed and signalled to the nucleus, through mitonuclear communication or mitochondrial retrograde signalling, remains poorly understood.

Using a population of progenitor cells residing in the larval eye-imaginal disc of *Drosophila melanogaster*, this thesis demonstrates that the eIF2α-kinase PERK and its downstream target ATF4 mediate mitonuclear communication in response to disturbed protein handling within mitochondria.

PERK has been widely recognised as a sensor of protein folding within the lumen of the endoplasmic reticulum. Activation of PERK triggers a response called Integrated Stress Response (ISR) that attenuates translation rates, which in turn induces ATF4 to transcribe genes with cytoprotective function. This work now shows that the *Drosophila* genome encodes a PERK isoform that is targeted for mitochondrial import and fulfils a similar function in this organelle. The transcriptional response through ATF4 confirmed known ISR target genes and additionally showed that *Drosophila* ATF4 functions as an inducer of the mitochondrial Unfolded Protein Response (UPR^{mt}) as well. A comparison with mitonuclear signalling in other model organisms argues for substantial rewiring of the response during evolution, though most proteins originated at the base of metazoa.

This thesis utilised *Drosophila* imaginal disc progenitor cells that build the adult eye. During development of the tissue, the PERK-ATF4 response protects fitness of cells with defects in the mitochondrial electron transport chain (ETC). Intriguingly, this adaptation can be hi-jacked by growth-promoting signalling pathways to enhance their oncogenic potential.

In conclusion, this thesis defines a molecular signalling pathway activated by ETC defects and links the pathway to *in vivo* phenotypes.

Zusammenfassung

Homöostase innerhalb einer Zelle ist abhängig von vielfältigen enzymatischen Netzwerken, die alle grundlegenden Prozesse in einer Zelle kontrollieren. Damit eine Zelle auf Stress – im Sinne eines gestörten Gleichgewichts – reagieren kann, hat sie im Laufe der Evolution adaptive Antworten entwickelt, von denen viele auf der Transkription von Genen beruht, deren Proteinprodukte den Stress abbauen und damit Homöostase wieder herstellen sollen. Ein bestimmter Stress, von dem bekannt ist, dass er eine solche transkriptionelle Antwort hervorruft, ist die Aggregation oder Missfaltung von Proteinen. Verschiedene, spezifische Antworten der Zelle auf Protein-Missfaltungs-Stress innerhalb des Zytosols oder des Endoplasmatischen Retikulums sind gut in der wissenschaftlichen Literatur charakterisiert. Stress durch Missfaltung von Proteinen innerhalb der Mitochondrien wurde auch mit einem transkriptionellen Effekt in Verbindung gebracht. Allerdings ist bis heute nicht geklärt, wie Missfaltung innerhalb der Mitochondrien registriert und ein Signal zum Zellkern übermittelt wird – also wie die Mitochondrien-Zellkern Kommunikation funktioniert.

Unter Verwendung einer Vorläuferzell-Population in der Augen-Imaginalscheibe von *Drosophila melanogaster* konnte nun in dieser Arbeit gezeigt werden, dass die Kinase des Translations-Initiations-Faktors 2α, genannt PERK, und ihr untergeordnetes Ziel-Protein, genannt ATF4, diese Mitochondrien-Zellkern Kommunikation vermitteln, wenn die Faltung von Proteinen in den Mitochondrien gestört ist.

PERK ist detailliert beschrieben als Sensor für Protein-Missfaltung im Lumen des Endoplasmatischen Retikulums. Eine Aktivierung von PERK löst eine Antwort aus, die als Integrierte Stress Antwort (ISR) bezeichnet wird. Diese Antwort inhibiert die Translation innerhalb der Zelle, was zu einer Aktivierung von ATF4 führt, welches in der Folge im Zellkern die Transkription von Genen induziert, deren Proteinprodukte eine schützende Wirkung für die Zelle haben. Diese Arbeit zeigt nun, dass das Genom von *Drosophila melanogaster* eine Isoform von PERK enthält, welche PERK für den Import in Mitochondrien bestimmt, wo PERK eine ähnliche Funktion wie im Endoplasmatischen Retikulum erfüllt. Die transkriptionelle Antwort durch ATF4 bestätigt viele bekannte ISR Ziel-Gene und zeigte weiterhin, dass das ATF4 Protein von Drosophila eine zusätzliche Funktion als Auslöser der mitochondrialen Protein-Missfaltungs-Antwort (UPR^{mt}) spielt. Ein Vergleich mit der Mitochondrien-Zellkern Kommunikation in anderen Modellorganismen spricht für eine substantielle Weiterentwicklung dieses

Kommunikations-Systems während der Evolution, ausgehend von der Entstehung des Großteils der involvierten Proteine bereits an der Basis mehrzelliger Tiere.

Diese Arbeit verwendet als Modell die Vorläuferzellen der Imaginalscheibe, welches das Auge der adulten Fliege hervorbringt. Während der Entwicklung dieses Gewebes, schützt der PERK-ATF4-Effekt die Fitness von Zellen, mit eingeschränkter Funktion der mitochondrialen Atmungskette. Interessanterweise kann eben jener Effekt von Signalwegen, die selbst Wachstum induzieren können, ausgenutzt werden, um ihren wachstums-fördernden Effekt noch zu verstärken.

Zusammenfassend definiert diese Arbeit einen molekularen Signalweg, der von Defekten in der Atmungskette ausgelöst wird, und verbindet dessen intrazelluläre Wirkung mit den Auswirkungen auf die Entwicklung der Fliege.

Acknowledgements

Foremost I deeply wish to thank Prof. Ingrid Lohmann for keeping me in her group after my Master thesis. I am very grateful for her support and a feeling of trust in my abilities to work independently.

I want to thank Prof. Joachim Wittbrodt for his challenging questions and comments since my Master studies. And not less importantly, for sending "urgent" Reference Letters from the middle-of-nowhere.

I want to thank Prof. Aurelio Teleman for his valuable suggestions and his general understanding.

I am very grateful to Jun.-Prof. Steffen Lemke, whose never-ending interest, suggestions and encouragement were always very motivating.

I also appreciate the input from Prof. Bruce Edgar, who was a member of my first TAC meeting.

I am further grateful to Prof. Michael Boutros for allowing me to carry out the primary RNAi screen in his lab.

I am grateful for the help I received from many talented students that worked with me during the course of my PhD thesis. Foremost, my gratitude goes to Christian Altbürger and Jonas Theelke, who stayed with me for years and who contributed their efforts and ideas to this work and our paper. In addition, I want to thank Daniel Habibian, Pauline Jeckel and Karen Groß for the great time we had working together on projects not part of this thesis.

I further want to thank my former lab mates, Dr. Zongzhao Zhai and Dr. Hanat Tuekenbay (a.k.a. Nati Ha), for their support and friendship.

General thanks I want to express to the current and former members of the Lohmann lab for the productive working atmosphere. Specifically, I highly appreciated the fly food prepared by Bernhard Glass and the organisational efforts of Dr. Petra Kaspar and Justyna Lisges.

I wish to thank the INF685 Kinderkrippe and INF159 for taking care of Lara, and our nanny Anna-Lena Dumbeck for taking care of Julie.

I need to thank as well Jana's family, Regina, Dietmar, Susi and Friedi for huge efforts in looking after Julie in London and for giving Lara some summer holidays that allowed me to finish the writing of this thesis.

I also want to thank part of my family, my father, my grandma and my uncle for the continued support and love.

I am grateful to have many good friends, who have supported me throughout this work and life, one way or another.

My old school-friends Christian "Scholle" Scholz and Christopher "Grossi" Grosser. We celebrated three "round birthdays" during the time of my PhD, thinking of the good old days like grandfathers. From the same category, I have to mention my friend Anne Sennhenn, who had the best wedding I ever attended (I cannot remember much, since I blacked out during the party, but it was awesome).

My old University friends that I have lived with during the times of our Bachelor and Master studies in an arrangement termed by other people "Vorhölle". Dr. Falco "Falconist/Smeggn" Krüger, Benjamin "Oldest" Trageser and previously Mathias "Labsi" Labs. My studies as well as the time after it would have been boring without your company and friendship.

I also want to thank the new friendships we experienced thanks to our kids, Eva and Ricardo, "Jacki" and Torsten, Daria and Shachar, as well as our old colleague Hanat and Mira. May fortune be with your families.

I am indebted to the "3rd floor COS student crew", Jessi, Linda, Tobi and Jonas, as well as the "Sandwich Club" that developed out of it. Working with you made hard work much easier. Many thanks also go to Ana Barata for great discussions.

No more words, I would not be here finishing this PhD without ♡**Jana, Lara & Julie**♡

Finally, I want to congratulate Geraint Thomas for winning the Tour de France 2018 on the day I finished the writing of this thesis. Great Ride.

Frequently used Abbreviations

BDSC	–	Bloomington Drosophila Stock Center
bZIP	–	basic leucine Zipper
C/EBP	–	CCAAT-containing Enhancer binding protein
COX	–	Cytochrome-c oxidase
dsRNA	–	long, double-stranded RNA
eIF2α	–	eukaryotic Initiation Factor 2 alpha
ETC	–	Electron transport chain
GOF	–	Gain-of-function
IIS	–	Insulin/Insulin-like signalling
ISR	–	Integrated Stress Response
LOF	–	Loss-of-function
ND	–	NADH:ubiquinone oxidoreductase
NR	–	nutrient restriction
RNAi	–	RNA interference
shRNA	–	short-hairpin RNA
UPR^{ER}	–	Unfolded Protein Response of Endoplasmic Reticulum
UPR^{mt}	–	Unfolded Protein Response of Mitochondria
VDRC	–	Vienna Drosophila Resource Center

Publications and Contributions

The following article is related to this thesis, but has not been published yet:

Sebastian Sorge, Jonas Theelke, Christian Altbürger and Ingrid Lohmann. An ATF4-mediated transcriptional adaptation of electron transport chain disturbance primes progenitor cells for proliferation *in vivo*. submitted.

In the following people are listed who contributed experimental data to this thesis:

Jonas Theelke (as student helper and lab rotation student) helped with several experiments in the late stage of my PhD project, specifically: practically carried out most cell culture experiments; dissected larval eye-antenna discs for LDH-GFP reporter analysis.

Christian Altbürger (for his B.Sc. and M.Sc. thesis as well as in-between as student helper) helped with several experiments in the early stage of my PhD project, specifically: helped with the evaluation (visual inspection of many flies) of the primary RNAi screen; all his other direct contributions (TEM analysis together with EM Core facility; Su(H)-GFP reporter TUNEL labelling analysis; early phenotypic characterisation of Delta,COX7a phenotypes) are part of his M.Sc. thesis and cited accordingly.

Dr. Jana Friedrich prepared the schematic Illustration of Figure D1 according to my idea and lent me the outline and format of her PhD thesis.

I – Introduction

The work I am presenting in my thesis addresses aspects of two broad questions of basic biological research: How do cells respond to defects in their sub-cellular compartments or organelles? and How do organisms regulate organ size during development?

Both questions are fundamental in their respective fields, cell biology and developmental biology, and, at least for the results presented here, are interconnected in the sense that adaptations to organelle defects can have profound consequences for the proliferative behaviour of the cells in a cell-autonomous manner. As part of this introduction I want to provide an overview of both fields and emphasise the model organism and tissue I have been working with.

Part One: Control of organ growth during development

Most terrestrial animal phyla, including for example birds, mammals and holometabolous insects, follow a determinate growth mode. Once the adult, sexually-mature stage has been reached final organismal size is fixed (Hariharan2016). Therefore, the final size and shape of the adult is established during embryonic and juvenile development of these organisms. In most cases, this developmental growth is plastic towards intrinsic (for example genetic or epigenetic) or extrinsic (for example nutrition) modulation, allowing both long-term and short-term adaptations to environmental stimuli.

While plasticity of organismal growth represents a generally favourable mode of development, it also requires extensive communication between developing organs to

regulate growth. Overall, growth scaling has to be proportional between most organs to assure bilateral symmetry (Palmer and Strobeck, 1986), while at the same time crucial organs do not scale at all, such as the Central Nervous System upon malnutrition ("brain sparing") in mammals (Dobbing and Sands, 1971) or *Drosophila* (Cheng et al., 2011). Together, these observations suggest that both organ-autonomous and systemic signalling cascades interact to drive appropriate growth. In the following paragraphs, I want to give an overview of the molecular understanding of growth coordination and regulation in *Drosophila*, a model that despite its evolutionary distance to humans has been at the frontier towards a molecular understanding in this research area.

Organ-intrinsic regulation of growth in *Drosophila* imaginal discs

Transplantation experiments in various species indicated an autonomous mode of organ growth already many decades ago. The first to describe this property were Harrison, Twitty and Schwind in a series of studies, performing transplantation experiments between related salamander species with different growth kinetics (Harrison, 1924; Twitty and Schwind, 1931). The same observation was later made in different species that allow these experiments, including serial transplantations of imaginal tissues of *Drosophila* (Hadorn, 1963). Since then, the *Drosophila* imaginal discs - epithelial primordia that build most of the adult fly's external structures, including eyes, wings, antennae and legs - have been a favourite model of developmental biologists to study growth, patterning and the signalling pathways that control these processes. Noteworthy examples with implications beyond the fly include the discovery of "cell competition" between cells with different fitness (Morata and Ripoll, 1975) or the identification of the Hippo pathway and most of its molecular components (Harvey et al., 2003; Justice et al., 1995; Tapon et al., 2002; Udan et al., 2003; Wu et al., 2003).

Drosophila imaginal discs are primordia of adult structures. They are specified during embryogenesis, grow through proliferation during the larval stages and differentiate to build the adult fly during metamorphosis. As mentioned earlier, transplantation and

regeneration experiments (Bryant and Levinson, 1985; Hadorn, 1963) showed a capacity of imaginal discs or fragments of them to grow to the appropriate size even in ectopic environments. More recently, studies using clones with differing proliferation rates have shown that the disc-autonomous size regulation is also stable under these conditions (Martin et al., 2009). So, while cell competition per definition involves alterations of proliferation rates, growth of a clone of cells can only occur at the proportional expense of another clone, so that final tissue size and architecture is undisturbed by this process.

In contrast to these experiments, which primarily described the properties of wild-type tissue, genetic or pharmacological modulation of signalling pathways can severely disturb the autonomous growth regulation. In fact, most of our current knowledge of the molecular determinants of growth regulation within a tissue come from studies, where gain- or loss-of-function mutants in signalling pathways show phenotypes of in- or decreased growth. What has been far more difficult to address though, is the actual contribution of any of these pathways (and other processes) to the wildtype's internal growth regulation (schematically illustrated in Fig. I1).

The main signalling pathways that contribute to imaginal disc growth in *Drosophila* are to a large degree used in similar ways in different imaginal discs and are also utilised as regulators of growth and patterning in other animal systems. A requirement as growth promoting signals in the wing imaginal disc has been attributed to the Insulin/Pi3K, the Hippo, the Tor, the EGFR/ras, the Myc and the JAK/STAT pathway (reviewed in (Hariharan, 2015). Closer examination of these requirements enforces the interpretative problems outlined in Fig. I1 and further reveals another fundamental discrimination in growth regulation: the balance between hypertrophic and hyperplastic growth. In principle, an increase in size of an organ could be achieved by increasing the cell volume or by increasing the number of cells. Within the *Drosophila* larva, both processes co-occur: While most tissues constituting the fundamental parts of the larva (the "larval tissues") have polyploid cells with large cell volumes (employing hypertrophic growth through endoreplication), the "imaginal tissues", as precursors of the future adult fly, maintain a roughly uniform small cell size and grow through cell proliferation.

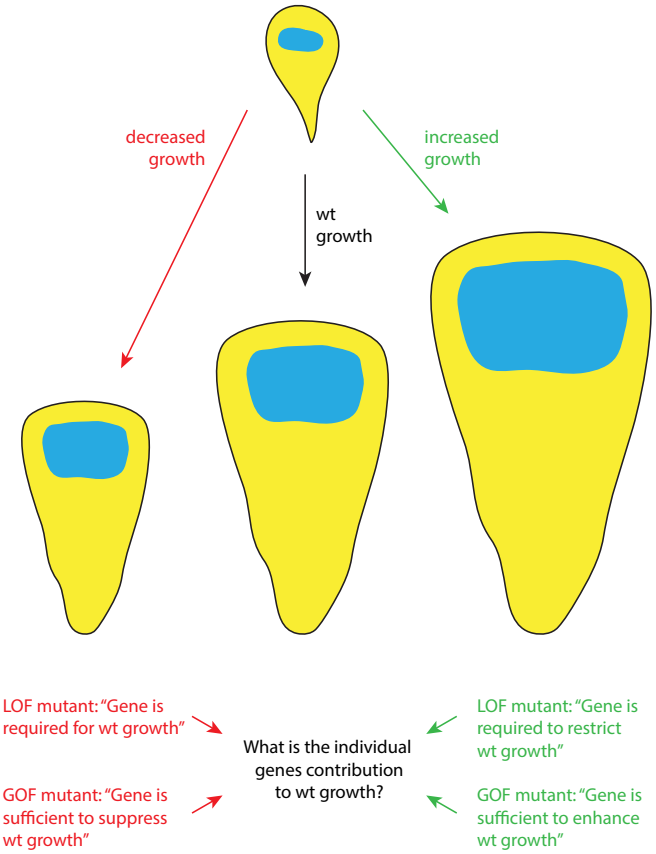

Figure I1: Schematic Illustration of wing disc growth
Early wing disc (top) can grow to wildtype size (middle) or show decreased (left) or increased (right) growth in mutant animals. Typical conclusions that can be drawn from these experiments are indicated, as well as the primary question (middle), which is not easily answered by these experiments.

Though not yet considered in this way by the research community, I consider pathways like Myc or Tor, which both primarily drive cellular hypertrophy, through increased ribosomal gene transcription or ribosome activity, respectively, to be more general requirements, which act upstream of virtually any other process. For example, pioneering work by Laura Johnston on Drosophila Myc (Johnston et al., 1999) has shown that hypomorphic *Myc* mutants have smaller cells, while over-expression of Myc increases cell size. The study further showed that Myc expression decreased the number of cells in G1-phase of the cell cycle, which was interpreted as promoting cell cycle G1-S progression. In my view, any pathway that increases cellular mass accumulation (through effects on translation) is expected to accelerate the G1-S transition, as the purpose of G1 is mass accumulation to allow genome replication and no requirement for external

signals regulating S-phase entry exists in the imaginal discs. A more probable explanation might therefore be that the length of the G1 phase is determined by the speed at which a cell translates new proteins in preparation of S-Phase.

Overall, genetic and molecular analyses on imaginal disc development have revealed a number of signalling pathways acting in progenitor cells to coordinate growth. Yet, despite substantial progress in understanding how these pathways are controlled and what the primary outputs are, a picture how these outputs shape appropriate growth are poorly understood. In the next paragraph, I will describe in greater detail the signals that have been identified as growth regulators in the *Drosophila* eye imaginal disc, present several opposing models of eye growth and provide a new perspective.

Inter-organ growth coordination in the *Drosophila* larva

Adaptations to environmental conditions or spontaneous developmental defects require systemic signalling cascades to coordinate growth between organs and to synchronise primordia development with the overall development of the organism. "Growth sparing" in response to starvation describes the selective growth of some organs under conditions where no external nutrients are available. This situation could be a consequence of a) a direct dependency on nutrient levels in the hemolymph that quantitatively differs between different organs; b) a different dependency on hormonal or other systemic signalling cues that are modulated in response to malnutrition, or c) signalling cascades operating in spared tissues that uncouple its growth from the rest of the body. While a) has not been investigated, evidence for both other possibilities have been shown. The laboratory of Alex Gould has shown that CNS sparing is mediated through Jeb/Alk-RTK signalling that uncouples CNS proliferation from a dependency on systemic insulin signalling (Cheng et al., 2011). While their study also showed that wing disc growth is spared to some degree, the mechanism remains unknown.

Several laboratories have contributed to our understanding of how systemic hormone signalling is modulated in response to malnutrition, thereby explaining the response of

the larval tissues that are sensitive to malnutrition and do not show sparing. To date, the most significant hormone contribution to growth of larval and imaginal tissues is insulin/insulin-like signalling (IIS) (Britton et al., 2002; Brogiolo et al., 2001). Insulin-like peptides (Ilps) are secreted from neurosecretory cells in the brain to direct larval growth or produced locally in some tissues and bind to the single insulin receptor (InR) to activate PI3K/Akt-signalling (Edgar, 2006). Within most larval tissues, PI3K/Akt activation through InR as well as Tor activation through the amino acid transporter Slimfast are strictly required to allow growth (see (Teleman, 2010) for review). Decreases in dietary nutrient uptake directly reduce Tor activity and indirectly reduce IIS activity through decreased secretion of Ilps from the brain. As mentioned before, some tissues can uncouple their PI3K/Akt and Tor signalling output from these inevitable growth-reducing effects of nutrient restriction and spare growth (Cheng et al., 2011).

An important question in the field that began to be solved over the last years, is how Ilp secretion from the insulin producing cells (IPCs) of the brain is regulated in response to changing nutrient availability. To this day, several signalling systems have been identified to signal these changes from the larval fat body (FB) to the IPCs. The laboratory of Pierre Léopold identified the tumor necrosis factor homologue of *Drosophila*, Eiger, to be released from the FB in response to a low-protein diet. In the IPCs, Eiger activates JNK signalling through its receptor Grindelwald, which suppresses secretion of Ilps from the IPCs, thereby reducing IIS activity in peripheral tissues (Agrawal et al., 2016). Through the same genetic screen, they identified a second signal with opposite function. Under conditions of sufficient nutrient uptake, the FB releases a ligand called stunted, which activates its receptor methuselah in IPCs to allow ILP secretion (Delanoue et al., 2016).

Another interesting question is how the imaginal tissues can feedback on overall larval development, since proper development of the imaginal tissues is one of the most fundamental necessities for adult life. Delayed pupation in response to defects of imaginal disc development have been described for a long time (Simpson and Schneidermann, 1975; Simpson et al., 1980). More recently, a Ilp-like ligand, called Dilp8, was identified to trigger this response through effects on ecdysone production (Colombani et al., 2012; Garelli et al., 2012). Further analysis identified Lgr3 as the

receptor for Dilp8, which has no insulin-related function, and the specific expression of Lgr3 in neurons innervating the neurosecretory cells of the prothoracic gland, which are the site of ecdysone synthesis and release (Colombani et al., 2015; Vallejo et al., 2015). Interestingly, these studies revealed that Dilp8-Lgr3 signalling is required to buffer against developmental noise even in the wildtype, as fluctuating asymmetry is increased in *Dilp8* or *Lgr3* mutants.

In summary, growth of larval tissues is regulated through direct cell-autonomous effects, such as the translation of amino acids availability into Tor activity, as well as non-cell autonomous, hormonal effects through the insulin signalling cascade. Many aspects of growth sparing and a more detailed understanding of the temporal modes of growth are still required to gain a better overall understanding of organ growth regulation.

Growth regulation in the eye-antenna disc

The *Drosophila* eye-antenna disc differs from the other imaginal discs with respect to the timing of differentiation. While other imaginal tissues enter their terminal differentiation programme after pupation, eye differentiation starts already during the early 3rd larval instar. At this time, the first R8 photoreceptors are specified at the posterior equator and subsequently a self-propagating wave called the morphogenetic furrow (MF) moves anterior wards. In front of the MF, cells are synchronised in their cell cycle and enter the stepwise specification/differentiation regime behind the MF (reviewed in Baker, 2001; Kumar, 2011). Proliferation of eye progenitors is asynchronous during early stages, with an overall high density of mitotic cells, and later becomes synchronised in front of the MF, creating the so-called First Mitotic Wave (FMW) and behind the MF, the Second Mitotic Wave (SMW; see Figure I2).

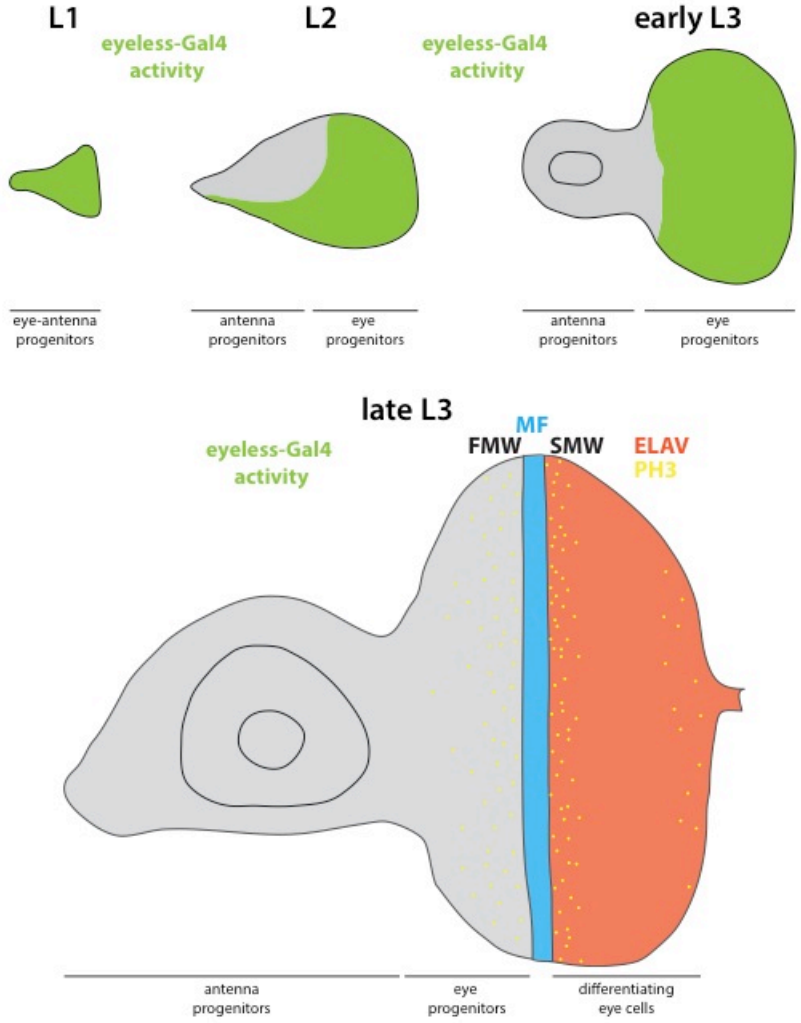

Figure I2: Schematic Illustration of eye-antenna disc development
Illustration based on microscopic study of fixed eye-antenna discs throughout larval development (from late embryo/L1, through L2, early L3 to late L3). The size of the discs in the scheme is approximate. Eyeless-Gal4 activity in green is based on observations with several UAS-transgenes induced by ey-Gal4. There is no activity of ey-Gal4 by the late L3 stage. Morphogenetic Furrow (FW), First and Second Mitotic Wave (FMW and SMW), mitotic ($PH3^{+}$) cells indicated by yellow dots and area of differentiation (marked by ELAV) in red.

In addition to the growth promoting pathways I mentioned in the previous paragraph, eye growth requires activation of the Notch pathway (Dominguez and de Celis, 1998; Papayannopoulos et al., 1998) as well as the activity of a group of transcription factors termed the retinal determination network (Kumar, 2010). At present, several models explaining growth regulation co-exist and I will discuss them next.

The Notch signalling pathway was shown to be activated at the dorsal-ventral boundary ("equator") of the eye, due to differential expression of the two Notch ligands,

Delta and Serrate, and a Notch-modifying enzyme, Fringe, in the ventral or dorsal compartment (Dominguez and de Celis, 1998; Papayannopoulos et al., 1998). Over-expression of the intracellular domain of the Notch receptor was shown to induce hyperplasia and is apparently able to compensate for endogenous Notch activation at the equator (Dominguez and de Celis, 1998). Subsequent studies then tried to link local Notch activation with proliferation occurring throughout the disc. These studies identified target genes of Notch at the equator, such as the Pax6-like transcription factor eyegone (Chao et al., 2004; Dominguez et al., 2003) or the ligand of JAK/STAT signalling, Unpaired (Chao et al., 2004). Based on these and other reports, several models have been proposed to explain how Notch activation at the equator instructs growth of the whole eye-antenna disc (reviewed in (Estella and Baonza, 2015). Though different in molecular mechanism, these models ultimately rely on secretion of a ligand (Unpaired or Hedgehog) from an organiser to direct growth.

Experimental observations and modelling of morphogen gradients by Wartlick, Jülicher and Gonzalez-Gaitan have suggested that a moving gradient of the morphogen decapentaplegic (dpp; as well as another unidentified molecule) accounts for the proliferation pattern of mid to late 3rd larval instar eye-discs (Wartlick et al., 2014). In this "temporal model", cell division is triggered "when their signalling levels have increased by 60%" since the last cell division" (Wartlick et al., 2014). Other modelling approaches of eye disc growth have casted doubt upon this model and instead suggested again that the cytokine Unpaired would instruct growth (Fried et al., 2016; Vollmer et al., 2017). Apparently, there is no consensus at this time.

I illustrated in Fig. I1 the problem that Gain- or Loss-of-function experiments often do not inform about the actual contribution of a gene to the wild-type phenotype. As an example, adult flies without eyes (and cuticle instead) could have lost eyes through various mechanisms, such as a lack of proliferation of eye progenitors; overgrowth of cuticle progenitors; through selective death of eye progenitors; or through a change in cell fate, to name a few. A further complication for our understanding is the fact that many of the genes found to be required for eye growth so far, act in strikingly linear

pathways, where finally only the most downstream gene appears to have all the growth-regulating activity. An example for this phenomenon is the dorsal-ventral (DV) compartment cascade, involving Fringe, Caupolican/Araucan/Mirror, Delta, Serrate and Notch, culminating in the activation of eyegone, which is apparently able to replace any mutant of these upstream genes (Chao et al., 2004; Dominguez et al., 2003). Together with the general controversy on how morphogen gradients could function (Alexandre et al., 2015), these drawbacks illustrate the need for a conceptually deeper understanding of what discriminates truly instructive from rather permissive signals.

In the wild-type eye disc, the DV cascade establishes Notch signalling at the equator of the disc. Any disruption of the cascade prevents eyegone expression, leading to a loss of eyes. Expressing an activated form of Notch (Dominguez and de Celis, 1998) or directly eyegone (Dominguez et al., 2003) restores eye growth. In this scenario, eyegone activity appears to be required in some form, but the equator itself appears dispensable for the growth promoting role. This assumption, together with the notion that ectopic eyegone expression non-autonomously induces the Unpaired cytokine (Chao et al., 2004), seems compatible with the model of Vollmer and colleagues suggesting Unpaired as the secreted factor controlling eye size (Vollmer et al., 2017). Unfortunately, such a model cannot readily explain the differential growth kinetics of eye discs over-expressing Delta, which exhibit higher proliferation rates in the ventral compartment only (Dominguez and de Celis, 1998, S. Sorge this thesis). If Unpaired is very stable and diffuses very fast (Vollmer et al., 2017), its effects should spread roughly equally under these conditions too, yet the increased mitotic indices are very local. One might therefore argue that Unpaired is just one permissive signal required to allow growth. Interestingly, a recent study by the laboratories of Konrad Basler and JP Vincent found that during wing disc development, the growth-enabling function of the dpp morphogen does not require the typical concentration gradient, but that uniform, low-level activation of dpp signalling is sufficient to allow proliferation, suggesting as well that the role of dpp in growth regulation is permissive (Bosch et al., 2017).

In order to better understand eye growth, one needs to consider the process in its entirety. The studies by Wartlick and Vollmer focus on the later phases of eye disc development, where proliferation rates are slowing down ("growth termination"). They describe the biophysical properties of secreted growth factors or their gradients to explain the gradual decline in proliferation over time. Indeed, growth termination contributes significantly to final eye size and shape. Given the early onset of differentiation in the posterior part of the eye, the prolonged progenitor state in the anterior part needs to be met by decreasing proliferation rates to prevent disproportionate growth of the anterior compartment.

The studies addressing the contribution of the Notch pathway and eyegone, instead focussed on the earlier stages of development, where indeed most mitotic rounds take place (approximately 6 rounds of division take place in approximately 48 hours from early L1 to early L3). During this time, eyegone activity is required for growth (Wang et al., 2008), but the necessary output of its activity has not been clearly identified. Since the role of Unpaired as a bona fide growth-promoter has also been questioned (Gutierrez-Aviño et al., 2009; Wang and Huang, 2009), it appears unlikely that Unpaired functions as an instructive division cue during these early stages.

In summary, most of the available literature suggests a number of pathways or transcription factors to be required for eye growth, but none of them could be claimed to have a clear instructive role in determining proliferation rates. One explanation could be that the crucial factor has simply not been identified yet or that the complex combinatorial action of these processes has not been understood in sufficient detail. Another possibility is that no instructive cue is required, so that cells divide at the "maximum speed" allowed by the action of many permissive cues with partially overlapping function. Such a model is compatible with most observations made so far:

1) As long as growth termination in the 3rd larval instar is in place, final eye size is determined by the size and shape of the eye disc at the onset of differentiation. So, the most crucial parameter for final eye size is the trigger to induce differentiation once a defined size has been reached (by asynchronous, "maximum-speed" proliferation of progenitors).

2) If 1) is correct, pure decreases in cell cycle length in the early progenitor compartment would not impact on final eye size, because differentiation would be triggered earlier and the growth termination cascade would still maintain proper size. Indeed, imaginal disc growth can become temporally uncoupled from larval growth under nutrient restriction (Cheng et al., 2011) or other disturbances of larval development and importantly, accelerations of cell cycle phasing do not change tissue size in the wing disc (Neufeld et al., 1998) or the eye disc (S. Sorge, unpublished observation).

3) The "maximum speed" would be determined by the cells' ability to progress through the cell cycle. While the metabolic requirements of cell cycle progression are still in the process of becoming understood (Cai and Tu, 2012; Vander Heiden et al., 2009), a general dependency on nutrients is obvious. Both, systemic signalling through ILP release from the brain and direct cellular sensing of amino acids through Tor and other pathways, can couple the cells' speed of cell cycle progression to the overall availability of nutrients and thereby overall developmental growth (increase in mass), though this coupling apparently is not a linear connection (see "sparing"). In that model, the main determinant of the growth speed of wild-type imaginal disc progenitors would be the set of proteins that determine uptake and use of nutrients to fuel metabolism and the necessary anabolic reaction.

Part Two: Cellular stress signalling and metabolic adaptation

Cellular survival, cell growth or cell division require nutrient uptake to maintain ATP levels, to replace or synthesize new proteins or to build other macromolecules such as RNA or DNA. Generally, the strict requirements for growth - either in cell volume or cell numbers - differ from the requirements of homeostasis or survival. A good illustration of this is found in many unicellular organisms, which are directly exposed to their environment and usually have limited abilities to move to a more favourable location. Microbes under starvation can arrest their cell cycle in a G_0-like phase, but within minutes re-enter the cell cycle to grow and proliferate as long as nutrients are available (reviewed in (Cai and Tu, 2012). Multi-cellular organisms have additional constraints on proliferation

and growth (see above), but cellular growth or division nevertheless requires nutrient availability to the cell. Animals have therefore evolved circulatory systems, storage tissues and systemic signalling cascades, who together are able to maintain nutrient levels within physiological levels throughout the body. In *Drosophila*, the fat body (FB), in an analogous fashion to vertebrate liver and adipose tissue, appears to be the primary organ involved in nutrient homeostasis. In addition to systemic events, cells can directly sense nutrient concentrations, for example through the Tor pathway introduced above (Efeyan et al., 2012; Hara et al., 1998). Importantly, Tor signalling and other stress-response pathways (see below) are not merely sensing nutrients to induce a quiescent state under starvation, but induce specific adaptations to counteract starvation.

Besides the rather obvious requirement of nutrients for growth or proliferation, a recently emerging concept is that the cellular metabolic state is directly linked to proliferative behaviour, so more than a mere requirement. Almost a century ago the German physiologist Otto Warburg described the glycolytic metabolism of cancer even in the presence of oxygen, hence called "Aerobic Glycolysis" or "the Warburg effect" (Warburg et al., 1924). His findings and especially his hypotheses that dysfunctional mitochondria are the cause of cancer, have been controversially discussed ever since (see (Senyilmaz and Teleman, 2015). But by now, "the Warburg effect" has become an important driver of advancement both in cancer and basic biological research, as Aerobic glycolysis seems to be a rather universal metabolic state of proliferating cells (Koppenol et al., 2011; Vander Heiden and DeBerardinis, 2017; Vander Heiden et al., 2009). Other metabolic demands of cancer cells that directly dictate their proliferative potential have recently been discovered (DeNicola and Cantley, 2015; Faubert et al., 2017; Mashimo et al., 2014). Therefore, at present it seems like a fair assumption that the metabolic state of a cell, which is determined by the intracellular concentrations of the relevant nutrients as well as the set of metabolic enzymes and their activity, has direct consequences for the speed of cell cycle progression. Overall, the scientific literature is compatible with the above-mentioned "maximum speed" of division model I have proposed.

For the remainder of this introduction I want to focus on intracellular stress-response pathways and their role in acute or chronic adaptation to stress during development or disease.

The Unfolded Protein Response of the Endoplasmic Reticulum

I have outlined several responses of cells to shortages in nutrient levels in the previous paragraphs. In addition to this single stress, cells are continuously exposed to a large number of additional, exogenous stresses. These include, but are not limited to, stress from temperature fluctuations (heat), osmotic or oxidative stress. To cope with these natural insults, cells have evolved detoxifying systems to buffer against or react to changes, like the transcriptional heat-shock response (Ashburner and Bonner, 1979; Richter et al., 2010) or the glutathione redox system (Hwang et al., 1992). Besides external impairments of cellular homeostasis, internal protein folding can be disturbed by many natural processes or specific toxins. To date, the best characterised organelles' stress response is the Unfolded Protein Response of the Endoplasmic Reticulum (UPR^{ER}).

The Endoplasmic Reticulum (ER) is the major cellular compartment for the folding and post-translational modification of membrane and secreted proteins. Unicellular eukaryotes possess a single pathway to monitor and maintain ER homeostasis, the Ire1 pathway, while multicellular eukaryotes have two additional pathways (see Korennykh and Walter, 2012 for review): In vertebrates, *Drosophila* and *C. elegans* three pathways with partially overlapping function build the core of the UPR^{ER}. ATF6 is a bZip-transcription factor initially targeted to the ER membrane. Upon ER protein folding stress, it is send to the Golgi, where proteolytic cleavage releases the cytoplasmic domain, which enters the nucleus to function as a transcriptional activator (Haze et al., 1999; Ye et al., 2000). Ire1 is an RNase incorporated into the ER membrane. Its ER-luminal domain is able to sense unfolded ER proteins, leading to lateral oligomerization and activation of the RNase domain. The RNase activity cleaves *Xbp1* mRNA to release an intron, leading to translation of the functional Xbp1 transcription factor (Mori, 2009). Both, the Ire1/Xbp1- and the ATF6-pathway primarily induce transcription of ER chaperones and

other enzymes (Cox et al., 1993; Yamamoto et al., 2007), aiming to decrease ER protein folding load and increasing ER protein folding capacity, respectively (Walter and Ron, 2011).

The third branch of the UPR^{ER} is mediated by the ER-resident eIF2α-kinase PERK (Harding et al., 2000). As the luminal domain of PERK is structurally related to Ire1, it is assumed that PERK senses ER protein folding stress in a similar, yet to be defined, way as Ire1. Accumulation of unfolded proteins in the ER lumen triggers PERK dimerization, cross-phosphorylation and finally phosphorylation of eukaryotic Initiation Factor 2α (eIF2α), leading to a slow down of translation initiation and thereby overall translation rates. While decreased overall protein translation decreases the protein burden for the ER, the response also triggers a relative increase in translation of open-reading frames (ORFs) with μORFs in their 5'-UTR. A prominent target amongst these mRNAs is a bZip transcription factor, called Activating Transcription Factor 4 (ATF4, Dever et al., 1992; Harding et al., 2000). The mammalian ATF4 mRNA carries two μORFs upstream of its main ORF that essentially fully block translation of ATF4 protein (Harding et al., 2000; Vattem and Wek, 2004). Only phosphorylation of eIF2α by one of four eIF2α-kinases increases the probability of ATF4 translation so that the protein can accumulate to relevant concentrations (for review see Kilberg et al., 2009). The structure and function of the *ATF4* mRNA is also conserved in *Drosophila* (Kang et al., 2015) and yeast (Hinnebusch, 1997), suggesting that ATF4 activity downstream of translation attenuation is a highly conserved response. Since the ATF4 response, activated downstream of PERK upon ER protein folding stress, is a much more general stress adaptation (see below for details), the PERK branch of the UPR^{ER} differs in that respect from the other two branches.

The Integrated Stress Response through ATF4

Translation and thereby functional activity of ATF4 requires phosphorylation of eIF2α by one of its kinases. Since the vertebrate genome encodes at least four eIF2α-kinases, which are activated by various different stresses, the term "Integrated Stress Response" (ISR) has been used (Harding et al., 2003). Similar to the broad input into the ISR, the

ATF4 output in terms of transcriptional targets covers a wide range of molecular functions and biological processes.

One of the first known transcriptional targets was another transcription factor, CHOP (or DDIT3; Harding et al., 2000), which appears to act as a negative feedback-regulator of ATF4 (Kilberg et al., 2009) and to induce apoptosis upon chronic stress situations (Demay et al., 2014). ATF4 further induces expression of other transcription factors that also act as potential dimerization partners, such as C/EBPβ and ATF3 (Pan et al., 2007; Thiaville et al., 2008). Other studies have linked ATF4 to the induction of the "Amino Acid Response" (AAR) by binding to "CARE" sequences (CCAAT-enhancer binding protein-activating transcription factor response element), thereby inducing amino acid transporter genes (CAT1, xCT, SNAT2) or ASNS, a gene encoding asparagine synthethase (Kilberg et al., 2009). More recently, a role for ATF4 in the regulation of one-carbon metabolism was shown in human cells (Bao et al., 2016) and in *Drosophila* neurons (Celardo et al., 2017). Another contribution from fly research to our understanding of ATF4 function came from cultured Drosophila cells, which showed ATF4-dependent induction of glycolytic enzymes in response to ER stress (Lee et al., 2015a), a response that is so far unique for *Drosophila* ATF4. And lastly, while this thesis was written, a study was published showing the transcriptional response to over-expression of ATF4 in cultured *Drosophila* cells (Malzer et al., 2018), confirming most of the target genes I had just introduced.

Overall, the transcriptional programme induced by ATF4 leads to a broad and relatively unspecific, general stress response, potentially improving cellular fitness through one of the many processes it activates. While some of its output has been proven to be beneficial for cellular fitness or survival (Bao et al., 2016; Celardo et al., 2017), in most of these experiments it is difficult to discriminate positive input from a single target gene with the overall impact of all target genes. Therefore, the physiological implications of the ATF4 response remain poorly understood and might be very context-dependent.

The Unfolded Protein Response of Mitochondria

In an analogous manner to the UPR^{ER}, a protective mitochondrial Unfolded Protein Response (UPR^{mt}) has been described (Martinus et al., 1996). Though conceptually similar to the UPR^{ER}, the UPR^{mt} remains less well characterised. Part of the explanation for this fact are evolutionary differences between the model organisms. The UPR^{mt} was first identified in human cells, where its activity was attributed to CHOP and C/EBPβ (Zhao et al., 2002). Later, a paralog of ATF4, ATF5, was implicated as the inducer of UPR^{mt} (Fiorese et al., 2016). Very recently, a multi-omics study in cultured human cells suggested that ATF5 and its UPR^{mt} target genes are not at all activated in response to mitochondrial stress (Quirós et al., 2017).

In *C. elegans*, where the UPR^{mt} is overall best described, a transcription factor (Atfs-1) with homology to ATF4 and ATF5 has been shown to mediate induction of mitochondrial chaperones, the classical UPR^{mt} targets (Haynes et al., 2010). A subsequent study then showed Atfs-1 to be contain a mitochondrial import sequence, leading to import into mitochondria, where it is degraded (Nargund et al., 2012). Defects in import, which can be caused by different defects to mitochondrial function, then lead to stabilisation of Atfs-1 in the cytoplasm and translocation to the nucleus, where it can act as transcription factor to induce mitochondrial chaperones (Nargund et al., 2012). Therefore, the *C. elegans* UPR^{mt} uses mitochondrial import as a sensor for mitochondrial (dys)function. Another important study in worms has also shed light on possible upstream mechanisms leading to UPR^{mt} activation. Yoneda and colleagues showed that genetic disturbance of large mitochondrial protein complexes (such as the complexes of the mitochondrial electron transport chain (ETC)) through RNAi acted as the most potent inducers of the UPR^{mt} (Yoneda et al., 2004).

In Drosophila, no apparent orthologue of either Atfs-1 or ATF5 is found. Technically, the protein with closest homology to both is ATF4. Interestingly, ATF4 has been linked to mitochondrial stress or dysfunction in a Drosophila model of Alzheimer's disease, where potentially PERK mediates its activation (Celardo et al., 2016; 2017). In a similar way, two studies in cultured human cells have linked defects in mitochondria to activation of the

ATF4-mediated ISR (Bao et al., 2016; Quirós et al., 2017). Under the conditions of these experiments, the classical mitochondrial UPR^{mt} target genes are not induced (Quirós et al., 2017), substantiating the molecular separation of ISR and UPR^{mt} in vertebrates. An apparent conundrum is the molecular trigger or sensor that activates either the ISR through ATF4 or the UPR^{mt} through ATF5 in response to mitochondrial dysfunction (Bao et al., 2016; Fiorese et al., 2016; Quirós et al., 2017).

The present state of research suggests substantial differences in the activation of the UPR^{mt} in the model organisms analysed to date. So far, the only consensus is the existence of a mechanism that activates mitochondrial chaperones, which at the same time is the defining criterion of UPR^{mt} activity. In the model organism I have been using for this study, the vinegar fly *Drosophila melanogaster*, no molecular mechanism for UPR^{mt} activation has been described.

Aims of this thesis

Growth of *Drosophila* imaginal discs is controlled by several signalling pathways and transcription factors in ways that are yet to be understood in molecular detail. Utilising the high proliferative plasticity of imaginal progenitor cells, the main general motivation of this study was to

> "identify novel mechanisms controlling proliferation of imaginal progenitor cells and final tissue size through an *in vivo* screen".

Building on the phenotypes discovered with $COX7a^{RNAi}$ as the foundation, the specific aims addressed in this thesis were:

1) To mechanistically dissect the intracellular response to knockdown of subunits of the electron transport chain (ETC).

2) To molecularly characterise the output of ATF4, which I found to be the mechanistic target of disturbed ETC function.

3) To define the genetic interaction between Notch signalling activation and ETC knockdown in inducing over-proliferation.

II – Results

Chapter One: A genetic screen for modifiers of eye growth

The entry point of my PhD project was RNAseq data generated in the lab by Z. Zhai that I used as a resource for an *in vivo* reverse genetic screen in the *Drosophila* eye to identify modifiers of eye growth. The rationale was that tumorous overgrowths, like the ones caused by knockdown of the transcription factor Cut in combination with activation of the Notch signalling pathway (Zhai et al., 2012), would show de-regulation of effector genes that themselves could promote eye growth, when over-expressed or knocked down by RNAi.

The RNAi screen

Therefore, I started my project by analysing the transcriptomic profile (by Microarray and RNAseq) of the Cut/Notch tumours performed by my colleague Z. Zhai (Zhai et al., 2012). Figure 1 shows a schematic representation of the model and the approach. The RNAseq data of ey>Dl>Cut^{RNAi} and ey>Dl>Cut^{RNAi}>p35 tumours was normalised to the control ey>Dl and differentially expressed genes were listed and plotted. As the transcriptome analysis was carried out in a single biological replicate by Z. Zhai, I focussed my attention on genes that showed the same direction of regulation in both genetic conditions, thereby excluding genes that were only found in one of the two tumours (see boxes in Figure 1).

In the first step, I ranked down-regulated genes according to their fold-change and chose candidates for the primary RNAi screen by the availability of UAS-RNAi flies in the Vienna Drosophila Resource Center (VDRC) library, as the genome-scale KK library of the VDRC was made available through Prof. Michael Boutros (DKFZ Heidelberg). In a second step, I chose 19 additional candidates, where UAS-RNAi flies could be obtained from the

Bloomington Drosophila Stock Center (BDSC). Table 1 (Appendix) lists all RNAi constructs and corresponding gene identifiers tested in my *in vivo* genetic screen.

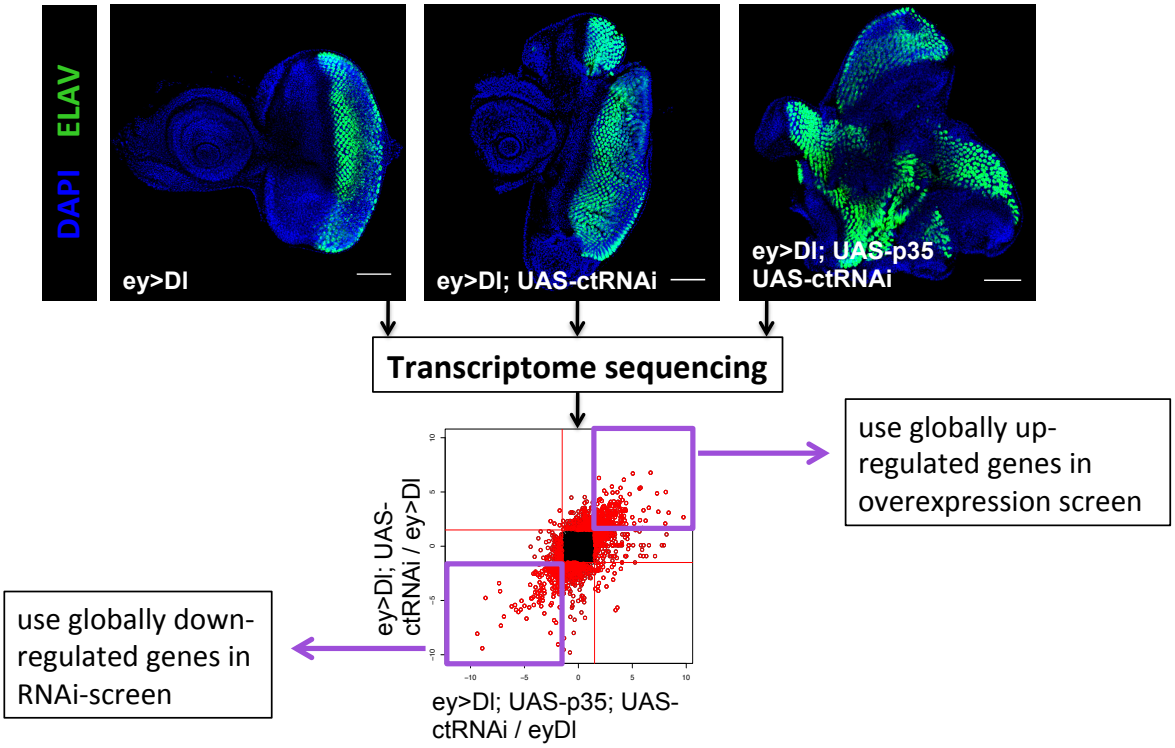

Figure 1: A schematic representation of the foundation of the RNAi screening approach
Representative images of tumorous overgrowths of eye-antenna disc with Delta over-expression (left), Delta over-expression with Cut knockdown (middle) and Delta over-expression, Cut knockdown and UAS-p35 over-expression (right). RNA-seq data from these discs was generated by Zongzhao Zhai and analysed by me. Candidates for the RNAi screen were from purple box to the lower left, candidates for the over-expression screen from purple box to the upper right. Scale bar in microscopic images is 50µm.

For the RNAi screen, I collected virgins from the two stocks ey>Dl/CyO and ey>Dl>Cut^{RNAi}/CyO and mated them with UAS-RNAi males. The screen was conducted with 25 virgins in big vials on standard fly food, in an incubator set to 27°C. After offspring had started to eclose, I categorised eye phenotypes by scoring each individual animal. Through this detailed screening, I found 19 genes to induce mild over-proliferation, two to induce complete lethality, two to result in severely reduced and malformed eyes and one to induce clear over-proliferation and tissue folding (Figure 2A,D). I did not detect obvious differences between the two backgrounds I used, implying that these phenotypes were not directly connected with Cut loss-of-function.

In a later experiment, I confirmed the initial phenotypes for the five genes that showed strong phenotypes in the primary screen. The two lethal knockdowns targeted the enzyme Glutamine synthase 1 and Rpn12, a component of the proteasome. In both cases, larvae showed strongly reduced or completely absent eye-antenna discs, arguing that their knockdown impaired development and viability of eye-antenna progenitors. The two lines showing reduced and malformed eyes in adult survivors targeted two un-described genes, CG7394 and CG10205. Through PCR-based genotyping I could show that these two lines harboured integration of the RNAi construct in a PhiC31 landing site producing off-target effects through over-expression of *tiptop* (Green et al., 2014), arguing that the phenotypes were not caused by the specific knockdown of these two genes (see Figure 2B). The single candidate causing clear over-proliferation of eye progenitors - COX7a - will be discussed in the following chapters.

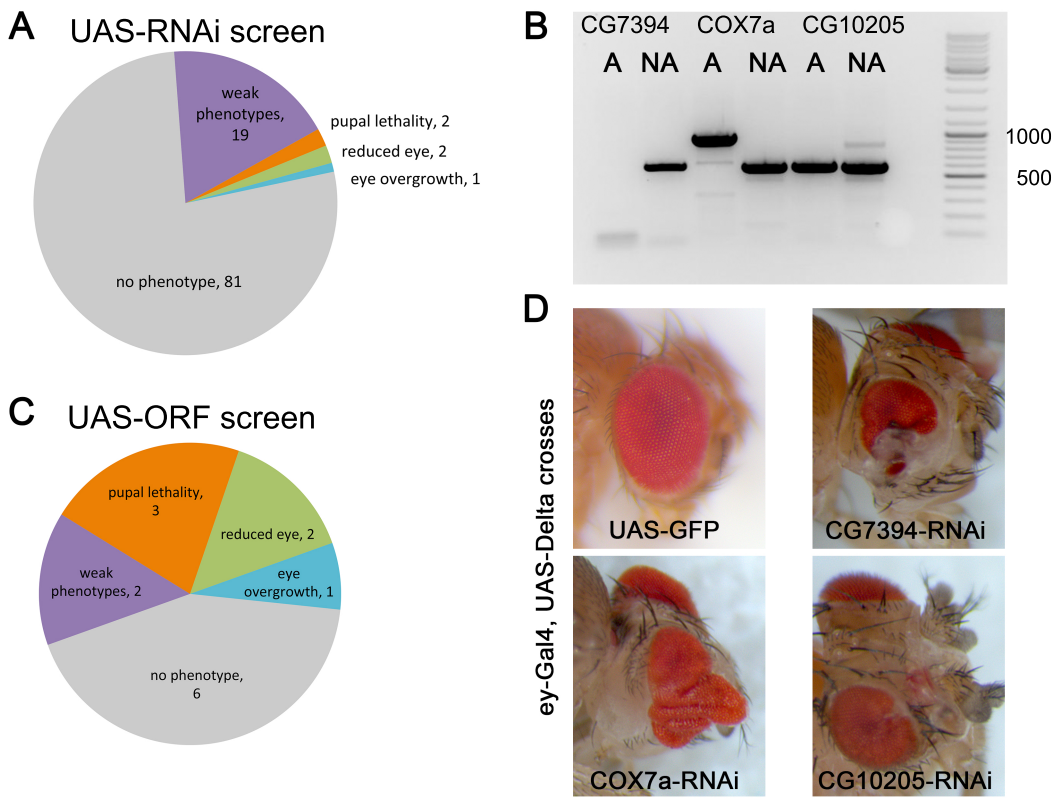

Figure 2: The results of the RNAi- and the over-expression screen

A) Schematic evaluation of phenotypes detected in the RNAi screen. **B)** Genotyping PCR from three RNAi lines of the Vienna KK library, which is subject to integration artefacts. Only the COX7a-RNAi showed a 1000bp PCR product (indicative of empty integration site) in the annotated (A) integration site. CG10205-RNAi showed integration in the A site (600bp PCR product) and therefore is subject to dominant insertion effects. CG7394-RNAi has no PCR product for A. All three have insertion into the NA (non-annotated) site. See (Green et al., 2014). **C)** Schematic evaluation of phenotypes detected in the over-expression (UAS-ORF) screen. **D)** Representative phenotypes of three RNAi constructs in the ey>Gal4, UAS-Delta background.

The over-expression screen

To complement the RNAi screen, I additionally investigated genes that I found up-regulated in Dl, Cut^{RNAi} and Dl, Cut^{RNAi}, p35 tumours. As no genome-scale libraries carrying open reading frames (ORFs) under UAS control exist, selection of candidates to test via over-expression was more restricted. Types of randomly inserted P-element constructs that allow over-expression of neighbouring genes through UAS sites in their 5'- or 3'-termini are insertions of the EP and EPgy2 elements that are available through the BDSC. I tested 17 of these lines but none induced a phenotype. As this agrees with previous attempts by Z. Zhai (personal communication), it appears as if these lines generally fail to support sufficient over-expression to cause phenotypes in the ey>Dl background. The UAS-ORF lines I tested were much more potent and I recovered eye phenotypes for 8/14 lines (Figure 2C). Of these, two showed either mild over-proliferation (mei-P26) or mild under-proliferation (dMyc), both at low penetrance, and five caused severe phenotypes leading to strongly reduced eyes (sequoia, CG6175) or full lethality (chinmo, Tis11, mutator 2). Over-expression of the *Drosophila* insulin receptor (InR), caused over-proliferation, but we decided not to pursue this candidate further, as Insulin signalling acts upstream of the known growth-promoting PI3K/Akt pathway (Britton et al., 2002).

In summary, through the *in vivo* screen I discovered several candidate genes that affected eye growth positively or negatively. Of these candidates, we decided to focus our attention on COX7a, the gene whose knockdown caused strong over-proliferation in the context of Notch signalling.

Chapter Two: COX7a is required for eye development

Cytochrome c oxidase subunit 7a (COX7a) is a nuclear-encoded, constitutively expressed subunit of the fourth complex (Cytochrome c oxidase) of the mitochondrial electron transport chain (ETC). Knockdown of COX7a - using the same RNAi construct I recovered through my screen - ubiquitously in *Drosophila* larvae or adults was shown to impair proper Complex 4 assembly and to reduce respiratory capacity (Kemppainen et al., 2013). Together with results on Complex 4 assembly in human cells (Nijtmans et al., 1998) or isolated mouse mitochondria (Lazarou et al., 2009), these findings suggest that COX7a is assembled into the complex at a late stage and that loss of COX7a attenuates Complex 4 function, but does not fully impair it.

The results I obtained through my screen suggested that reducing COX7a function by RNAi, and thereby Complex 4 function, promoted eye progenitor proliferation in combination with elevated Notch signalling.

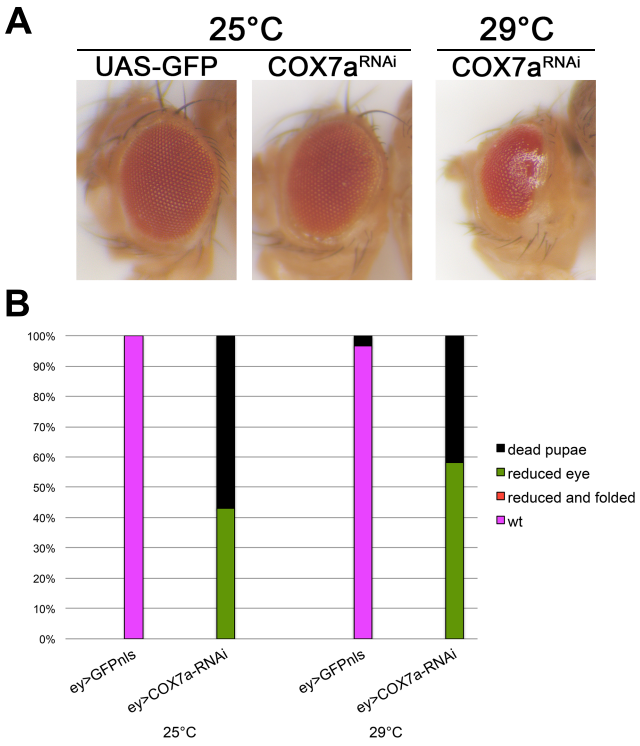

Figure 3: COX7a knockdown in the eye
A) Representative images of eye phenotypes caused by COX7a knockdown at indicated temperature. At higher temperature (higher Gal4 activity), size reduction and differentiation defects are qualitatively increased. **B)** Quantification of eye phenotypes suggests no significant difference in penetrance or lethality (n=180; 95; 122; 74).

To understand the nature of this phenotype, I analysed the effect of COX7a knockdown without Delta over-expression. In this setup (ey>COX7a^{RNAi}), I found adult eye size to be slightly reduced compared to the wildtype-looking control (ey>GFP), with visible differentiation defects at the posterior equator (Figure 3A,B). In addition, half of the offspring died either as pupae or as pharate adults that were unable to eclose (Figure 3D). To enhance COX7a knockdown, I raised offspring at 29°C (instead of 25°C before), which enhances activity of the yeast Gal4 protein. Under these conditions, I observed much stronger reductions in eye size in surviving adults (Figure 3C), while the proportion of dead pupae or pharates remained at a similar level (Figure 3D). I found similarly increased small-eye phenotypes when I enhanced knockdown efficiency by increasing the number of RNAi transgenes or through co-expression of Dicer2, a cellular protein required to process long double-stranded RNA molecules into functional 21-mers (data not shown). Together, these results argue that loss of COX7a function reduces eye size in a dose-dependent manner.

COX7a knockdown induces apoptosis and affects proliferation

Reduced eye size could be caused by decreased cell proliferation, by increased cell death or by other developmental defects. I performed immunofluorescent labelling (IF) with an antibody against cleaved Caspase 3, an indicator of apoptotic cell death. COX7a knockdown induced apoptosis in a few progenitor cells anterior to the morphogenetic furrow (MF), primarily in cells of the so-called first mitotic wave and in some cells in or posterior to the MF (Figure 4A,B; see also Introduction Figure I2). Under enhanced knockdown conditions, apoptosis was induced at an earlier developmental time point and more widely in the progenitor compartment (Figure 4C). In addition to cells of the FMW, apoptotic cells were observed more anteriorly, at the boundary between eye progenitors and (wildtype) antenna or cuticle progenitors (Figure 4C), arguing that their elimination might be induced by a cell competition mechanism (Lolo et al., 2012). Expression of p35, a baculoviral protein that inhibits apoptosis (Hay et al., 1994), failed to rescue the small-eye phenotype under standard conditions (Figure 4D,E), arguing that apoptosis is not primarily responsible for the development of this phenotype. The pattern of apoptotic cells further implied that apoptosis induction is triggered in progenitor cells at the time they are recruited into the FMW, so could be a consequence of a failure of cell cycle progression.

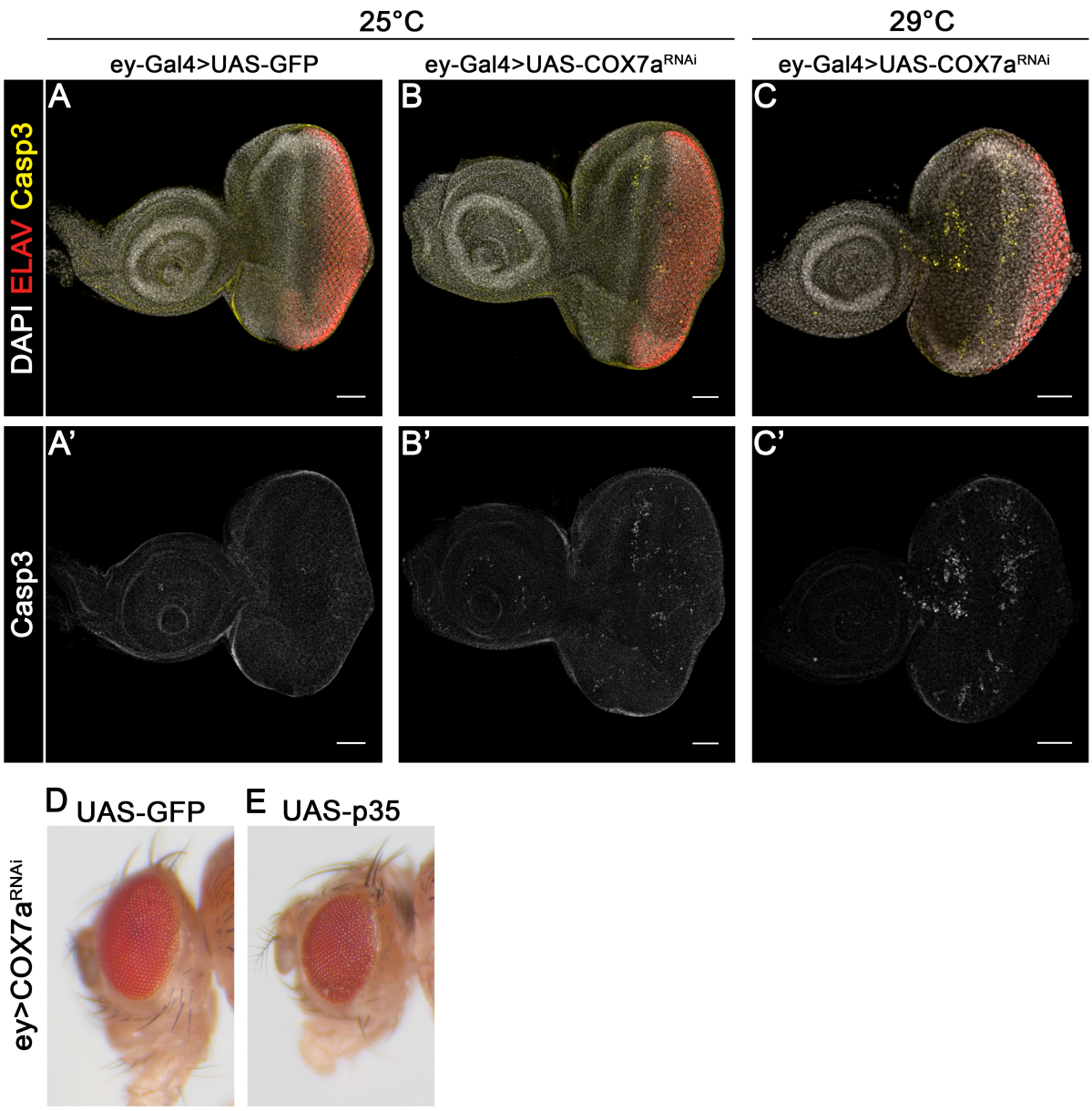

Figure 4: Apoptosis in COX7a knockdown eye discs

A-C) Microscopic images of eye discs with IF labelling of ELAV (red) to mark differentiating photoreceptors and cleaved Caspase-3 (yellow in upper panel; white in lower A'-C'). Apoptosis is induced at low levels in progenitors of the FMW (B, B'), but more strongly throughout the progenitor compartment at higher temperature (C, C'). **D-E)** Genetic rescue of apoptosis by expression of p35 (E) failed to rescue eye size reduction or differentiation defects induced by COX7a knockdown (D). Scale bar 50µm in microscopic images.

IF labelling of phosphorylated histone 3 (PH3) marks cells in mitosis and was used to assess proliferation. Wildtype discs display a typical pattern of PH3-positive cells, with dispersed labelling in progenitors, and two stripes of coordinated cell division, the first and second mitotic wave, separated by the MF (see Introduction Figure I2). Knockdown of COX7a had no major effect on the overall pattern of PH3-positive cells (Figure 5A, B),

though the SMW often appeared slightly disrupted and some aberrant cell divisions were detected in the MF or far posterior to the SMW. Increased COX7a knockdown further disrupted the SMW and appeared to increase proliferation in progenitors (Figure 5C), potentially in response to the increased cell death observed (see Figure 4C). Under these conditions, the size of the eye field was also clearly reduced relative to the size of the antenna in a few individuals, while overall there was no significant change (Figure 5D).

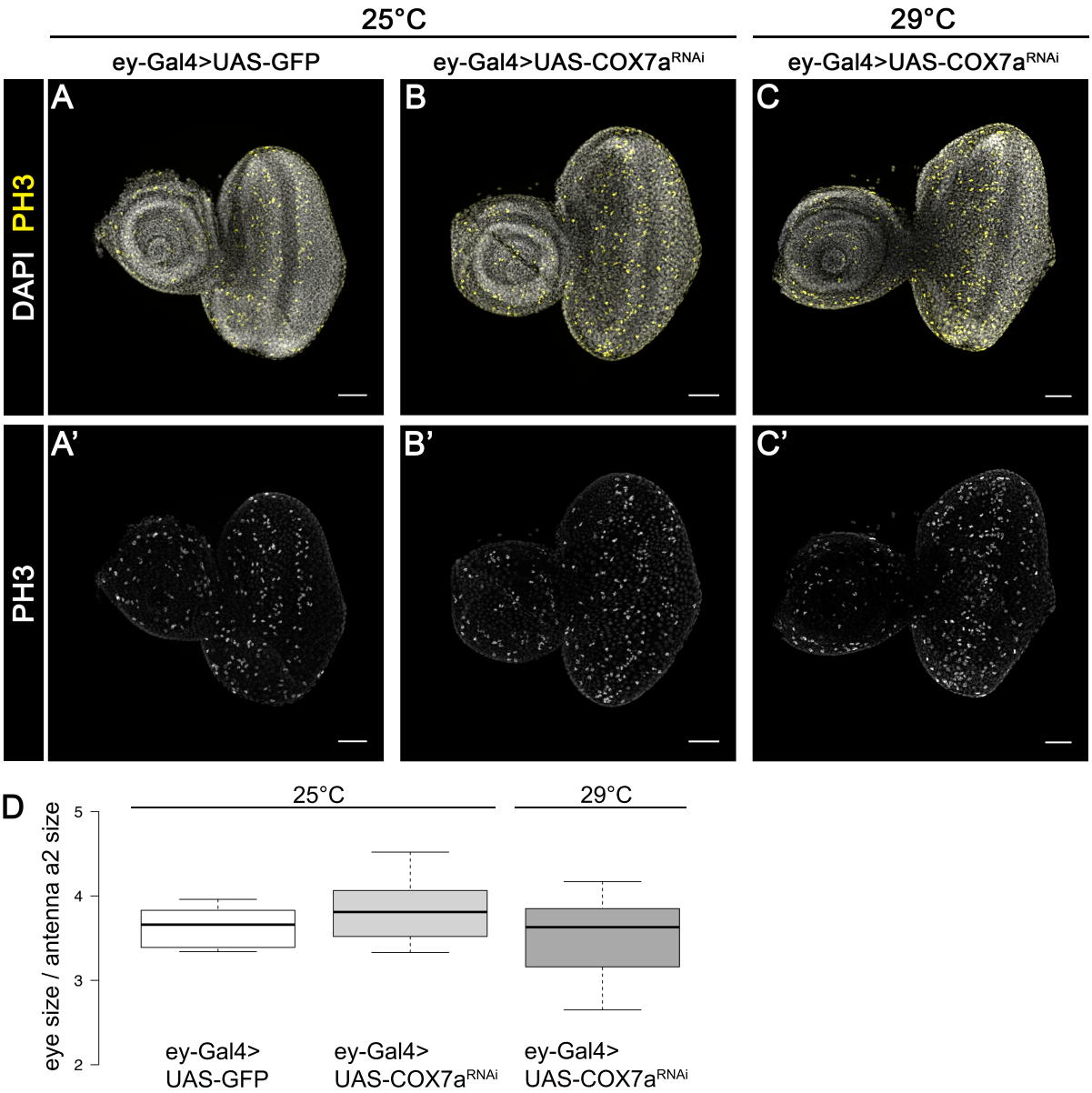

Figure 5: Proliferation in COX7a knockdown eye discs

A-C) Microscopic images of eye discs with IF labelling of phosphorylated Histone-3 (yellow in upper panel; white in lower A'-C'). Proliferation patterns are not visibly disturbed by COX7a knockdown in the progenitor compartment. The band of proliferation behind the MF, the SMW, appears broader, with ectopic divisions in the differentiation zone. **D)** Quantification of eye size relative to antenna segment a2. While individual discs with clear eye size reduction are detected at 29°C, there is no overall significant difference (n=6; 7; 7). Scale bar 50µm in microscopic images.

Finally, it is noteworthy that strong depletion of COX7a induced apoptosis in a way qualitatively and quantitatively distinct from the effects observed upon mild knockdown of COX7a, suggesting that upon enhanced knockdown secondary (non cell-autonomous) effects could mask primary (cell-autonomous) effects. Therefore, I carried out most analyses shown later at 25°C, under mild knockdown conditions.

COX7a knockdown causes differentiation defects

The adult eye phenotypes of COX7a knockdown show defects in the organisation of the hexagonal lattice, as well as instances of small ommatidia (see Figure 3B). Enhanced knockdown of COX7a enhanced the defects, in severe cases to the point where no structured array of ommatidia was visible anymore (see Figure 3C). As before, these phenotypes could be established for a variety of reasons, including failures in the recruitment of cells to the forming ommatidia or direct differentiation defects. The hexagonal lattice gives the eye its orderly appearance and is made by the interommatidial cells that are recruited in a stepwise fashion after the photoreceptor clusters have formed (Kumar, 2011). Disruptions of the precise pattern of the lattice (called rough eye phenotype), as observed upon COX7a knockdown, are generally caused by any alteration to the number of cells within each ommatidium (photoreceptors) or between ommatidia (pigment cells or interommatidial bristles). The results presented above suggested that proliferation in the SMW is impaired to some degree (see Figure 5B,C). The main requirement for the cell divisions in the SMW is to create a sufficiently large pool of progenitor cells to ensure proper recruitment of cells to the forming ommatidia. The adult eye morphology together with the IF results of the developing disc therefore suggest that the recruitment of photoreceptors to the ommatidia or the formation of the interommatidial lattice is impaired in several locations, primarily in the posterior part of the eye. This interpretation is further supported by high magnification imaging of photoreceptor clusters marked by the pan-neuronal marker ELAV. As shown in Figure 6, the regular arrangement of photoreceptor clusters is disrupted under mild knockdown conditions and even more so under enhanced COX7a knockdown (Figure 6A-D). The appearance of areas devoid of photoreceptors coincides with late mitotic events (see above and Figure 5) that appear to disrupt the arrangement of the apically located ommatidial clusters. In addition, the coordinated progression of differentiation is clearly defective, as clusters with aberrant photoreceptor numbers are detected (see red arrows in Figure 6B,D).

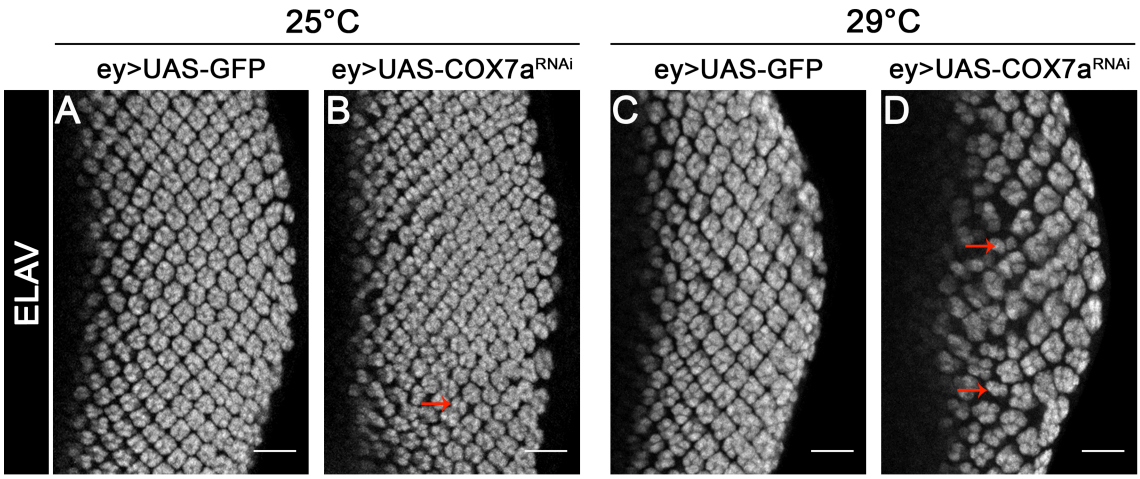

Figure 6: Differentiation defects upon COX7a knockdown

A-D) Microscopic images of eye discs with IF labelling of ELAV (white) to mark differentiating photoreceptors. COX7a knockdown (B,D) discs show formation of photoreceptor clusters with aberrant cell numbers (red arrows in B and D). Differentiation defects are more severe at 29°C. Scale bar 50µm in microscopic images.

In summary, disorganisation of the adult eye upon COX7a knockdown is caused by successive defects in the recruitment of progenitor cells to the ommatidia. It appears likely that these defects are a consequence of a proliferation defect posterior to the morphogenetic furrow, in the second mitotic wave. The decrease in adult eye size could not be attributed to a specific trait in the larval eye disc. Given that overall eye size is primarily controlled by proliferation of progenitors anterior to the MF, a possible scenario is that excessive progenitor cell death can neither be compensated for by increased proliferation nor be rescued by p35 expression.

Chapter Three: A genetic characterisation of COX7a knockdown phenotypes

Previous work on another small Complex 4 subunit, COX5a, suggested that *COX5a* mutant clones in the eye disc fail to induce expression of *Cyclin E* (*CycE*) and in consequence fail to enter S-Phase (Mandal et al., 2005). The molecular mechanism apparently involves activation of AMPK and p53 upstream of *CycE* (Owusu-Ansah et al., 2008). For technical reasons, I could not reproduce the CycE IF in COX7a knockdown discs. But genetically, over-expression of CycE, which alone has no effect on eye development, substantially rescued the reduced eye size caused by COX7a knockdown even under enhanced knockdown conditions (Figure 7A,B,D). Apoptosis was reduced in these rescued discs (Figure 7E,F), further substantiating the idea that apoptosis was induced as a consequence of a failure of cells to proliferate.

In another study, COX7a knockdown phenotypes in whole larvae or adults could be partially rescued by expression of Alternative oxidase (AOX) from *Ciona intestinalis* (Kemppainen et al., 2013). In situations of Complex 3 or 4 deficiencies, AOX can accept electrons from ubiquinol, reduce molecular oxygen and thereby maintain a principally functional ETC. The drawback of the enzyme is the diminished rate of proton pumping across the inner mitochondrial membrane and hence a reduced ability of mitochondria to produce ATP at Complex 5. Expression of AOX rescued most of the reduced eye phenotypes induced by COX7a knockdown (Figure 7A,C,D) and almost completely abolished the induction of apoptosis (Figure 7E,G).

Overall, expression of CycE and AOX rescued most aspects of COX7a knockdown-induced phenotypes in a similar fashion. Though inconclusive without further epistasis experiments and molecular understanding of the cascade, these data fit well to the model proposed by (Mandal et al., 2005). In this scenario, COX7a knockdown will attenuate ETC function, leading to decreased ATP production in the mitochondria. AOX expression maintains ETC function and ATP synthesis to a degree that prevents AMPK activation and the G1 checkpoint that prevents *CycE* expression and thereby cell cycle progression.

To further unravel potentially contributing pathways or processes, I continued to genetically screen for constructs able to rescue COX7a knockdown phenotypes. Consistent with the interpretation of Owusu-Ansah and colleagues (Owusu-Ansah et al.,

2008), scavenging of reactive oxygen species (ROS) through expression of Catalase or SOD2 had no effect on COX7a knockdown phenotypes. The converse experiment, knockdown of SOD2 had no effect either. More candidates have been evaluated at later stages of the project, but failed to indicate additional contributions to the development of COX7a knockdown phenotypes.

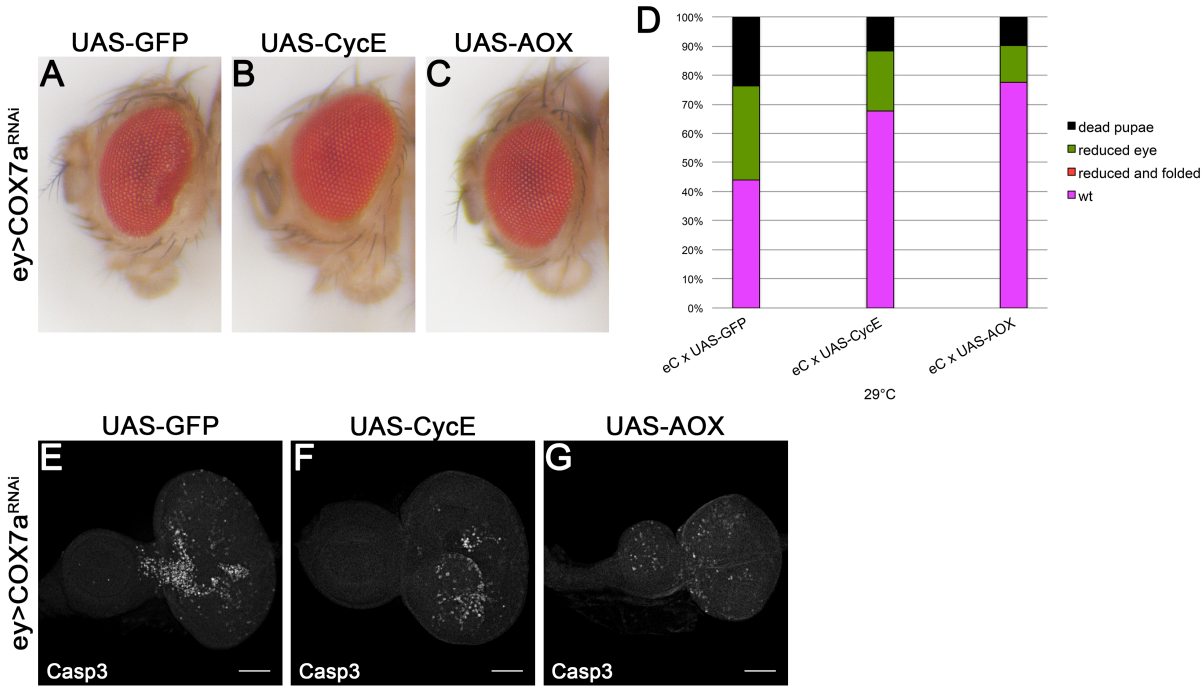

Figure 7: CycE and AOX partially rescue COX7a knockdown phenotypes

A-C) Expression of CycE or AOX in the ey>COX7a^{RNAi} background qualitatively rescues size reduction and differentiation defects of COX7a knockdown. **D)** Quantification of phenotypes in the same genotypes (as A-C) shows reduced incidences of lethality and size reduction (n=34; 34; 31). **E-G)** IF labelling against apoptosis marker cleaved Caspase-3 indicates reduction of strong progenitor apoptosis upon expression of CycE or AOX. Scale bar 50µm in microscopic images.

In the following chapters I will focus on the over-proliferation phenotype I initially found through the RNAi screen, as we considered the genetic interaction with the Notch signalling pathway to be the most intriguing aspect of COX7a loss of function.

Chapter Four: COX7a knockdown phenotypes and over-proliferation with Notch signalling follow different genetic requirements

I have described the phenotypes associated with COX7a knockdown in the *Drosophila* eye-imaginal disc in the previous chapters and clarified part of the genetic cascade responsible for the development of the cellular phenotypes. In this chapter, I have repeated most of the experiments, mentioned before in the context of COX7a knockdown, together with activated Notch signalling through over-expression of its ligand Delta. For simplicity I will refer to the combination of Delta over-expression and COX7a knockdown as "Delta,COX7a background or phenotypes", Delta over-expression alone as "Delta phenotype/background" and COX7a knockdown alone as "COX7a phenotype/background".

Delta, COX7a induces similar cellular phenotypes as COX7a or Delta alone

Over-expression of the Notch ligand Delta in eye progenitors increases eye size along the dorso-ventral axis (Dominguez and de Celis, 1998) via increased proliferation of the ventral compartment. The RNAi screen had shown that COX7a knockdown strongly increased proliferation in the Delta background and adult eye morphology suggested this effect to originate in the ventral compartment as well (see Figure 2). IF labelling of phospho-Histone 3 indeed showed a high density of PH3-positive cells in the ventral domain, both in Delta and Delta, COX7a late L3 eye discs (Figure 8A,B). At this late stage of development, when activity of the ey-Gal4 driver has already deceased, the increased size of the discs is clearly apparent (Figure 8B). IF labelling for Casp-3 showed apoptotic cells in the ventral tip of Delta discs (Figure 8C). Delta, COX7a discs showed apoptotic cells in a pattern that combined the individual patterns of Delta and COX7a (Figure 8D) and appeared to be roughly additive in quantitative terms as well (Figure 8E).

Delta over-expression induces a slight rough eye phenotype in the ventral domain with an irregular arrangement of the ommatidia. Delta, COX7a eyes appear similar to either Delta or COX7a phenotypes alone, without apparent differences at this level of analysis. Together, the genetic interaction between Notch activation and COX7a

knockdown primarily affects proliferation within the ventral part of the eye disc and induces cell death in the same progenitor domain.

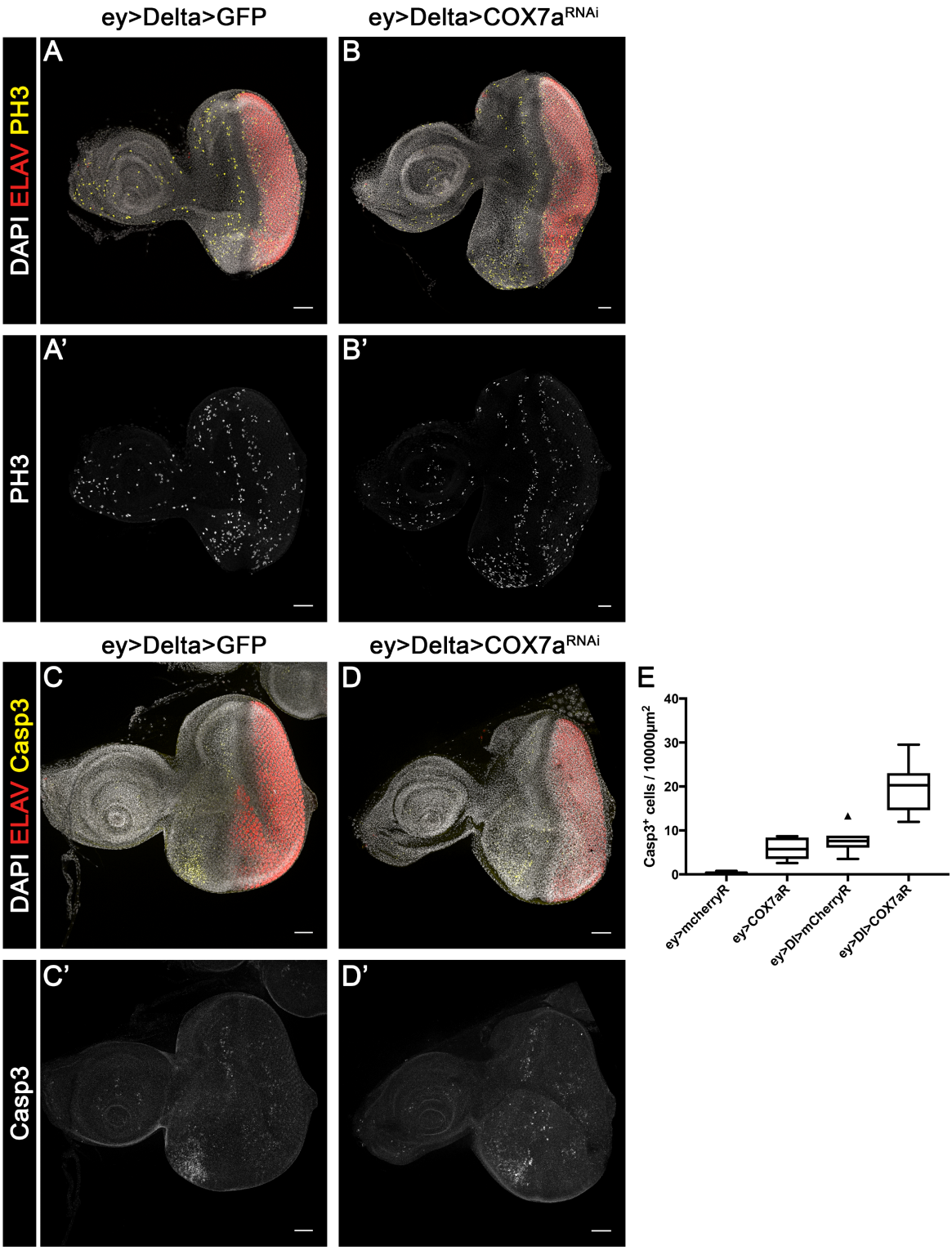

Figure 8: Proliferation and apoptosis in Delta, COX7a eye discs

A-B) IF labelling against ELAV and PH3 shows that both Delta and Delta,COX7a discs over-proliferate in the ventral compartment. **C-D)** Casp3 IF labelling indicates increased apoptosis in the ventral tip, where cells are over-proliferating. **E)** Quantification of apoptotic cells normalised to area (n=6 to 8).

Delta, COX7a phenotypes are driven by different genetic determinants than COX7a phenotypes

The results shown in Figure 7 strongly suggest that COX7a phenotypes are caused by a defect of cell cycle progression through decreased CycE expression. Apparently, the failure to enter S-Phase triggers apoptosis of progenitors anterior to the MF, which in turn seems to enhance proliferation of neighbouring cells. In order to investigate whether CycE and AOX expression would also rescue Delta, COX7a induced over-proliferation, I expressed them in this background. As the quantification of phenotypes shows (Figure 9A), neither of them substantially altered the distribution or severity of phenotypes recovered. In a similar way, inhibition of apoptosis with p35 expression did not rescue over-proliferation (Figure 9A), but slightly increased pupal lethality and caused overall more severe over-growths and even "metastases" in rare cases (Figure 9A, B).

These results clearly show that, while COX7a knockdown-induced cellular phenotypes are still present to some degree in the Delta, COX7a background (see Figure 8 for apoptosis), the molecular circuitry causing the small eye phenotype is not responsible for the genetic interaction with the Notch pathway. Ultimately, this suggests that the small eye phenotype of COX7a knockdown and the folded eye phenotype of Delta, COX7a are separable phenotypes, very likely acting through independent, parallel genetic pathways.

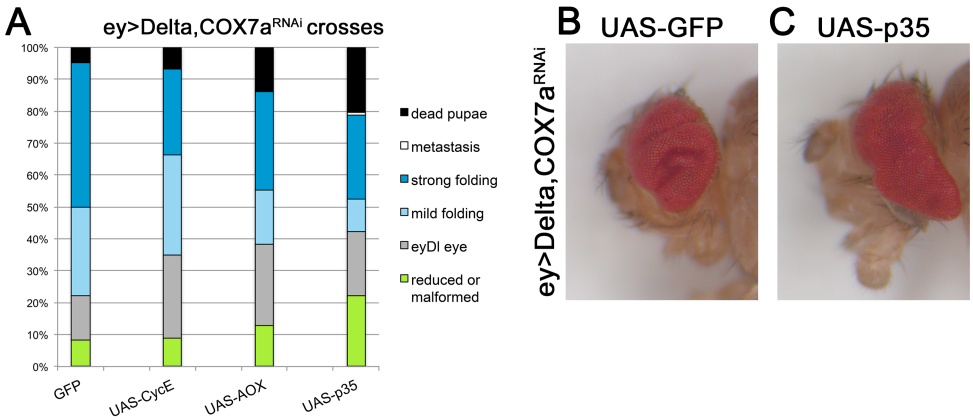

Figure 9: CycE, AOX or p35 do not inhibit Delta,COX7a over-proliferation

A) Quantification of phenotypes in the Delta,COX7a background. Neither expression of CycE, nor AOX, nor p35 substantially inhibits over-proliferation (n=108; 89; 94; 99). **B-C)** Representative images of adult eye phenotypes show qualitatively more severe malformations and outgrowth when apoptosis is inhibited by p35 expression in Delta,COX7a background. Part of the data in A) is also included in *Sorge et al, submitted*.

Chapter Five: Transcriptomic analysis reveals a nuclear response to COX7a knockdown

The results of the previous chapters implied an additional response to COX7a knockdown or a direct enhancement of the Notch signalling pathway output. Work from my student C. Altbürger had previously failed to indicate a difference in the output of Notch signalling as evidenced for by a transcriptional reporter (Altbürger, 2014). To unambiguously discriminate between these two and potential other possibilities, we decided to perform a transcriptomic analysis of the developing eye-antenna disc. My previous work had suggested that over-proliferation occurs already during earlier stages of larval development than the late L3 stage shown in previous experiments. Therefore, I decided to use early L3 larvae (96h AEL) at the onset of differentiation at the posterior equator of the eye disc. At this stage, there is relatively homogenous GFP labelling of all eye progenitors in ey>GFP discs, as well as fading GFP signal in the ventral part of the antenna, where the Gal4 driver was active earlier in development (Figure 10A). A second advantage of using this developmental stage, besides a high proportion of cells being affected by COX7a knockdown and/or Delta over-expression, is that only a minor fraction of cells of each disc are undergoing differentiation and thereby potential secondary affects from these cells (or their defects) are minimized. The significant drawbacks were the difficulty to dissect these small discs and the limited amount of material that could be obtained from them. At the time I carried out this experiment, the only established protocol for transcriptomic analysis from 50ng total RNA per sample, which was the maximum I could achieve, was Microarray analysis using Affymetrix Drosophila Genome 2.0 chips. I used one control genotype (eG: ey-Gal4/UAS-GFP) and four experimental genotypes (eD: ey-Gal4,UAS-Delta/UAS-GFP. eDC: ey-Gal4,UAS-Delta/UAS-COX7a-RNAi. eC: ey-Gal4/UAS-COX7a-RNAi and eN: ey-Gal4/UAS-Notch^{intra2}) in biological duplicates.

Distinct transcriptional responses

Analysis of the Microarray was carried out with Affymetrix software using the RMA algorithm for probe intensity interpretation and normalisation. Unless otherwise noted, fold changes and corresponding p-values were calculated against the control eG background. Overall, there was very high correlation between replicates (average

Pearson correlation of biological replicates 0.99746±0.0003), but also between the different genetic backgrounds (Figure 10B). The most unique transcriptional profile was seen for the over-expression of the intracellular domain of Notch (eN), correlating well with the most divergent disc morphology of this genotype at the time of preparation. The high correlation between genotypes (especially between eG, eC, eD and eDC) was also reflected in a relatively small number of genes showing significantly different expression (see Table 2, Appendix for summary).

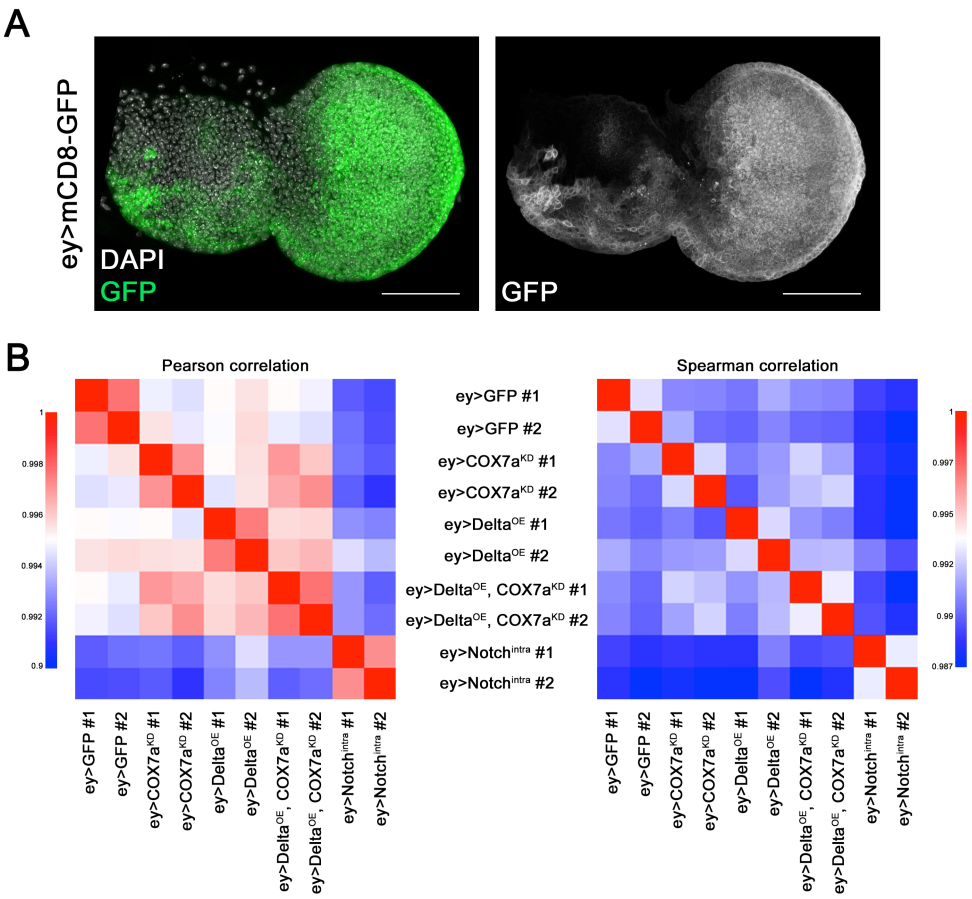

Figure 10: Early L3 eye-antenna disc transcriptomic analysis

A) Representative microscopic image of early L3 eye-antennal disc as was used for the transcriptomic analysis. Ey-Gal4 driven mCD8-GFP expression indicates driver activity throughout eye progenitor compartment and more weakly in antenna progenitors. **B)** Global representation of Microarray analysis of all ten samples, showing Pearson (left) and Spearman (right) correlation. Correlation is high between replicates, but also between most genotypes. Scale bar is 50µm in microscopic images.

Figure 11A shows the overlap of genes being differentially up-regulated in the four experimental genotypes using a relatively conventional cut-off of $p<0.05$ and fold-change>1.5. The biggest overlap was observed between eC and eDC (with 57% or 49% of genes shared, respectively) as well as between eD and eN (with 44% or 25% of genes shared, respectively). Applying the same threshold for genes down-regulated compared

to control ($p<0.05$ and fold-change>-1.5) yielded different results in terms of numbers and overlapping fractions (Figure 11B). The number of down-regulated genes was smaller than the number of up-regulated genes in all backgrounds but eN, where down-regulation was much more prominent. Further, down-regulated genes showed overall less overlap between the four genotypes (22% of down-regulated genes were found in at least two conditions compared to 35% of up-regulated genes), but the overlap appeared to be more general (58% of genes down-regulated in at least two conditions were also down-regulated in a third or all four genotypes, compared to 28% for up-regulated genes).

In conclusion, the transcriptome profiling revealed specific alterations of the transcriptome upon COX7a knockdown or activation of the Notch pathway that will be described in the following chapters.

COX7a knockdown transcriptional signature

To gain a broad overview of the transcriptional response, I performed GO term over-representation using DAVID (Huang et al., 2009). To perform the analysis with a larger set of genes, I used a lower stringency cut-off for this analysis (fold-change of ±1.5 and $p<0,1$). Table 3 (Appendix) summarises the results. The highest-ranking term amongst up-regulated genes in the Delta background was indeed "Notch signalling", confirming the general usability of the approach. In line with the interpretation mentioned above, down-regulation was less prominent and did not yield a single term for Delta over-expression (fold enrichment>2, $p<0.01$) and the single term "extracellular space" for COX7a knockdown. The highest-ranking term amongst genes up-regulated in the COX7a background was the KEGG (Kyoto Encyclopedia of Genes and Genomes) pathway "Glycolysis/Gluconeogenesis".

Analysis of individual genes confirmed the global trend, as the most highly induced transcript upon COX7a knockdown I found was *Impl3*, encoding the glycolytic enzyme lactate dehydrogenase (LDH). Other enzymes of glycolysis were induced to a lesser degree than LDH (Figure 11C). Though not detected by GO term enrichment, other genes with implications in cellular metabolism were also found up-regulated, including a transmembrane transporter for the disaccharide Trehalose (*Tret1-1*) and amino acid transmembrane transporter genes (*path, mnd, JhI-21*) (Figure 11D). Other noteworthy target genes were molecular chaperones predicted to localise to mitochondria (*Hsc70-2,*

Hsp22, *Hsc70-5*, *Hsc20*), a response classically referred to as the mitochondrial Unfolded Protein Response (UPR^{mt}) (Figure 11E).

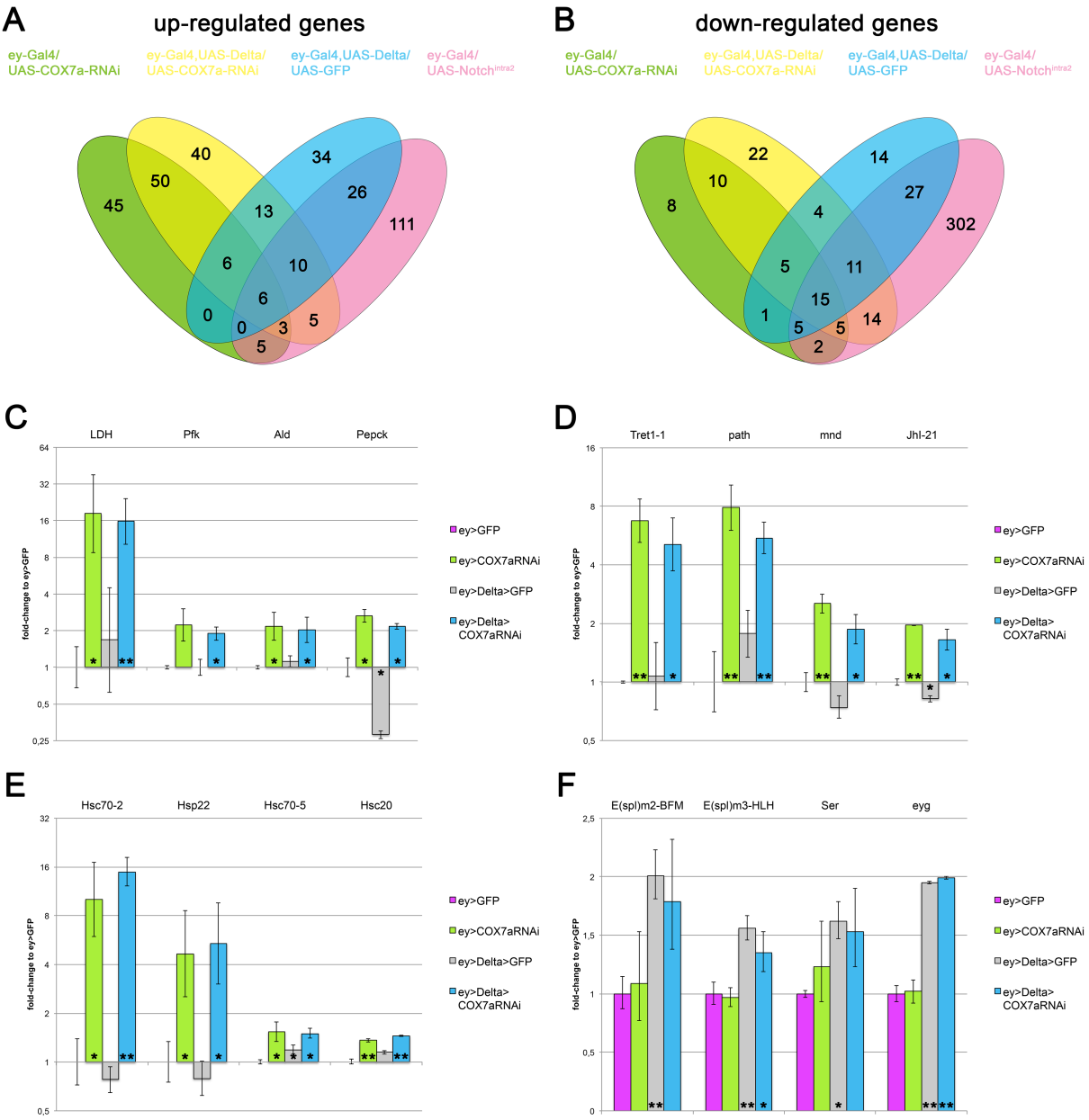

Figure 11: Global and genotypic-specific transcriptional responses

A-B) Overlap of up- (A) or down- (B) regulated genes in the four experimental genotypes relative to ey>GFP control. p<0.05 and fold-change>±1.5. **C-F)** Transcript levels of individual genes belonging to different groups: Glycolytic enzymes (C), nutrient transporter (D), mitochondrial chaperones (E) and Notch target genes (F). At this level of analysis, there is no indication for a direct transcriptional interaction between COX7a knockdown and Delta over-expression. Fold-change relative to ey>GFP shown. Y-axis shown with log2 scaling. Error bars denote SD. Asterisks indicate significance according to One-way ANOVA between multiple subjects (* p<0.05; ** p<0.01). Part of the data in C-F) is also included in *Sorge et al, submitted*.

To confirm the transcriptional response, I used an LDH-GFP enhancer trap insertion that reports transcriptional activity of the LDH locus (Wang et al., 2016). While GFP is hardly detectable in a control or Delta background, COX7a knockdown strongly induces GFP expression (Figure 12A-D). Furthermore, IF labelling against Tret1-1 in the LDH-GFP background confirmed induction of the protein in the same cells that up-regulate the GFP reporter (Figure 12E,F), suggesting a cell-autonomous response, potentially through the same transcriptional activator.

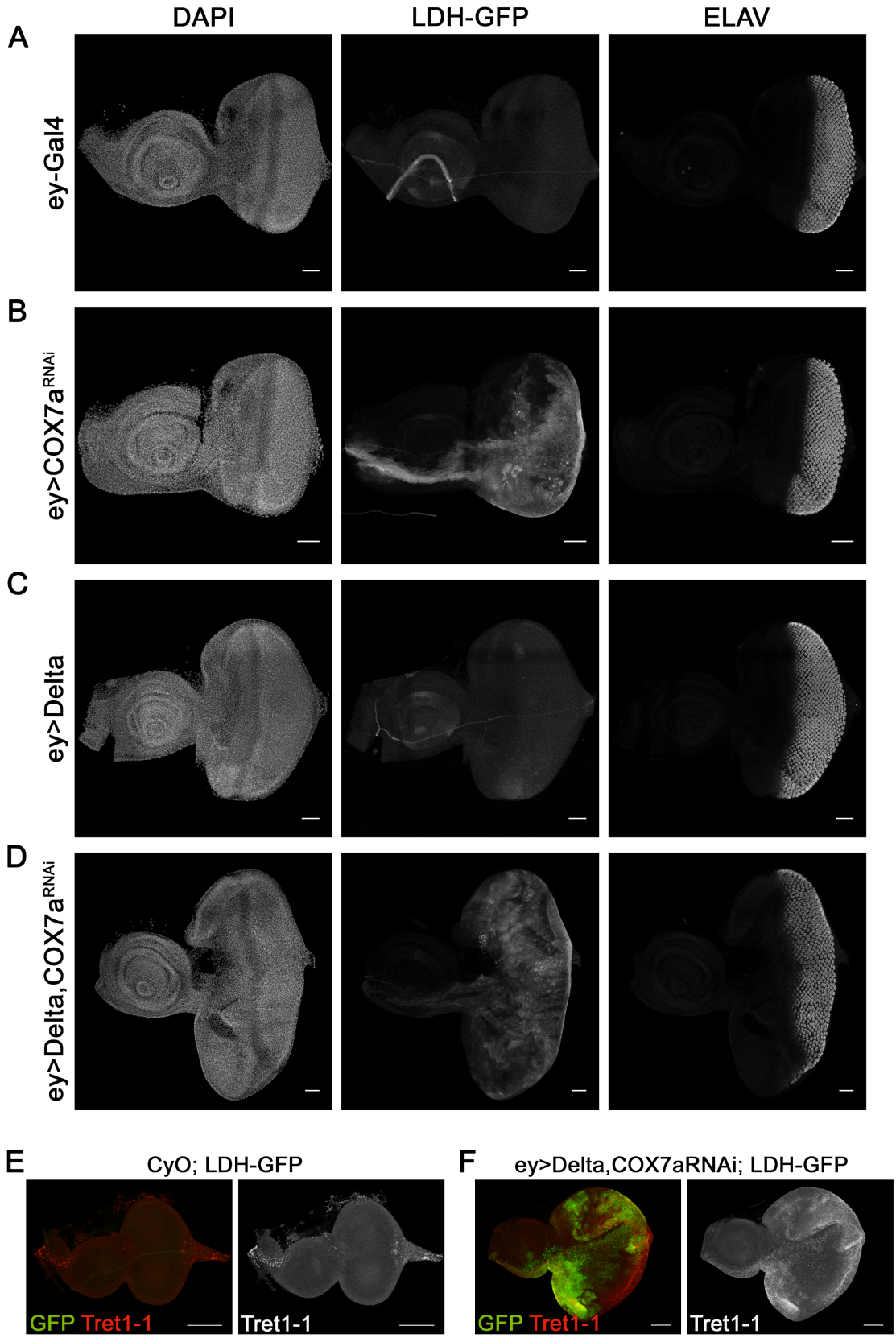

Figure 12: Confirmation of COX7a target genes

A-D) A LDH-GFP reporter (Wang et al., 2016) crossed into the respective backgrounds confirms LDH induction upon COX7a knockdown (C and D). **E-F)** IF labelling of Tret1-1 shows induction of the protein in LDH-GFP^{+} cells, indicative of a cell-autonomous effect. Scale bar is 50µm in microscopic images.

No transcriptional cooperation

Possibilities to explain the genetic interaction between the Notch signalling pathway and COX7a knockdown are a) a direct modulation of the Notch output by loss of COX7a or b) transcriptional cooperation or synergism between Notch/Su(H) and a yet unknown transcription factor mediating the response to loss of COX7a. If a) was true, one would expect to see an increase in the transcriptional output of the Notch target genes. As shown in Figure 11F, general Notch target genes of the *Enhancer of split* (*E(spl)*) complex (Jennings et al., 1994) or the eye-specific Notch target *eyegone* (Dominguez et al., 2003) were induced to the same or lower degree in Delta, COX7a discs compared to Delta alone. This result is in agreement with results obtained using a Notch reporter (Altbürger, 2014) and strongly suggests that the transcriptional output of the Notch pathway is not enhanced by COX7a knockdown. If b) was true, one would expect to see cooperative effects on the individual target genes or the induction of unique targets. As presented before, neither COX7a knockdown targets (Figure 11C-E) nor Notch targets (Figure 11F) are induced more strongly in Delta, COX7a discs. The overlap of induced genes (see Figure 11A) suggested 45 unique genes in Delta, COX7a discs (not found in Delta or COX7a alone). Closer examination of these genes revealed that only a small fraction (7/45) were indeed significantly ($p<0.05$ fold>1.5) induced in Delta,COX7a discs over both individual conditions. Later experiments showed that all genes tested by RNAi (4 out of 7 tested, see Chapter Eight) did not contribute to Delta,COX7a over-proliferation. Based on the very small number of unique targets and their apparent lack of involvement in the development of the phenotype, I concluded that transcriptional cooperation between the Notch pathway and COX7a cannot explain the genetic interaction.

In summary, the transcriptomic profiling showed distinct responses upon Delta over-expression and COX7a knockdown and no evidence for relevant crosstalk between the two genetic manipulations. The result therefore argued that the pro-proliferative effect of COX7a knockdown would be caused by a interaction between the modulated cellular functions downstream of the COX7a adaptation and the Notch pathway.

Chapter Six: ATF4 mediates the transcriptional response to COX7a knockdown

The transcriptomic adaptation upon COX7a knockdown showed up-regulation of a high number of genes with roles in cellular metabolism. Intrigued by the idea that attenuation of ETC function triggered an adaptive transcriptional response to restore or maintain cellular (metabolic) functions, I followed three different approaches to identify (the) factor(s) mediating the transcriptional response: Literature comparison of target gene sets, motif analysis in regulatory sequences of target genes and RNAi screening of candidate factors for rescuing ability.

Target gene and motif analysis suggest ATF4 as a potential regulator

As shown in Figure 11D, COX7a knockdown induces expression of several amino acid transporter genes. Through literature research, I found that their mammalian homologues (based on Flybase annotation: JhI-21 = SLC7A5; mnd = SLC7A7; path = SLC36A1/2/3; CG5535 = SLC7A1/3) were described as target genes of an amino acid response pathway mediated by activating transcription factor 4 (ATF4) together with a CCAAT-enhancer binding protein (C/EBP) (Kilberg et al., 2009). In a similar manner, ATF4 was described to regulate LDH and the same glycolytic enzymes I found in my transcriptome analysis in *Drosophila* S2R+ cells upon chemical induction of ER stress (Lee et al., 2015b). To confirm a potential involvement of ATF4 as a transcriptional regulator in the response to COX7a knockdown, I performed motif analysis in regulatory sequences of COX7a target genes with iRegulon (Janky et al., 2014). The highest-ranking motif found was human ATF4 (detected at 22/114 genes), followed by mouse Atf4 as third (15/114) and *Drosophila* ATF4 with Irbp18 (16/114) (see Figure 13A). Putative target genes with predicted ATF4 binding sites include, as expected from the previously mentioned experiments, *LDH, Ald, Tret1-1, path, JhI-21* and *mnd*, suggesting that these genes could be under direct transcriptional control by ATF4.

ATF4 is required for Delta, COX7a-induced over-proliferation

Over-expression of Delta in combination with COX7a knockdown induces over-proliferation of the larval eye-imaginal disc, leading to large, folded adult eyes (see Figure 2D). In the previous section I have shown that a comparison of target genes as well as *in silico* prediction suggested a transcription factor called ATF4 (cryptocephal in *Drosophila*) to mediate at least part of the transcriptional adaptation to COX7a knockdown. If this adaptation is mediated by ATF4 and if it is linked to the over-proliferation phenotype, loss of ATF4 should inhibit the genetic interaction with the Notch pathway and thereby over-proliferation.

Indeed, I found over-proliferation to completely depend on ATF4 function, as ATF4 knockdown by RNAi in the Delta, COX7a background rescued over-proliferation under all conditions tested (Figure 13B, C). Delta, COX7a, ATF4 discs and adult eyes largely resembled the Delta phenotype, arguing that loss of ATF4 function specifically impaired the effects induced by COX7a knockdown, while activation of the Notch pathway through Delta over-expression was independent of ATF4.

ATF4 becomes translated upon COX7a knockdown

ATF4 was first noticed as one of few proteins whose translation increases under conditions that generally attenuate global translation rates. The reason for this phenomenon are micro open-reading frames (μORFs) that prevent assembly of the ribosome at the ATF4 start codon. In *Drosophila*, both/all *ATF4* mRNA isoforms contain μORFs upstream of the proteins start codon, similar to the situation described for mammalian ATF4. As predicted from the mRNA structure and reports in other *Drosophila* tissues (Kang et al., 2017), ATF4 protein is undetectable in wild-type eye-imaginal discs by IF staining (Figure 13D). As expected from the previous results, COX7a knockdown induces ATF4 protein in the progenitor compartment (Figure 13D), exclusively until mid-L3 stages but not later. According to the transcriptomic analyses, *ATF4* mRNA is highly expressed in wildtype eye-imaginal discs and its levels remain unchanged under all conditions, strongly suggesting that the induction of ATF4 protein occurs via the described translational mechanism.

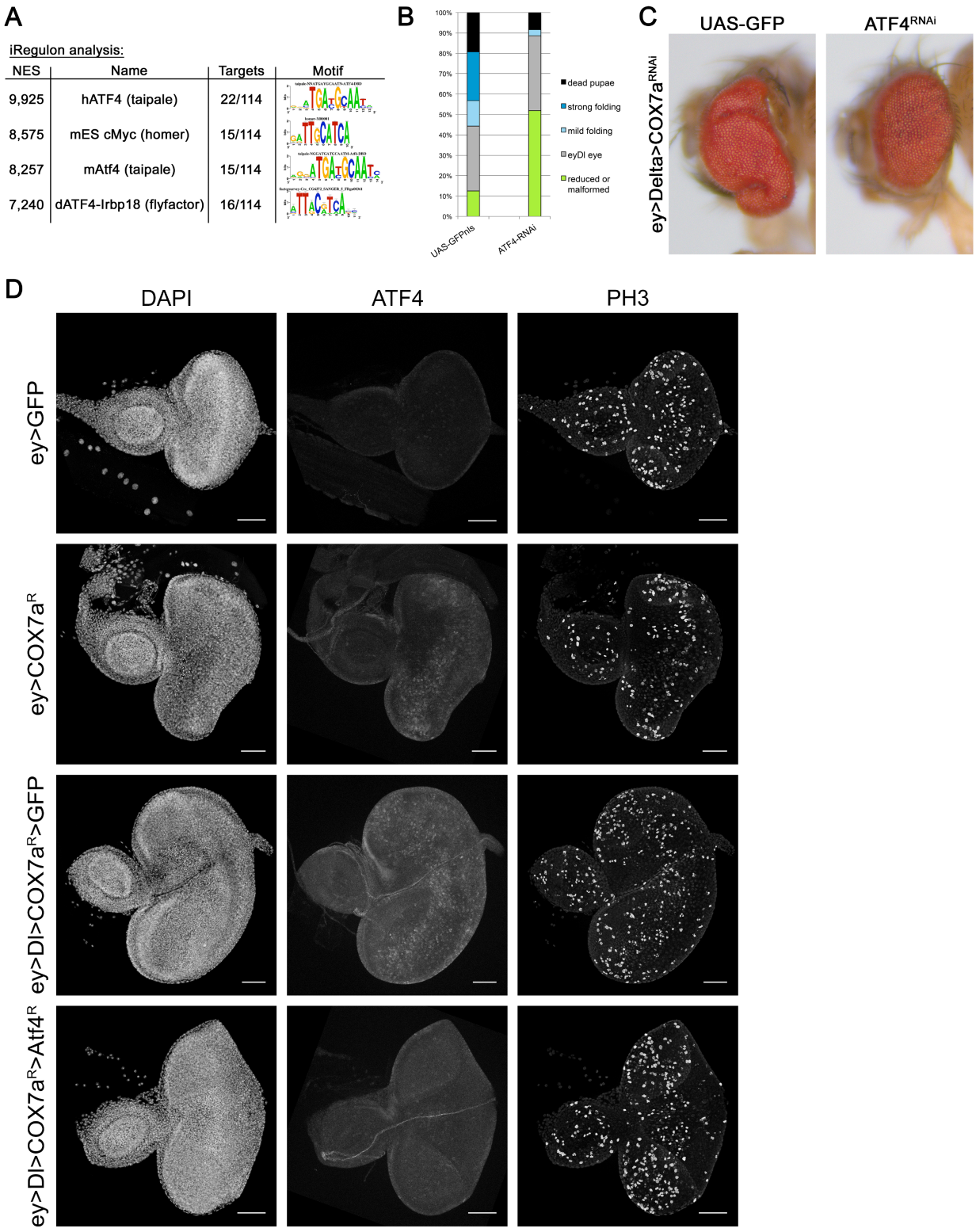

Figure 13: ATF4 activation upon COX7a knockdown

A) iRegulon motif prediction suggests ATF4 to regulate many of the target genes induced by COX7a knockdown. **B)** Quantification of adult eye phenotypes (n=67; 106). Knockdown of ATF4 in the Delta,COX7a background rescues over-proliferation. **C)** Representative images of adult eyes of crosses in B. **D)** Images of eye-imaginal discs showing IF labelling for ATF4 (middle column) and PH3 (right column). Knockdown of COX7a induces ATF4 (second and third row) in an *ATF4*-dependent manner (bottom row). Scale bar 50µm in microscopic images. Images in D are Z-projections (standard deviation mode). Part of the data in A-D) is also included in *Sorge et al, submitted*.

ATF4 is the main transcription factor downstream of COX7a knockdown

According to the results presented above, ATF4 was suggested to be the main factor contributing to over-proliferation in Delta, COX7a discs. To understand to which degree ATF4 regulates gene expression in response to COX7a knockdown, I performed a second transcriptomic analysis by Microarray. The genotypes included the ones of the first analysis (eG: ey-Gal4/UAS-GFP. eD: ey-Gal4,UAS-Delta/UAS-GFP. eDC: ey-Gal4,UAS-Delta/UAS-COX7a-RNAi. eC: ey-Gal4/UAS-COX7a-RNAi) as well as ATF4 knockdown in all backgrounds (eA: ey-Gal4/+; UAS-ATF4-RNAi/+. eCA: ey-Gal4/UAS-COX7a-RNAi; UAS-ATF4-RNAi/+. eDCA: ey-Gal4,UAS-Delta/UAS-COX7a-RNAi; UAS-ATF4-RNAi/+). A major difference to the first analysis was the use of a different food (with lower protein content) as will be explained below (see Chapter Eight).

Overall, this analysis worked similarly well as the first analysis. Pearson correlation between biological duplicates was almost the same as before (0.9968±0.0011). A comparison of both experiments together revealed a substantial difference between the two experiments (Figure 14A): in general, the similarity between different genotypes within the same experiment was greater than the similarity of the same genotypes between experiments. This surprising result suggests a common difference between the experiments that will be further analysed in Chapter Eight. The numbers of differentially regulated genes between genotypes was higher for most genotypes than in the previous analysis (see Table 4, Appendix).

Importantly, the second profiling largely confirmed the findings of the first analysis regarding the COX7a knockdown induced response. The vast majority of COX7a targets from the first analysis were also induced in the second analysis (86/115) using the same thresholds (Figure 14B). These targets included all previously mentioned genes except *Hsc70-5*, which was induced slightly weaker. Some of these targets were induced much more strongly (for example LDH, Tret1-1; compare Figure 11C and 14E). Surprisingly, the Delta response differed significantly from the previous result. Though the over-expression of Delta was stronger in the second array (4.9 fold versus 3.9 fold), only relatively few target genes were shared between the two experiments (Figure 14C). These targets included some of the canonical Notch targets mentioned before (*Ser*, *eyg*, *E(spl)m2-BFM*). Though conceptually interesting (and discussed further in Chapter Eight), I did not continue the analysis of these differences, but focussed on the main question I addressed with the second profiling.

The main finding of the second Microarray is that ATF4 is indeed required for the induction of the vast majority of COX7a knockdown induced target genes (431/472, Figure 14D). These included all the previously mentioned genes, some of which are shown in Figure 14E. Interestingly, pathetic induction is not stronger under nutrient restriction, but pathetic expression in controls requires ATF4 activity independently of COX7a knockdown. This apparent difference in the regulatory behaviour of pathetic compared to the other ATF4 targets hints at a different transcriptional mechanism, for example an interaction of ATF4 with a different cofactor.

In summary, my second transcriptome profiling confirmed the conclusions from the first analysis and established ATF4 as the main transcriptional activator downstream of COX7a knockdown. The comparison between the two analyses might furthermore reveal crucial adaptations or altered responses that could not be analysed within this thesis.

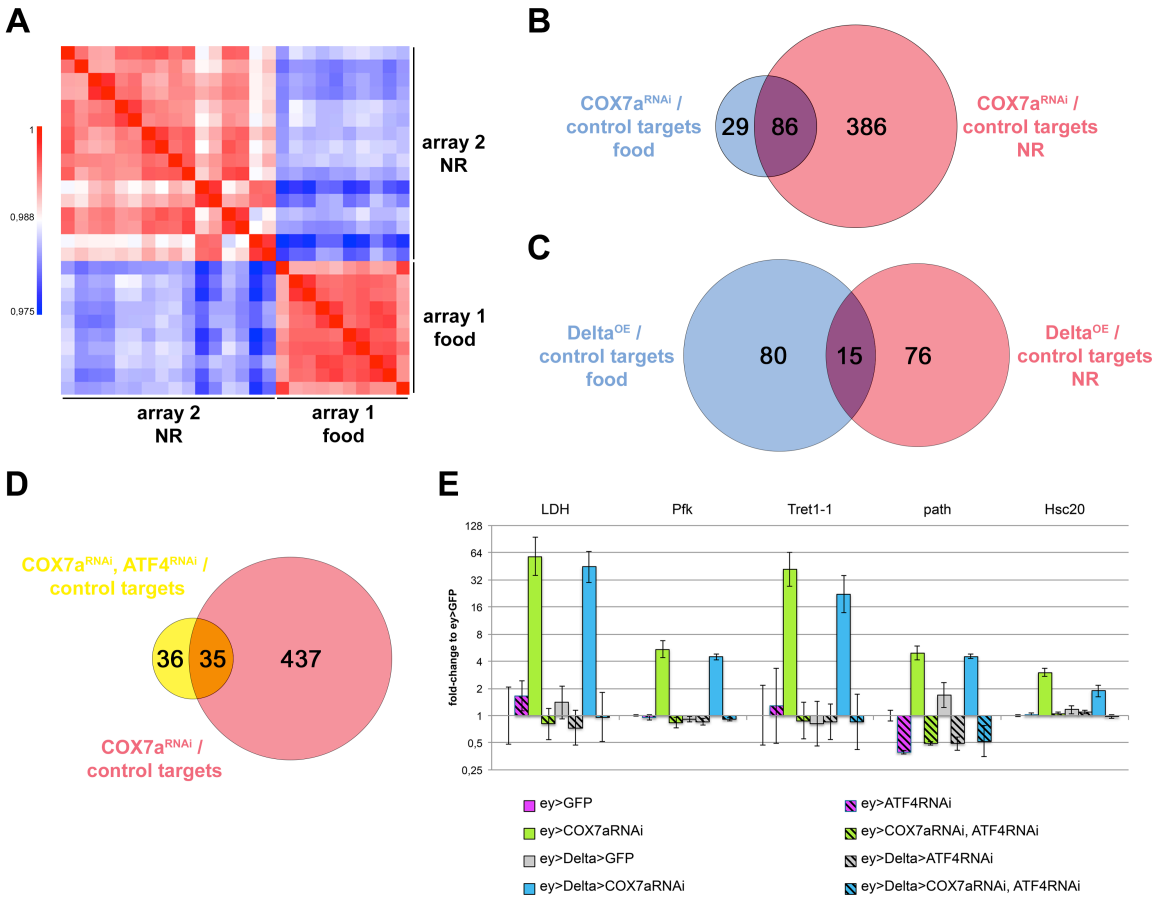

Figure 14: ATF4 mediates the COX7a transcriptional response

A) Global comparison of the two transcriptomic datasets. Pearson correlation indicates high similarities within each array. **B)** Overlap of COX7a target genes from first array (on normal food, in blue) with induced target genes from second array (under nutrient restriction, NR, in red) confirms majority of targets. **C)** Overlap of Delta targets is small. **D)** Overlap of COX7a with COX7a,ATF4 target genes highlights ATF4 as required for most COX7a knockdown targets. **E)** Representative examples of COX7a target genes and their dependence on ATF4. Fold change to ey>GFP; log2 scale; error bars are SD. Part of the data in B-D) is also included in *Sorge et al, submitted*.

Chapter Seven: A mitochondrial PERK isoform mediates ATF4 activation

In the previous Chapter I have presented evidence for ATF4 as the main transcriptional activator induced in response to lowered COX7a levels. Further, I have outlined that the induction of ATF4 protein is the consequence of a translational mechanism and not itself triggered by transcription. The mRNA structure of ATF4 predicts that translation of the ATF4 ORF requires phosphorylation of eIF2α. I performed IF staining for p-eIF2α. Control eye-antenna discs show weak, homogenous, cytoplasmic staining (Figure 15A), while COX7a knockdown discs show strong staining in relatively few progenitor cells (Figure 15B). Whether there is a more subtle induction of p-eIF2α throughout the progenitor compartment, as might be expected from the ATF4 staining, could not be clarified with this analysis. Nonetheless, the data indicates that eIF2α is phosphorylated in response to COX7a knockdown, suggesting that one of the two eIF2α kinases known in *Drosophila* is activated downstream of COX7a loss.

PERK is required for Delta, COX7a-induced over-proliferation

The two eIF2α-kinases encoded by the *Drosophila* genome, GCN2 and PERK, have been described to be activated by amino acid limitation and ER protein folding stress, respectively (Harding et al., 2000; 1999). As no reagent to directly detect activation of the kinases was available, I tested their possible involvement in the COX7a phenotypes by RNAi-mediated knockdown in the Delta, COX7a background. The phenotypic quantification showed that PERK is required for Delta, COX7a-induced over-proliferation in a similar manner as ATF4, while GCN2 function appears to be dispensable (Figure 15C). This result is surprising, as Delta,COX7a-induced over-proliferation apparently requires an amino acid-poor diet (see Chapter Eight), which would mechanistically fit well to GCN2 activation. In contrast, ER protein folding stress, the only signal activating PERK described so far, is not an expected consequence of COX7a knockdown. Yet, the same connection was observed in *Drosophila* neurons without *pink1* or *parkin* function (Celardo et al., 2016), though this study failed to provide a solid mechanistic basis for this interaction.

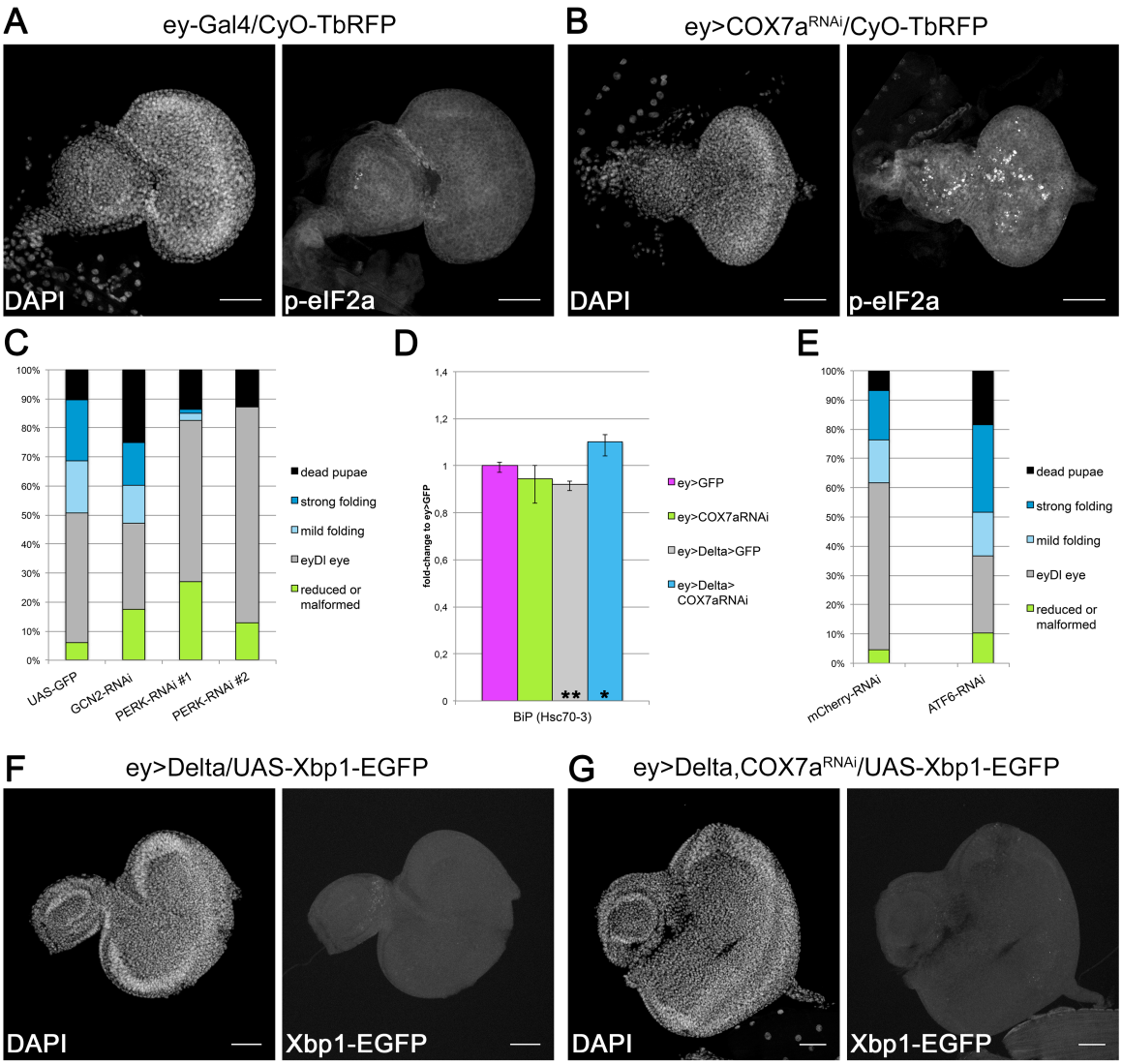

Figure 15: PERK mediates Delta,COX7a phenotypes

A-B) IF labelling of phospho-eIF2α suggests increased levels upon COX7a knockdown. **C)** Quantification of adult eye phenotypes in the Delta,COX7a background suggests PERK is required for over-proliferation (n=67; 68; 74; 39). **D)** Transcript levels of ER chaperone BiP from first Microarray analysis. BiP levels fluctuate minimally. **E)** Quantification of adult eye phenotypes in the Delta,COX7a background suggests ATF6 is not required for over-proliferation (n=89; 87). **F-G)** The Xbp1-EGFP reporter is undetectable in the Delta (F) and Delta,COX7a (G) backgrounds, suggesting that the Ire1/Xbp1 branch of the UPR^{ER} is not activated. Scale bar 50µm in microscopic images. Images in A,B,F,G are Z-projections (Average for DAPI; Maximum for p-eIF2α and Xbp1-EGFP). Part of the data in C-E) is also included in *Sorge et al, submitted*.

To answer the question whether COX7a knockdown indeed causes ER stress, I aimed to understand if the two other branches of the ER stress response pathway (UPR^{ER}) are likewise activated or required in my model. ATF6 is a transcription factor of the same family as ATF4 and has been described to mediate activation of some of the specific UPR^{ER} target genes in mammalian model systems (Ye et al., 2000). The Ire1/Xbp1 pathway is the third branch of UPR^{ER} and was shown to regulate the partially same set of ER chaperones and enzymes as ATF6 (Cox et al., 1993; Yamamoto et al., 2007). *BiP*

(*Hsc70-3* in *Drosophila*) is the classical readout of UPR^{ER} activation, regulated by both Xbp1 and ATF6 (Yamamoto et al., 2007). My *in vivo* transcriptome does not show up-regulation of *BiP* in response to COX7a knockdown (Figure 15D). Likewise, ATF6 knockdown failed to inhibit Delta, COX7a-mediated over-proliferation (Figure 15E) and a reporter for activity of Xbp1 (Ryoo et al., 2007) was not induced in the Delta,COX7a background (Figure 15F,G).

Together, the data suggested that COX7a knockdown does not induce the typical ER stress response pathways. In conclusion, this suggests a mechanism of PERK activation independent of its localisation or function in the UPR^{ER}.

PERK isoform B localises to mitochondria

The *Drosophila* genome encodes three different PERK mRNA and protein isoforms that differ in their first exon, which contains the 5'-UTR, the most N-terminal amino acids including the N-terminal signal peptide and, similarly to ATF4, μORFs (Figure 16A). I used several tools for prediction of protein localisation, to understand if the different protein isoforms might differ in their sub-cellular localisation. While several tools gave rather unspecific results, MitoProt (Claros and Vincens, 1996) predicted PERK isoform B to contain a potential mitochondrial targeting sequence (with 55% probability of export to mitochondria).

To test if the different N-termini indeed governed localisation to different cellular compartments, I cloned (all the following experiments on PERK localisation were performed together with my student Jonas Theelke) the N-termini of PERK isoform B and isoform A (which appears to contain the expected signal peptide for the secretory pathway) and fused them to EGFP. Isoform C was left out in this experiment, as it is not expressed in imaginal discs according to publicly available databases. The constructs were transfected into *Drosophila* S2R+ cultured cells and localisation was assessed live and after fixation. Live-imaging showed both EGFP constructs to be expressed in different subcellular patterns: While A_EGFP was usually found in a punctate pattern and occasionally at the plasmamembrane, $RB^{N\text{-}term}$-EGFP was detected in a more filamentous compartment. Both constructs were expressed at very low levels compared to a co-transfected cytoplasmic mCherry driven from the same strong actin promoter. The reason most likely is that the cloning strategy included the start codons of μORFs located few nucleotides upstream of the PERK ORFs (Figure 16B). As these μORFs contain weak

translation initiation sequences (Acevedo et al., 2018; Kozak, 1986), they are probably skipped at certain frequencies and allow translation of the downstream PERK ORFs.

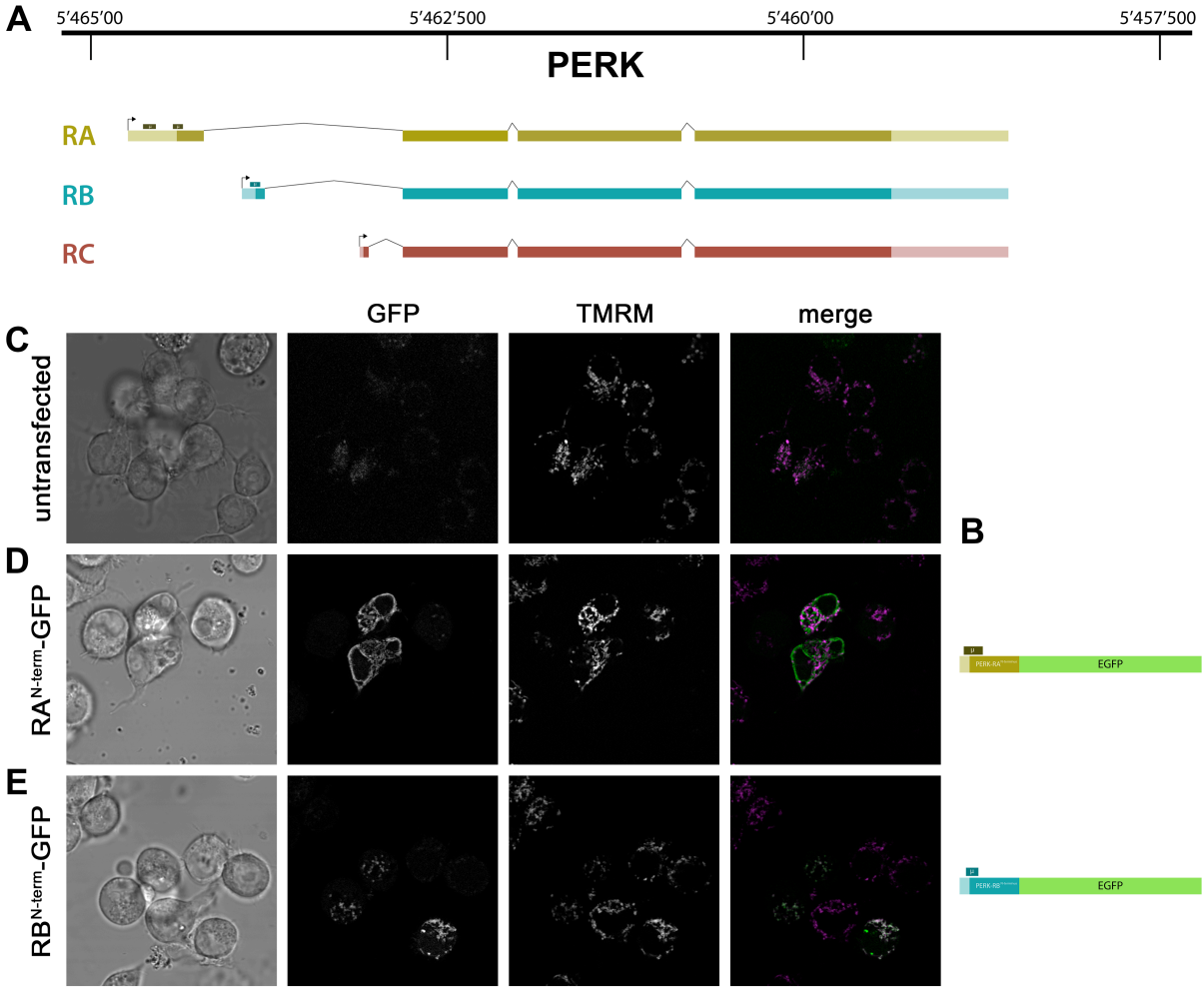

Figure 16: PERK isoform B contains a mitochondrial signal peptide

A) Schematic representation of the genomic PERK locus. PERK locus shown in reverse orientation (centromer to the right). Three mRNA isoforms encoding three protein isoforms are transcribed from the PERK locus, differing in the first exon, which contains the 5'-UTR and N-terminus of the proteins. PERK-RA (olive) contains two µORFs (small squares above mRNA) upstream of the translational start site. PERK-RB (cyan) contains one µORF. **B)** Synthetic PERK-EGFP fusions used in transient transfections of S2R+ cells. Constructs contained PERK 5'-UTR (including µORFs) and 180nt coding sequence as well as EGFP sequence. **C-E)** *Drosophila* S2R+ cells transfected with PERK-RA$^{N\text{-}term}$-EGFP (D) or PERK-RB$^{N\text{-}term}$-EGFP (E). Cells were treated with 100nM TMRM prior to imaging. TMRM accumulates in mitochondria and shows typical filamentous morphology of mitochondria. PERK-RB$^{N\text{-}term}$-EGFP (E) extensively co-localises with TMRM, while PERK-RA$^{N\text{-}term}$-EGFP (D) and TMRM are rather mutually exclusive.

To understand if the observed EGFP localisation corresponds to mitochondria, I labelled mitochondria with the cationic fluorescent dye tetramethylrhodamine-methyl ester (TMRM, (Scaduto and Grotyohann, 1999). As expected from the *in silico* prediction, $RB^{N\text{-}term}$-EGFP extensively co-localised with TMRM, while the $RA^{N\text{-}term}$-EGFP fusion and TMRM were found to be rather mutually exclusive (Figure 16C-E). I further attempted to confirm the finding by IF staining of the EGFP fusion constructs. While a-ATP5a staining (a mitochondrial Complex V subunit) confirmed the filamentous mitochondrial signal seen with TMRM and $RB^{N\text{-}term}$-EGFP during live imaging, the EGFP fusions were hardly detectable after fixation and, if detectable, $RB^{N\text{-}term}$-EGFP appeared to have spread throughout the cell, obviously presenting a fixation artefact. IF labelling of Calreticulin (a ER-resident protein) showed a punctate pattern, clearly discrete and largely non-overlapping with ATP5a, as would be expected.

Together, the results presented above indicate that the N-terminal sequences of the two different PERK isoforms can differentially affect the proteins localisation, with isoform B being imported into mitochondria. Despite further examination being necessary, this mitochondrial PERK provides a solid mechanistic explanation for PERKs involvement in activation of ATF4 downstream of the mitochondrial defect caused by COX7a knockdown.

Chapter Eight: Internal and external dependencies of Delta, COX7a over-proliferation

In the previous chapters I have outlined a molecular pathway that responds to reduced COX7a levels by inducing transcription of target genes through the transcription factor ATF4. I have further shown that this ATF4-mediated transcriptional adaptation is required for the over-proliferation phenotype that I had initially found and that is a consequence of activation of the Notch signalling pathway interacting with the downstream targets of the COX7a-PERK-ATF4 axis. It therefore appeared likely that one or several downstream targets of ATF4 would be responsible for the increased proliferative capacity and that their knockdown would be able to rescue the over-proliferation phenotype.

Impact of ATF4 target genes on Delta, COX7a-induced over-proliferation

In an attempt to understand how the ATF4 adaptation increases the proliferative capacity of eye progenitors, I screened selected target genes by RNAi in the Delta,COX7a background. As shown in Chapter Five, ATF4 induces a relatively wide range of target gene groups, collectively referred to as the "integrative stress response" (ISR). Many of these targets encode proteins involved at various stages of cellular metabolism. Since a metabolic contribution to cell proliferation is widely acknowledged in mammalian biology (Vander Heiden et al., 2009), I first focussed on this group of genes.

The use of "aerobic glycolysis" (or the "Warburg effect") is a metabolic adaptation of cancer cells that correlates with their proliferative potential. As mentioned before, ATF4 induces glycolytic enzymes, lactate dehydrogenase (LDH) and the main sugar transporter (Tret1-1). So, at least from a theoretical point of view, eye progenitors depleted of COX7a could be forced into a glycolytic metabolism and this adaptation alone might be the reason for the increase in proliferation. Practically, I found that knockdown of LDH or Tret1-1 in the Delta,COX7a background strongly increased proliferation (Figure 17A). Knockdown of LDH in the Delta background also led to slightly folded eyes (Figure 17B) and over-expression of LDH in the ey-Gal4 background slightly decreased eye size (Figure 17C). Together, these results suggest that the transcriptional induction of glycolysis is not responsible for over-proliferation.

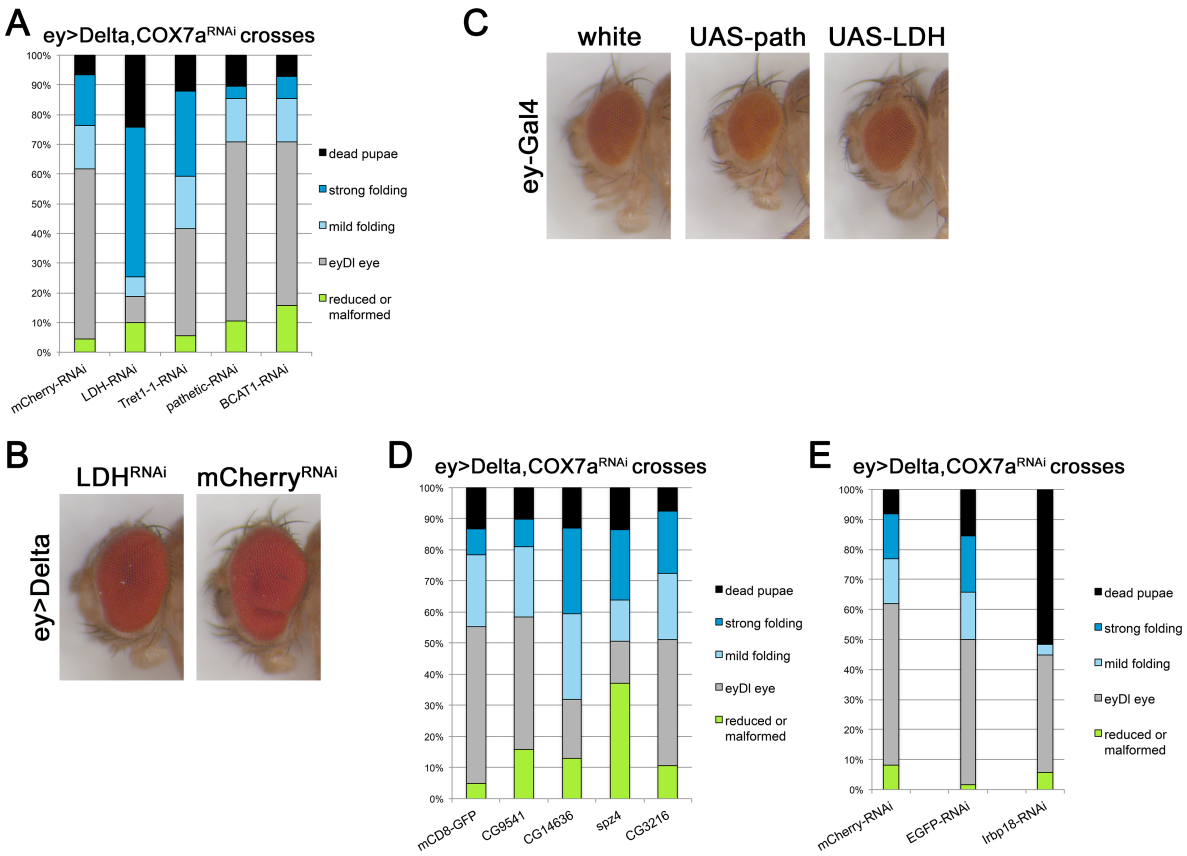

Figure 17: ATF4 target genes and their contribution to Delta,COX7a over-proliferation

A) Quantification of adult eye phenotypes in the Delta,COX7a background (n=89; 91; 91; 48; 96). Interference with carbohydrate metabolism (LDH, Tret1-1) strongly enhances over-proliferation. **B)** Knockdown of LDH in the Delta background induces a slight over-proliferation phenotype. **C)** Over-expression of LDH, but not path, in the ey-Gal4 (wildtype) background slightly reduces eye growth. **D)** Quantification of adult eye phenotypes in the Delta,COX7a background (n=83; 89; 69; 97; 94). None of these "unique" targets is required for over-proliferation. **E)** Quantification of adult eye phenotypes in Delta,COX7a background (n=87; 64; 87) showing two controls and rescue of over-proliferation by knockdown of Irbp18 (C/EBPγ). Part of the data in A) and E) is also included in *Sorge et al, submitted*.

Amino acids are required for protein synthesis and can be metabolised to generate ATP as well. The ATF4 target genes are rich in amino acid transporters (path, Jhl-21, mnd, CG5535) and metabolic enzymes (BCAT1) and the cellular capacity to increase amino acid uptake or use (especially under conditions of a low protein diet, see below) could be envisioned as an explanation for over-proliferation. I knocked down three of the transporters and BCAT1 but failed to observe a reproducible, clear effect on Delta,COX7a over-proliferation. At best, there was a slight trend for very mild attenuation of over-proliferation with path and BCAT1 knockdown (Figure 17A). As over-expression of path was not affecting eye size in the ey-Gal4 background (Figure 17C), a single amino acid transporter does not appear to be a good explanation for ATF4-mediated over-

proliferation. For genetic reasons I could not analyse double knockdowns of amino acid transporters in the Delta,COX7a background, which might have been more promising.

I further tested four candidates found to be uniquely or cooperatively induced by Delta and COX7a-knockdown. None of the four affected over-proliferation (see Figure 17D).

I found a single gene, whose knockdown abolished over-proliferation in the same way as ATF4 and PERK knockdown. This gene (called *Irbp18* in *Drosophila*) encodes a basic leucine-zipper (bZip) transcription factor homologous to mammalian C/EBPγ and was shown to be one obligate heterodimeric interactor of ATF4 in *Drosophila* (Reinke et al., 2013). Irbp18 knockdown blocked over-proliferation and was found to be lethal for half of the offspring (Figure 17E). Interestingly, *Irbp18* was transcriptionally induced in response to COX7a knockdown according to the second microarray, but not significantly induced in the first analysis. Further, Irbp18 belongs to the genes induced under nutrient restriction in genetic controls (see below), making it an interesting candidate for future studies to explain the food dependency that I will present next.

COX7a phenotypes are nutrient dependent

While screening candidates in the Delta,COX7a background, I repeatedly noticed that the number of offspring per vial seemed to affect the over-proliferation phenotype. I observed the general trend that vials with many larvae had a higher proportion of offspring with strong over-proliferation of the eye, while vials with few offspring tended to have very few or no strong phenotypes. Furthermore, crowding slowed down larval development (time to pupation), so apparently had a general negative impact on development. To properly quantify the impact of crowding, I picked freshly hatched L1 larvae from the same cross in defined numbers into fly food vials. I chose 40 larvae per vial to represent a very low density and 120 larvae to represent a high density (crowding). The results of the experiment (Figure 18A) confirmed the previous notion that crowding increases Delta,COX7a-induced over-proliferation.

Potential ways to explain the crowding effect are manifold. Larvae could secret substances into the food that negatively affect their own development in a dose-dependent manner. Larvae could also compete for nutrients in the food. Interestingly, I observed a similar dependency of Delta,COX7a phenotypes, but also of the COX7a phenotype, on the composition of the food as I had observed for crowding (illustrated in

Figure 18B). I tested various food recipes to understand which component of the food could be limiting and drive over-proliferation of Delta,COX7a. As shown in Figure 18C, lowering the yeast content (as the main source of protein) of an otherwise identical food formulation and with identical numbers of larvae per vial, increased the proportion of strong phenotypes, arguing that a lack of amino acids would be required for COX7a-dependent eye phenotypes.

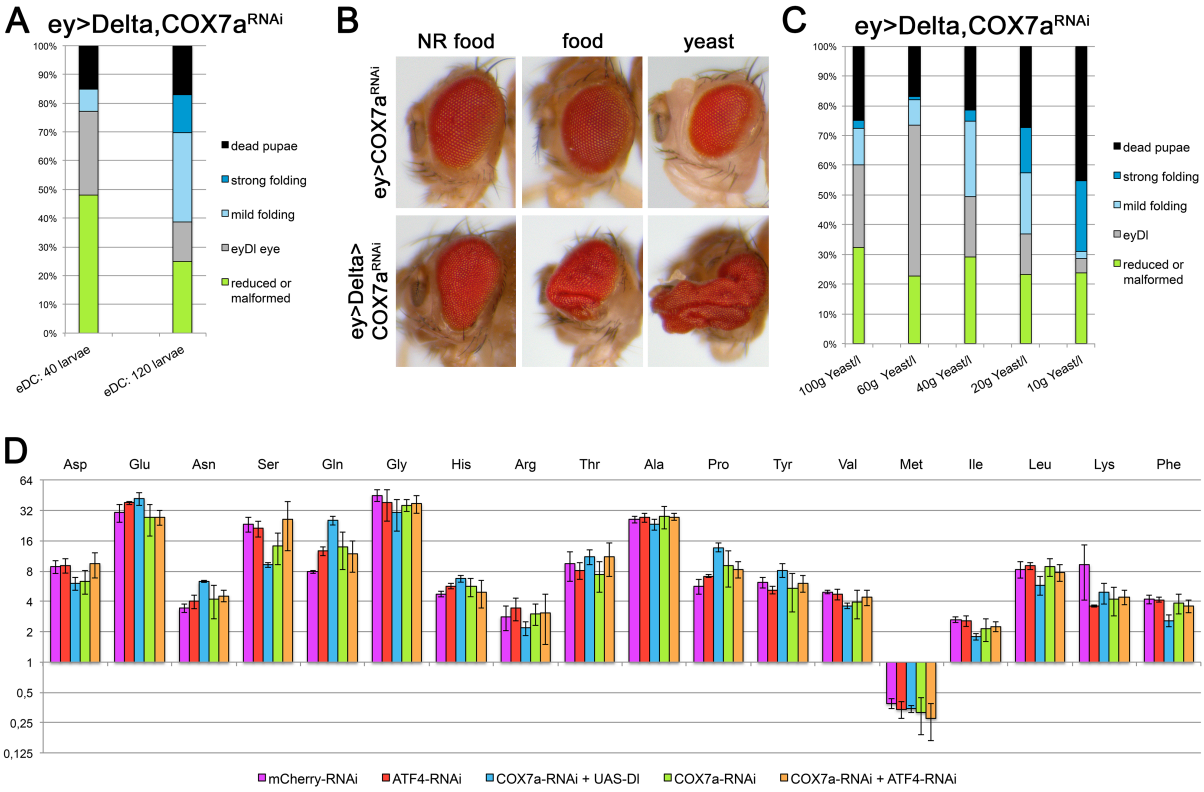

Figure 18: Nutrient dependence of COX7a phenotypes

A) Quantification of adult eye phenotypes of offspring from the same cross reared under low or high larval density (40 or 120 larvae per vial, respectively) (n=79; 181). **B)** Representative images of COX7a (upper row) and Delta,COX7a (lower row) phenotypes in dependence on the larval diet (NR food = amino acid-restricted fly food; food = normal fly food; yeast = living yeast paste on apple-juice agar plate). **C)** Quantification of adult eye phenotypes of offspring from the same cross reared on fly food with different yeast concentration (100g per liter to 10g per liter). **D)** *In vivo* metabolomics analysis of free amino acids in eye-antenna discs of indicated genotypes. For this experiment, Gal4 activity was based on ey-Flpout (stock: ey-Flp, act>CD2>Gal4, UAS-GFP). The experiment failed to reveal significant differences in free amino acid concentrations upon COX7a knockdown. Mean of four replicates with SD shown on log2 scale. Part of the data in B-C) is also included in *Sorge et al, submitted*.

Though many experiments (shown above and below) were based on such a low-protein diet, I should note some conceptual problems: a) A late L3 larva of a given size will have to take up a given amount of essential amino acids from the food. If the food is poor in protein and therefore essential amino acids, the larva will have to take up more food to reach a certain size. As a consequence, a larva on a low-protein diet will consume

much more sugar. A low-protein diet is therefore automatically a high-sugar diet and effects are hard to discriminate. b) It is unknown at present, how the larval diet affects concentrations of nutrients and hormones in the hemolymph (the fly's equivalent to blood). Therefore, it is an assumption that a low-protein diet would also translate into low amino acid levels in the hemolymph.

To investigate if COX7a-depleted eye discs lack certain amino acids, as the low-protein dependency and reports from cultured human cells lacking mitochondrial function (Birsoy et al., 2015; Sullivan et al., 2015) suggest, I analysed amino acid content through metabolomics. In the setup I used, I could not detect significant changes of a single amino acid upon COX7a knockdown or the double knockdown of COX7a and ATF4 (Figure 18D). In summary, though amino acid import and metabolism are prominent transcriptional features downstream of COX7a and COX7a phenotypes are subject to modification by differing amino acid concentrations in the diet, my experiments failed to clarify the exact connection between dietary restrictions and eye disc development under conditions of COX7a knockdown. Future work should clarify, whether the lack of differences is due to experimental difficulties or whether disc cell metabolism is indeed well buffered against the cell-autonomous defects, that we (see below) and others have shown in cultured cells.

The transcriptional signature of amino acid limitation

In Chapter Six I have shown a global comparison between the two transcriptomic datasets I generated, focussing on the effects of COX7a knockdown and Delta over-expression under the two dietary conditions. I have also outlined that the differences in the transcriptomes were much greater under nutrient restriction.

The data also allowed me to ask, what transcriptional changes are induced by nutrient restriction in genetic controls (ey>GFP and ey>Delta>GFP), as these might hint at the apparently higher capacity for proliferation. Overall, I found a high number of genes to be differentially expressed under nutrient restriction within one genotype using the same thresholds as before ($p<0.05$; $-1.5<fold>1.5$): in ey>GFP controls 538 up and 322 down; in ey>Dl>GFP 621 up and 666 down. The overlap of induced or repressed genes was generally high (about 2/3 of ey>GFP genes shared with ey>Delta>GFP), suggesting a common difference. GO-term analysis of shared down-regulated genes showed a strong enrichment of neuronal GO-terms (see Table 5) and the list of shared

down-regulated genes included many genes well known for their functions during later eye disc development. Together this data suggests that the discs under nutrient restriction were of significantly younger developmental age, despite my efforts to sample at an equivalent developmental stage. The most notable GO-term amongst shared up-regulated genes was the JNK pathway (including the TNF-ligand Eiger and core components of the cascade). At present it remains unknown, which cell population expresses these genes and whether this reflects the younger age or an actual increase in stress signalling within the tissue under nutrient restriction.

An important finding from this comparison was that nutrient restriction did not induce an ATF4-like transcriptional signature. This result is in agreement with the lack of GCN2-dependence of the over-proliferation phenotype (see Chapter Seven) and the *in vivo* metabolomic analysis. Together, the primary conclusion from these findings is that the dependency of the phenotypes on nutrient restriction is not triggering the cellular amino acid limitation (GCN2-ATF4) pathway, but rather appears to be a non-cell autonomous or a systemic effect.

Conceptually, ey>Delta>GFP discs are able to proliferate more in response to COX7a knockdown under nutrient restriction. Therefore, specific adaptations could be induced in these discs and these genes might allow a more meaningful interpretation. Three of the most highly induced genes (by nutrient restriction) exclusively in ey>Delta>GFP are Prophenoloxidase 1 and 2 (PPO1/2) and Hemese (He). All three genes are well described specific markers of *Drosophila* immune cells, the hemocytes (Kurucz et al., 2003; Rizki et al., 1985). Recently, PPO1 and PPO2 activity in eye disc-attached hemocytes was shown to correlate with an immunosuppressive phenotype in Notch/PI3K tumours (Villegas et al., 2018), suggesting that the melanization process triggered by PPO1/2 acted tumour suppressive. My data confirmed PPO1/2 induction upon Delta over-expression, though only under nutrient restriction. In summary, the data suggests that nutrient restriction sensitizes the immune system and that interactions between cells of the disc epithelium and the attached hemocytes could be part of the over-proliferation phenotype.

Chapter Nine: Mitochondrial defects of COX7a loss of function

The *in vivo* model I presented in all previous Chapters allowed me to study the consequences of reduced expression of COX7a in a developing epithelium. The main strength of this approach is the obvious biological significance of the phenotypes, as they morphologically and functionally disrupt an organ of the fly. Using these phenotypes as a readout and available genetic tools to probe gene function, I was able to reveal the signalling cascade activated downstream of COX7a knockdown. But so far, my experiments could not yet explain the direct consequences of COX7a knockdown on mitochondrial respiration or ETC function. To add another level of analysis, we decided to complement the *in vivo* model with a less complex and better accessible *in vitro* model. Therefore, we decided to study COX7a depletion in cultured *Drosophila* S2R+ cells, specifically aiming at a metabolomic understanding of loss of COX7a function.

COX7a-depleted S2R+ cells show metabolic alterations consistent with reduced ETC function

Studies in different human cell lines have recently indicated a main function of mitochondrial respiration to be the maintenance of aspartate biosynthesis to allow proliferation (Birsoy et al., 2015; Sullivan et al., 2015). Cells unable to respire exhibit electron acceptor deficiency that inhibits mitochondrial aspartate production, which ultimately inhibits cell cycle progression. Intrigued by the metabolic phenotypes upon loss of respiration, I used COX7a depletion in cultured *Drosophila* cells to test if reduced COX7a expression recapitulates some phenotypes associated with a full loss of respiration.

I performed the COX7a knockdown with the identical dsRNA construct used *in vivo* and could show a strong reduction in COX7a mRNA levels four days after treatment (levels reduced to 1.9%±0.23% SD; n=6). I note that this reduction is much stronger (corresponding to approximately 50-fold reduction) than the reduction observed in the eye disc transcriptomes (approximately 6-fold reduction). COX7a depletion almost completely blocked cell proliferation, reminiscent of the situation in cultured human cells without respiration. In the initial days of the RNAi treatment, cells still divided up to once within four days, but failed to show a robust increase in cell number after splitting compared to control cells (Figure 19A).

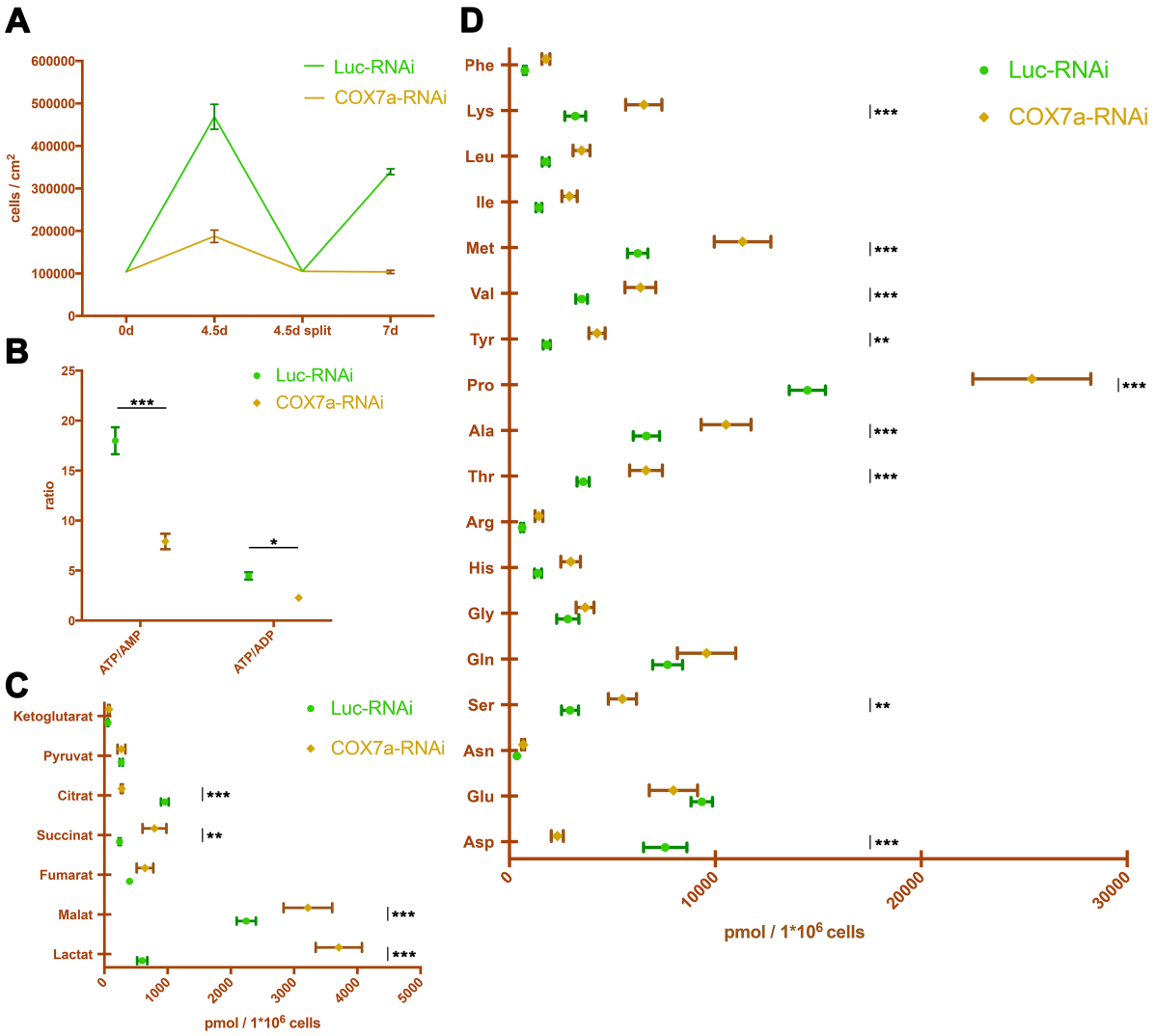

Figure 19: COX7a depletion in S2R+ cells

A) Typical growth curve of S2R+ cells treated with control (Luciferase) or COX7a dsRNA (at 0d). Error bars denote SD. **B)** Ratio of ATP to AMP and ADP is decreased after COX7a knockdown. Mean of three replicates with SD shown. **C)** Lactate, malate and succinate levels are increased after COX7a knockdown, while citrate levels are reduced. Mean of three replicates with SD shown. **D)** Free amino acids in S2R+ cells show several significant alterations after COX7a knockdown. Mean of three replicates with SD shown. Asterisks indicate significance according to Two-way ANOVA analysis (*=p<0,05; **=p<0,01;***=p<0,001). Part of the data in A-D) is also included but presented differently in *Sorge et al, submitted*.

A major aim of the cell culture model was to investigate metabolic consequences of reduced COX7a expression. To this end I collected cell pellets of control cells (Luciferase-RNAi) and COX7a-RNAi cells in triplicates and submitted them to the Metabolomics Core Facility of COS/University Heidelberg for the analysis of amino acid, thiols, adenosines and organic acids. The major results showed decreased ATP levels upon COX7a knockdown as both ATP/AMP and ATP/ADP ratios were decreased (Figure 19B). Concentrations of intracellular lactate, malate and succinate were increased, while citrate

was found reduced (Figure 19C). Levels of several amino acids were strongly altered, including a prominent reduction of aspartate, while many amino acids with more reduced carbon were more abundant upon COX7a knockdown (Figure 19D).

In summary, strong COX7a depletion in cultured cells recapitulated many aspects of cultured human cells devoid of respiration. Though actual respiration of COX7a-depleted cells was not assessed, loss of COX7a probably induces mitochondrial defects equivalent to a strong reduction of respiratory capacity.

Mitochondrial morphology and function are not altered in vivo

The results from cultured cells depleted of COX7a suggested that strong COX7a knockdown induces cellular phenotypes reminiscent of a full loss of respiration. As said before, the *in vivo* knockdown of COX7a is less severe and therefore a full inhibition of ETC function and respiration not expected. Still, I was interested in investigating if defects in mitochondrial morphology or function could be detected. Transmission electron microscopy (TEM) on COX7a knockdown eye discs had previously been carried out by C. Altbürger (Altbürger, 2014). Within this data I measured mitochondrial diameter as a readout of mitochondrial morphology, but failed to detect significantly altered mitochondrial diameters upon COX7a knockdown (Figure 20A). Light microscopic analysis with a GFP reporter targeted to mitochondria or IF staining of a Complex V subunit likewise failed to indicate obvious differences, while a positive control, knockdown of the mitochondrial fusion protein opa1, exhibited a clear loss of long, filamentous mitochondria (Figure 20C-E). Together, the data suggested that *in vivo* COX7a knockdown does not alter mitochondrial morphology.

A more direct readout to assess respiratory function is TMRM labelling (see Chapter Seven). TMRM is passively incorporated into mitochondria depending on the membrane potential across the inner mitochondrial membrane. TMRM therefore is a measure for membrane potential, which is produced by the electron transport chain, but which does not necessarily correlate with respiratory activity. As *ex vivo* culturing and imaging of imaginal discs is subject to various external effects that are difficult to control, I decided to test TMRM incorporation in a setup where GFP labelled clones expressed COX7a-RNAi, allowing me to compare TMRM intensity in the clone with the surrounding wildtype cells. In these clones, I failed to detect any difference in TMRM incorporation

(Figure 20B), arguing that the membrane potential was kept intact at least under this experimental condition.

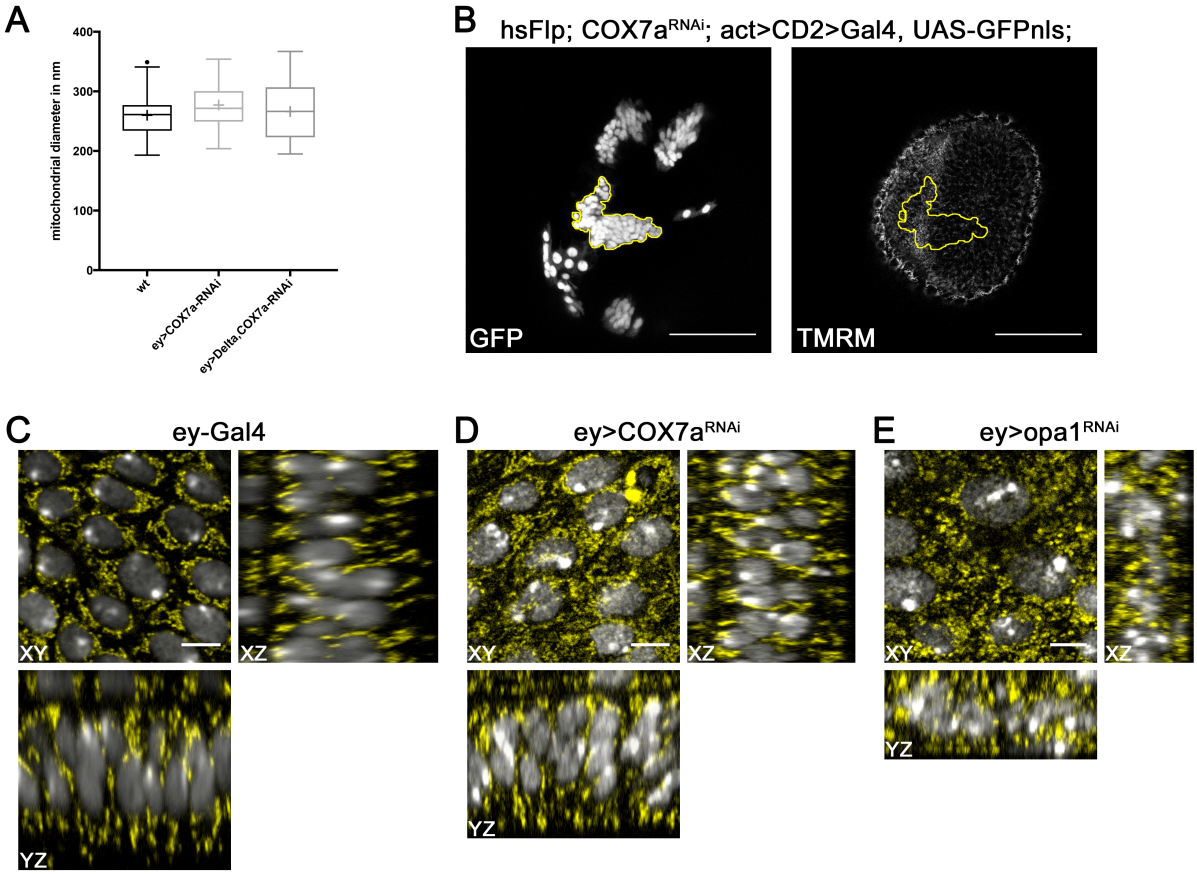

Figure 20: Mitochondrial morphology is unaltered upon COX7a knockdown

A) Mitochondrial diameter in TEM analysis (Altbürger, 2014) does not show significant differences according to One-way ANOVA (n=49; 50; 46). **B)** Heatshock-induced clones (labelled with GFP, outlined in yellow) expressing COX7a RNAi incorporate TMRM normally. **C-E)** XY, XZ and YZ views of eye disc cells showing nuclei in white and mitochondria (IF labelling of ATP5a) in yellow. Control (C) and COX7a knockdown (D) eye progenitors have long, filamentous mitochondria, occasionally spanning the whole apico-basal length of a cell. Knockdown of opa1 (E) disturbs mitochondrial morphology, leading to more singular, round mitochondria. Scale bar 50µm in B; 5µm in C-E. The data in A) is also included in *Sorge et al, submitted*.

Though more conclusive results could be generated by directly measuring oxygen consumption, my results generally (within this Chapter and Chapter Eight) argue that *in vivo* COX7a knockdown represents a mild attenuation of ETC function or might even induce the ATF4 response independently of an actual functional impairment.

Chapter Ten: A generalisation of COX7a-induced phenotypes in the *Drosophila* eye disc

Throughout this thesis I have characterised various phenotypes caused by RNAi-mediated knockdown of COX7a during eye development. Within this last Chapter I want to provide evidence for a more general and global picture of how mitochondrial function and specific proteins are required. Along this line I want to answer three questions:

1) Does knockdown of other ETC subunits show similar phenotypes as I described for COX7a?

2) Is diminished ATP production via oxidative phosphorylation triggering the ATF4 response downstream of COX7a/ETC knockdown?

3) Is the ATF4 response interacting specifically with Notch signalling?

COX7a phenotypes represent a common ETC knockdown effect

COX7a is a small, accessory subunit of Complex IV of the ETC and was shown to be required for the assembly of the fully functional Complex (Jacobs). As no indication for a unique role of COX7a existed in the literature, I reasoned that knockdown of other ETC subunits would cause similar phenotypes and induce the ATF4 response. In total, I tested 18 RNAi lines targeting 15 ETC subunits and found that most of them (11/15 subunits) induced phenotypes similar to COX7a or stronger (Figure 21A-D). These subunits included 6/6 Complex I subunits; 1/3 Complex III subunits and 4/4 Complex IV subunits. For Complex II, I could only test two non-canonical subunits and both scored negative (see Table 6 for summary of all subunits with associated phenotypes). As depicted in Figure 21A,B, some subunits showed slight reductions of eye size and minor differentiation defects when knocked down alone, but over-proliferation in combination with Delta over-expression. Due to the similarity with the COX7a phenotypes I termed these subunits "COX7a-like". Other subunits showed high pupal lethality and severe defects in eye size and organisation in adult survivors, with or without Delta over-expression, and I termed these according to one member of the group "ND75-like" (Figure 21C,D). Overall, the results suggest that knockdown of ETC subunits is potently disturbing eye development.

Over-proliferation of Delta,COX7a discs requires ATF4 function downstream of COX7a knockdown. COX7a-like subunits showed the same cooperation with Notch

signalling, so might be expected to show the same ATF4 response. To test this, I used the LDH-GFP reporter, which is induced downstream of COX7a knockdown in an ATF4-dependent manner, as a readout for ATF4 activation. I found the reporter induced for 5/7 subunits tested (see Figure 21E,F and Table 6, Appendix), including COX7a-like and ND75-like subunits. Importantly, all subunits showing over-proliferation (COX7a-like) with Delta over-expression scored positive for ATF4 activity.

In summary, RNAi-mediated disturbance of ETC subunits generally induced ATF4 activation and eye phenotypes reminiscent of the results obtained for COX7a.

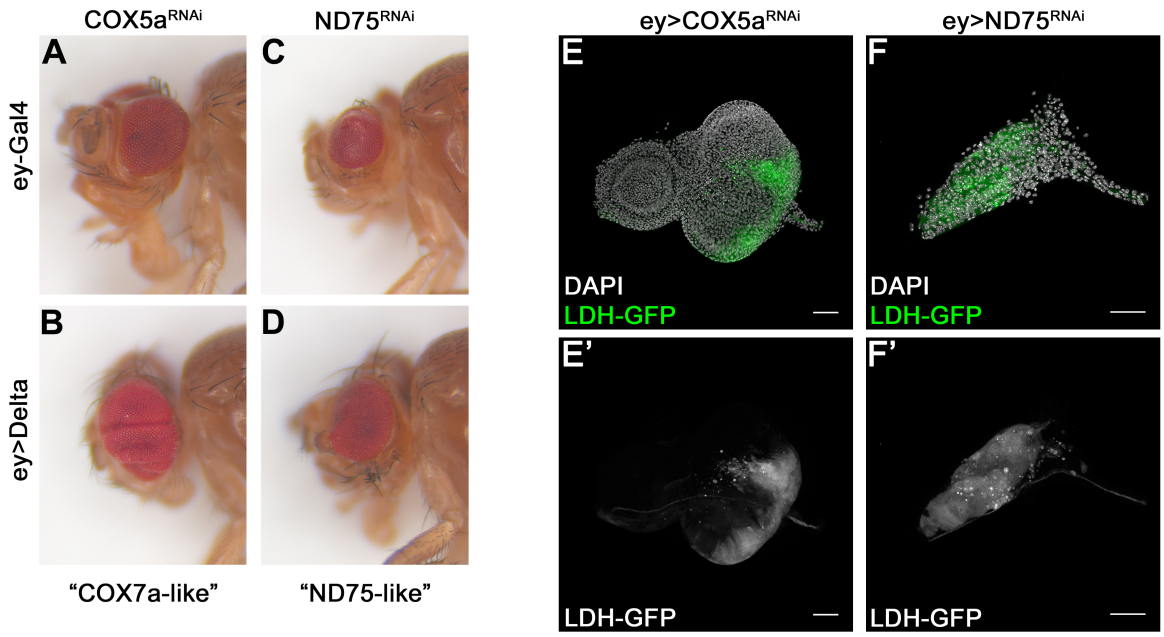

Figure 21: Phenotypes associated with knockdown of other ETC subunits

A-D) Representative images of adult eye phenotypes in ey-Gal4 (A,C) or ey>Delta (B,D) backgrounds for knockdown of ETC subunits COX5a or ND75. COX5a knockdown caused phenotypes reminiscent of COX7a knockdown, therefore termed "COX7a-like". ND75 is the founding member of the more severe "ND75-like" group. **E-F)** LDH-GFP induction by COX5a (E) and ND75 (F) knockdown in ey-Gal4 background. Both induce LDH-GFP, arguing for the same ATF4 response. Scale bar 50µm in microscopic images.

ETC phenotypes are not a consequence of general metabolic interference

ETC subunits form and functionally contribute to their ETC complexes. As the ETC itself is primarily required for ATP production with concomitant removal of electrons (as electrons are used by the ETC to reduce molecular oxygen), the common phenotypes of ETC subunit knockdown (see above) could be explained through their shared role in respiration. Along this argument, knockdown of ETC subunits would impair cellular respiration and ATP production and this metabolic impairment would cause ATF4 activation and eye phenotypes. If that was the case, interference with metabolic reactions occurring upstream of the ETC should lead to similar defects. I tested this hypothesis by interfering with various metabolic reactions, from pyruvate import into mitochondria to various steps of the tricarboxylic acid (TCA) cycle. Surprisingly, I found that neither pyruvate import (through Mpc1^{KD}), nor pyruvate dehydration (through muc^{KD} and Pdhb^{KD}), nor enzymes of the TCA cycle (through CG5214^{KD}, Idh3B^{KD} and l(1)G0255^{KD}) affected eye development in Delta^{OE} conditions (Figure 22A), despite some of these lines' functionality had been confirmed before (Homem et al., 2014). Furthermore, knockdown of the TCA cycle enzyme CG5214 did not induce the LDH-GFP reporter in a similar way as most ETC subunits (Figure 22B,C), substantiating the idea that metabolic disturbance at this level does not activate ATF4.

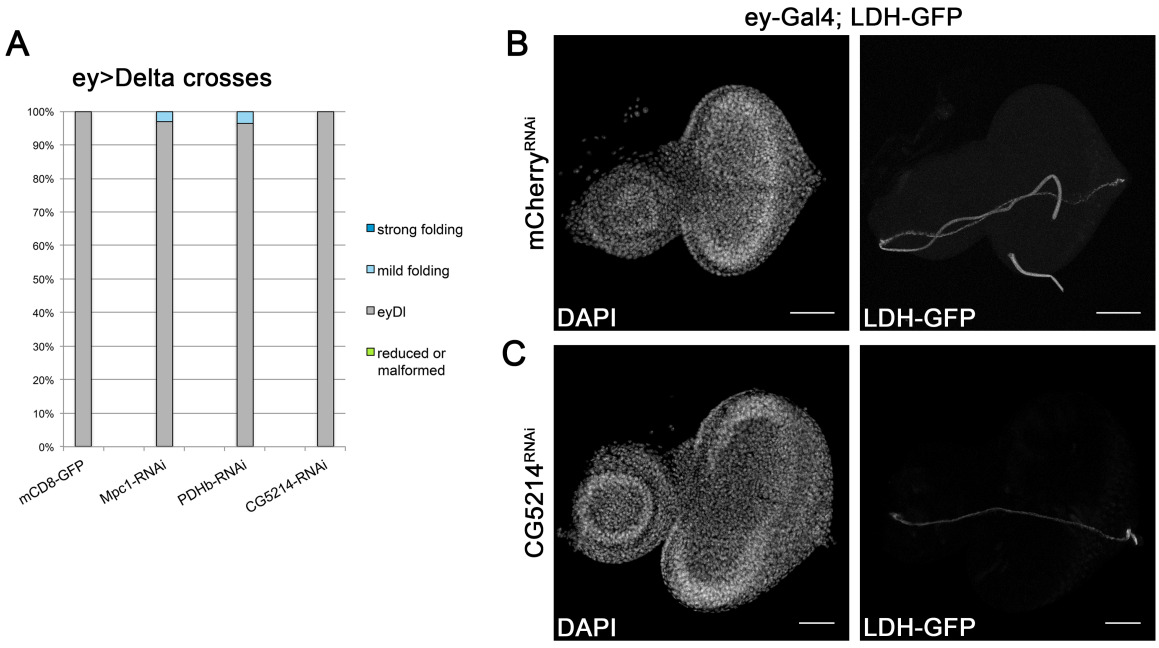

Figure 22: Metabolic enzymes other than the ETC do not cause comparable phenotypes
A) Quantification of adult eye phenotypes in the ey>Delta background (n=209; 97; 85; 77). Knockdown of metabolic enzymes upstream of the ETC does not induce clear phenotypes. **B-C)** Microscopic images of early/mid-L3 eye-antenna discs showing DAPI (left) and LDH-GFP reporter (right). Knockdown of TCA cycle enzyme CG5214 does not induce reporter expression. Scale bar 50µm in microscopic images. Average projection for DAPI and Maximum Projection for LDH-GFP shown.

In summary, defects in metabolic reactions that supply the electron transport chain with reducing equivalents are not equally required as ETC subunits during eye development and do not show the same ATF4 response. A likely explanation for these differences is that the ATF4 response is not triggered by a metabolic defect, but through impaired ETC complex assembly (see Discussion).

Interactions between the ATF4 response and oncogenic EGFR/Ras signalling

For the third and last question I wanted to understand if the cooperation between the ATF4-mediated transcriptional adaptation and a growth-promoting pathway was also a more general phenomenon. I decided to use the well-known oncogene Ras^{v12}, which induces overgrown eyes, typically with dorsal-anterior cuticle and eye outgrowths and black necrotic patches within the eye, when over-expressed with eyeless-Gal4 (Figure 23A). Knockdown of COX7a in the ey>Ras^{v12} background induced severe tissue folding and reduced the typical ras^{v12} eye phenotype (Figure 23A,B). Likewise, larval eye discs where more heavily overgrown (Figure 23E,F). The growth-enhancing effect of COX7a was again ATF4-dependent as co-knockdown of ATF4 rescued eye size and morphology back to the level of Ras^{v12} alone (Figure 23C,G). Knockdown of PDSW, a COX7a-like ETC subunit that induces over-proliferation with Delta over-expression, also induced strongly folded eyes, though to a lesser degree than COX7a (Figure 23D,H).

Overall, these results suggest that the ATF4-mediated adaptation can promote proliferative effects of different signalling pathways in the eye-antennal disc.

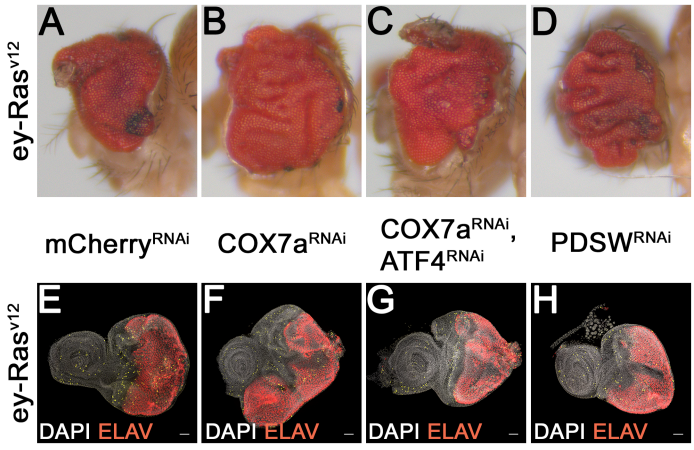

Figure 23: ETC subunit knockdown enhances Ras-dependent over-proliferation
A-D) Representative images of adult eyes, showing increased folding and overgrowth upon COX7a (B) or PDSW (D) knockdown. **E-H)** Eye-antenna discs (DAPI in white, ELAV in red, PH3 in yellow) of the same genotypes, similarly reflecting ETC knockdown-induced over-proliferation. Scale bar is 50µm.

Appendix

Fbgn Identifier	Vienna line #
FBgn0038020	*31173*
FBgn0032727	31294
FBgn0032727	31295
FBgn0031865	33149
FBgn0262473	100078
FBgn0001254	100148
FBgn0039795	100398
FBgn0030102	100501
FBgn0038207	100504
FBgn0036364	100515
FBgn0031049	100603
FBgn0034470	100671
FBgn0032350	100689
FBgn0035193	101272
FBgn0026190	101283
FBgn0034075	101484
FBgn0036173	**101490**
FBgn0259219	101585
FBgn0001226	101669
FBgn0039299	101807
FBgn0259209	101898
FBgn0032285	101911
FBgn0038682	102220
FBgn0034162	102243
FBgn0035379	102389
FBgn0259209	102399
FBgn0259219	102469
FBgn0031505	102590
FBgn0259209	102757
FBgn0034860	102880
FBgn0035917	102980
FBgn0036846	103759
FBgn0010441	103774
FBgn0038020	*103798*
FBgn0039136	104014
FBgn0260440	104092
FBgn0001227	104341
FBgn0037906	104557
FBgn0039494	104609
FBgn0015657	104618
FBgn0037515	104634
FBgn0020381	104726
FBgn0024294	104817

Fbgn Identifier	Vienna line #
FBgn0039102	104906
FBgn0019643	105064
FBgn0031560	105067
FBgn0032284	105076
FBgn0025712	105183
FBgn0038720	105194
FBgn0000153	105436
FBgn0260632	105491
FBgn0039620	105518
FBgn0263773	105596
FBgn0038115	105629
FBgn0030493	105695
FBgn0033402	106198
FBgn0036742	106421
FBgn0035165	106452
FBgn0030544	106526
FBgn0020439	106560
FBgn0040817	106561
FBgn0030737	106649
FBgn0040529	**106661**
FBgn0035147	106750
FBgn0015872	106911
FBgn0035089	106938
FBgn0029648	107046
FBgn0034412	107067
FBgn0034903	107199
FBgn0034709	107301
FBgn0035173	107339
FBgn0001230	107356
FBgn0027496	107588
FBgn0034974	107603
FBgn0033970	**107665**
FBgn0027790	107768
FBgn0027790	107768
FBgn0027843	108184
FBgn0000591	108226
FBgn0025678	108439
FBgn0014018	108469
FBgn0025456	108999
FBgn0032727	109718
FBgn0000120	109860
FBgn0005592	110277
FBgn0033679	110467

Fbgn Identifier	BL line #
FBgn0034443	25875
FBgn0029114	28519
FBgn0250839	28771
FBgn0010226	28885
Fbgn0262473	31044
Fbgn0262473	31477
FBgn0000250	31713
FBgn0052627	33549
FBgn0028693	**34560**
FBgn0000250	34775
FBgn0002789	34963
Fbgn0262473	35628
FBgn0000250	37484
FBgn0001142	**40836**
FBgn0001145	40949
Fbgn0027843	41836
FBgn0000533	41961
Fbgn0024294	41972
Fbgn0024294	42818

Table 1: RNAi stocks tested in primary RNAi screen

Blue marks single stock with over-proliferation phenotype, Green marks two Vienna KK stocks showing dominant phenotypes, Grey marks two stocks showing complete lethality.

background	p<0.05 up-regulated fold>1.5	p<0.05 down-regulated fold>-1.5
ey>COX7a-RNAi	115	51
ey>Delta, COX7a-RNAi	133	86
ey>Delta	95	82
ey>Notch-intra	166	381

Table 2: Differentially regulated genes in first Microarray
Numbers of genes showing differential regulation relative to ey>GFP control.

	ey>COX7a-RNAi			**ey>Delta**		
	term	fold enrichment	p-value	term	fold enrichment	p-value
up-regulated fold>1.5 p<0.1	Glycolysis / Gluconeogenesis (KEGG)	8	6,80E-04	Notch signaling pathway (GO_BP)	16.8	6,10E-09
	Cytochrome P450 metabolism (KEGG)	6.9	1,30E-03	compound eye development (GO_BP)	9.5	8,80E-07
	glutathione metabolic process (GO_BP)	10.2	1,40E-03	cell fate specification (GO_BP)	18.9	1,30E-04
	mitochondrion (GO_CC)	2.7	2,10E-03	transcriptional repressor activity (GO_MF)	16.2	1,80E-03
	gluconeogenesis (GO_BP)	31.9	3,70E-03	sensory organ development (GO_BP)	9	2,20E-03
down-regulated fold>-1.5 p<0.1	extracellular space (GO_CC)	3.2	5,50E-03	-		
	-			-		
	-			-		
	-			-		
	-			-		

Table 3: GO-term analysis of first Microarray analysis
GO-term enrichment was calculated with DAVID using lower stringency p-value than before to increase numbers of genes for the analysis.

background	p<0,05 up-regulated fold>1.5	down-regulated fold>-1.5
ey>ATF4-RNAi	67	77
ey>COX7a-RNAi	472	386
ey>COX7a-RNAi, ATF4-RNAi	71	202
ey>Delta, GFP	91	180
ey>Delta>ATF4-RNAi	118	280
ey>Delta, COX7a-RNAi	443	232
ey>Delta, COX7a-RNAi, ATF4-RNAi	125	163

Table 4: Differentially regulated genes in second Microarray
Numbers of genes showing differential regulation relative to ey>GFP control.

	shared in controls NR versus food		
	term	fold enrichment	p-value
up-regulated fold>1.5 p<0.05	mRNA binding (GO_MF)	3.6	3,70E-05
	imaginal disc derived wing morphogenesis (GO_BP)	2.9	2,20E-04
	protein binding (GO_MF)	2	3,00E-04
	regulation of alternative mRNA splicing (GO_BP)	4.6	6,80E-04
	protein ubiquitination (GO_BP)	3.1	1,80E-03
down-regulated fold>-1.5 p<0.05	plasma membrane (GO_CC)	2.8	1,70E-08
	axon guidance (GO_BP)	4.9	5,60E-06
	learning or memory (GO_BP)	9.8	7,00E-05
	neuromuscular junction (GO_CC)	6.8	5,10E-04
	olfactory learning (GO_BP)	6.9	4,90E-04

Table 5: GO-term analysis for food dependency
GO-term analysis with DAVID for genes showing differential regulation between different larval diet in genetic controls (ey>GFP and ey>Delta>GFP).

Complex	Subunit	reduced eye with ey-Gal4	over-proliferation with ey>Dl	LDH-GFP induction
1	ND-PDSW	+	+	+
1	ND-49	+	+	n.d.
1	ND-23	+	+	n.d.
1	ND-42	+	-	n.d.
1	ND-75	+	-	+
1	NP15.6	+	-	n.d.
2	CG6629 (SdhB)	-	-	n.d.
2	SdhAL	-	-	n.d.
3	UQCR-6.4	-	-	n.d.
3	UQCR-11	-	-	-
3	UQCR-Q	+	-	+
4	COX5a	+	+	+
4	COX6a	+	-	-
4	COX6c	+	-	+
4	COX7a	+	+	+

Table 6: Summary of ETC knockdown phenotypes
Subunits of ETC complexes tested by RNAi within this thesis. + means yes; – means no; n.d. means not determined. This Table is also included in *Sorge et al, submitted*.

III – Discussion

This thesis uncovered the kinase PERK to link defects in the mitochondrial electron transport chain (ETC) to the transcription factor ATF4, thereby inducing a transcriptional stress response.

In the first part of my Discussion I will summarise the major findings of this work, discuss these in the context of the literature and provide an evolutionary perspective on cellular stress signalling.

Part One: A mitochondrial PERK connects ETC defects with the ATF4-induced integrative stress response (ISR) and mitochondrial unfolded protein response (UPR^{mt})

Cellular stress response pathways have evolved to protect cells against a number of internal or external insults. The first to be identified and molecularly characterised was the classical heat-shock response, which triggers expression of molecular chaperones to counteract protein misfolding and aggregation upon heat exposure (Ashburner and Bonner, 1979; Richter et al., 2010). Similarly, mitochondrial proteostasis is maintained through the mitochondrial unfolded protein response (UPR^{mt}), which specifically induces mitochondrial chaperones and proteases (Zhao et al., 2002).

To date many stresses and signals have been described that can trigger the UPR^{mt}. However, our molecular understanding on how these are sensed and translated into a transcriptional or translational response is still poor (Jensen and Jasper, 2014). This can

be partially explained by evolutionary differences between model organisms that complicate the overall picture.

The ATF4-induced transcriptomic response

Recently, Quiros and colleagues (Quirós et al., 2017) conducted a multi-omics approach in cultured human cells to identify a common stress response, which they found activated by four different mitochondrial inhibitors that target different key mitochondrial processes. They found rather distinct effects on the level of mRNA and protein upon treatment with all four inhibitors, but the core response shared by all conditions was mediated by ATF4 and included "cytoprotective genes, which reprogram cellular metabolism through activation of the integrated stress response (ISR)" (Quirós et al., 2017). Further, the authors showed that neither the inhibitors applied in the experiment nor the original conditions used to define the mammalian UPR^{mt} (Münch and Harper, 2016; Zhao et al., 2002) induced the ATF5 target genes of the UPR^{mt} (mitochondrial chaperones and proteases). Considering that their are several technical issues within Quiros et al. too, the mammalian mitochondrial stress response remains controversial. To move forward, disputes between the current publications need to be clarified and the molecular mechanisms that activate either the ATF4-mediated ISR or the ATF5-mediated UPR^{mt} need to be defined precisely.

As with mammals the mitochondrial stress response in *Drosophila* is only poorly understood and studies deciphering the molecular basis are essentially missing. My work now for the first time showed that ATF4 is activated in response to the knockdown of ETC subunits, arguing that this form of mitochondrial stress triggers the same response as in human cells (Quirós et al., 2017), probably through a different molecular mechanism as I will discuss later. The target genes regulated by ATF4 in the eye disc are partially overlapping with several mammalian studies (Khan et al., 2017; Kilberg et al., 2009; Quirós et al., 2017), though the situation in *Drosophila* is different. *Drosophila* ATF4 (dATF4) is the common homologue of human ATF4 (hATF4) and ATF5 (hATF5), which are defined as regulators of the ISR and the UPR^{mt}, respectively. Some functional conservation in the regulation of ISR target genes has been found between dATF4 and

hATF4 (Celardo et al., 2017; Kang et al., 2017), but a transcription factor with functional analogy to hATF5 in mediating the UPR^{mt} has not been described.

My transcriptomic data suggests that dATF4 unites both functions: it induces ISR and UPR^{mt} target genes simultaneously. As part of this thesis I showed ATF4-dependent induction of mitochondrial chaperones Hsc70-5 (human HSPA9), Hsp22 (human CRYAB) and Hsc20 (human HSCB) in response to ETC knockdown. A recent study, published while this thesis was written, showed induction of Hsc70-5 and Hsp22 in cultured *Drosophila* cells that over-expressed dATF4 (Malzer et al., 2018). A result, which is in line with my data and substantiates the role of dATF4 in the regulation of these mitochondrial chaperones. However, both, my data and those of Malzer et al. do not show ATF4-dependent regulation of Hsp60 (human HSPD1), another mitochondrial chaperone and classical UPR^{mt} target (Yoneda et al., 2004).

Therefore, dATF4 is containing most, but not all of the classical UPR^{mt} activity. hATF4 and hATF5 are paralogues with the last common ancestor in Ray-finned fishes (according to the Ensembl database) and dATF4 is most likely orthologous to that last common ancestor. The scenario I have just described, in which dATF4 possesses activity of both vertebrate paralogues, therefor argues for the evolutionary model of sub-functionalisation (Lynch and Force, 2000).

In *C. elegans* the UPR^{mt} is well defined. A transcription factor called Atfs-1 is released from mitochondria under stress and induces UPR^{mt} targets in the nucleus (Haynes et al., 2010; Nargund et al., 2012). Atfs-1 is orthologous to dATF4 and hATF4/hATF5 on the level of protein sequence, but functionally analogous to hATF5 and dATF4, in respect to the UPR^{mt} activity presented in this thesis (the functional analogue of hATF4 and dATF4 in mediating the ISR is called Atf-5 in *C. elegans*).

Overall, the coupling of various types of mitochondrial stress to an ATF4-like transcription factor is shared throughout the animal kingdom, but has evolved differently at the mechanistic level. In the next paragraph, I will present another evolutionary novelty in *Drosophila*, namely how mitochondrial stress is molecularly linked to the induction of ATF4.

Mitochondrial PERK activates ATF4 in response to mitochondrial stress

My results clearly show that PERK, the ER-resident eIF2a-kinase, is required to activate ATF4 downstream of ETC knockdown. A conceptually similar finding has been made by Celardo and colleagues, in two publications studying a *Drosophila* model of Parkinson's disease (Celardo et al., 2016; 2017). In their system, PERK is required to activate ATF4 in response to mitochondrial defects of *pink1* and *parkin* mutants in the *Drosophila* CNS. They revealed the ER stress marker BiP to be induced in muscles of these mutants, and conclude that PERK is activated by canonical ER stress. They finally conclude their argumentation stating that "It is possible that defective mitochondria at the ER contact points are causing the activation of ER stress" (Celardo et al., 2016).

The data I presented in this thesis similarly link ATF4 activation to a different mitochondrial defect in a different tissue of the fly. This effect also requires PERK, but in the absence of canonical ER stress, as neither an ER stress reporter nor UPR^{ER} transcripts were found induced. Therefore, these data argue for a role of PERK in mediating this response independently of ER stress. To investigate this potentially new function, I first performed sequence analysis and found indications for differential sub-cellular localisation of the three PERK isoforms found in *Drosophila*. Subsequent experiments showed that the *in silico* predictions were correct and that the N-terminus of PERK isoform B indeed targets a protein to mitochondria. Based on the experiments carried out so far, I cannot fully exclude a contribution of ER-resident PERK to ATF4 activation, but the emerging picture points towards the mitochondrial PERK that becomes activated upon ETC defects.

Several modes of action for mitochondrial PERK are conceivable, the two most likely will be explained here and are depicted in the general overview in Figure D1. Model A: In an analogous fashion to PERKs mode of action within the ER (Ma et al., 2002), PERK could be imported into mitochondria and inserted into the inner or outer mitochondrial membrane, where it would sense mitochondrial protein folding status via interactions with mitochondrial chaperones or through directly interacting with unfolded proteins (Korennykh and Walter, 2012). In that model, knockdown of ETC subunits as I performed them, would disturb ETC complex assembly and thereby release chaperones from PERK

leading to its activation. Indeed, knockdown or mutational loss of small, accessory ETC subunits (like COX7a) has been shown to disturb assembly of the complexes, leading to the formation of smaller sub-complexes and most likely to the accumulation of subunits that cannot be incorporated (Kemppainen et al., 2013; Nijtmans et al., 1998; Stroud et al., 2016). Less straight-forward in Model A is the explanation on how PERK within the inner mitochondrial membrane could directly phosphorylate cytoplasmic eIF2α.

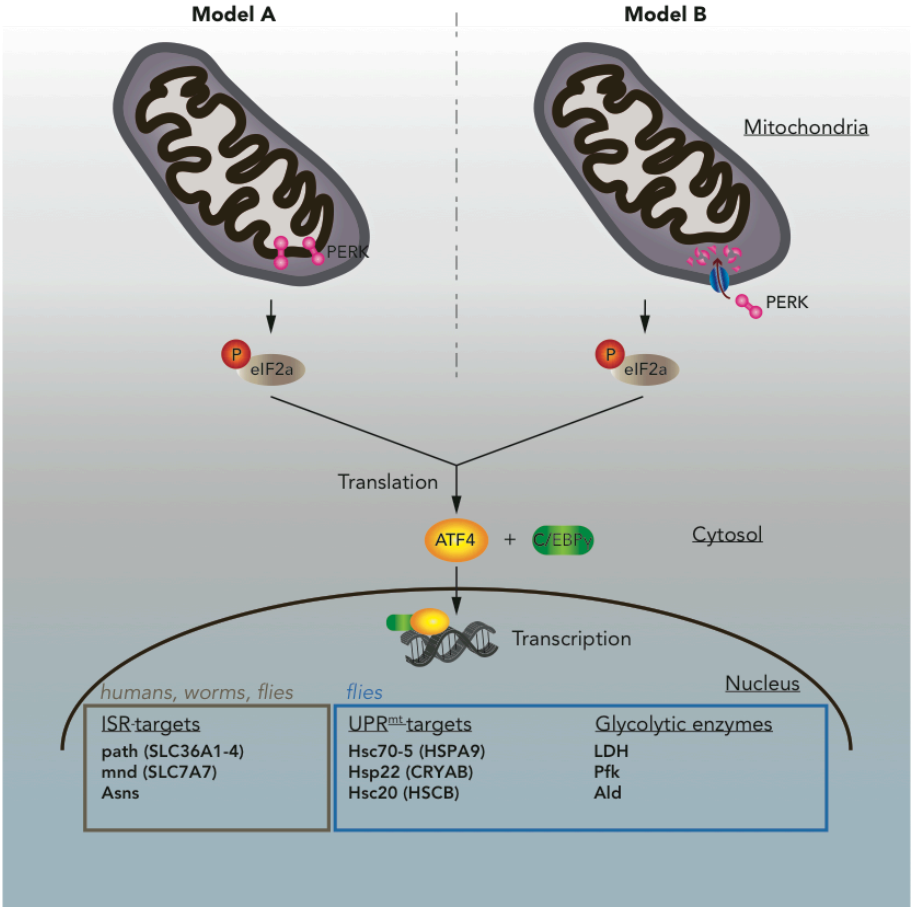

Figure D1: Two models for a mitochondrial PERK
In Model A, PERK resides in the inner mitochondrial membrane, where it senses the folding status of the mitochondrial matrix in a similar manner to its described function in the ER membrane. In Model B, PERK gets imported into mitochondria, but gets degraded immediately. Upon defects in import efficiency, cytoplasmic PERK accumulates and phosphorylates eIF2α.

Model B suggests the import of PERK into mitochondria, followed by degradation, similar to what has been described for the *C. elegans* transcription factor Atfs-1 as discussed earlier (Nargund et al., 2012). Defects in the import efficiency would lead to

cytoplasmic accumulation, dimerization and phosphorylation of eIF2α. As I failed to detect co-localisation of PERK with a mitochondrial marker by IF in fixed tissue (preliminary, see Sorge et al. in preparation), Model B is currently the more plausible one.

Future research will need to clarify the biochemical properties and interactions of PERK inside mitochondria and the mechanism of how a mitochondrial PERK protein phosphorylates eIF2α.

ETC defects trigger the PERK-ATF4 response

Mitochondria are exposed to stresses during their normal function, for example superoxide radicals and related ROS species as a consequence of respiration. In addition, research over the last decades has characterised several exogenous stressors, mostly chemical or genetic that elicit adaptive responses and could potentially occur outside the laboratory as well. As mentioned before, general conclusions are hard to draw, as different approaches are often hard to compare and even the response to the same stresses can be interpreted differently (Quirós et al., 2017).

Within this thesis, I have analysed many mitochondrial ETC subunits and found that knockdown of the majority of them induced the ATF4 response. At the same time, enzymes involved in metabolic reactions, which fuel the ETC with reducing equivalents do not induce ATF4 and are generally not causing phenotypes in the developing eye. Therefore, my data suggest that cells are particularly sensitive to alterations in the level of ETC subunits. Surprisingly, a similar finding has been made in a seminal *C. elegans* study (Yoneda et al., 2004). Yoneda and colleagues showed that mitochondrial chaperone "induction was specific to perturbed mitochondrial protein handling, as neither heat-shock nor endoplasmic reticulum stress nor manipulations that impair mitochondrial steps in intermediary metabolism or ATP synthesis activated the mitochondrial chaperone genes" (Yoneda et al., 2004). Thus, results from *C. elegans* are consistent with the overall implications of my results presented in this thesis and together suggest that disturbances of protein folding or complex assembly are the most potent inducers of the mitochondrial UPR.

A unified picture of the Drosophila mitochondrial stress response

As I have outlined in the previous sections, the mitochondrial stress response has undergone substantial evolutionary changes despite a general conservation of most of the active players. Another difference is the terminology used in published literature as the ATF4-response is referred to as the Integrated Stress Response (ISR) and any activity regulating mitochondrial chaperone and protease mRNA levels is termed mitochondrial Unfolded Protein Response (UPR^{mt}).

All data published in *Drosophila* so far suggest that dATF4 regulates ISR and some UPR^{mt} target genes simultaneously. My work demonstrates that PERK links mitochondrial stress to ATF4, generating the transcriptional response that is shared with ER stress (Lee et al., 2015a) and can be induced by over-expression of dATF4 (Malzer et al., 2018). My work further indicates that the obligate ATF4 co-factor Irbp18 (C/EBPγ) is crucially required for this transcriptional response, though a more detailed analysis of its contribution is necessary.

Some UPR^{mt} target genes from mammalian or *C. elegans* studies are not under control of dATF4. These include the Hsp60 chaperonins (HSPD1 in mammals, hsp-60 in *C. elegans*) and *CG5045*, the ClpP protease (CLPP in mammals, clpp-1 in *C. elegans*) (Yoneda et al., 2004; Zhao et al., 2002). It therefore appears likely that these UPR^{mt} effectors could be under the control of a different pathway, which is apparently not activated upon ETC knockdown in the eye disc. While Yoneda and colleagues did not focus on these aspects, their hsp-6 and hsp-60 transcriptional reporters appear to respond quantitatively different to the stresses they used, implying that they could be regulated through different molecular pathways (Yoneda et al., 2004).

In conclusion, the *Drosophila* mitochondrial stress response is triggered by the mitochondria-localised eIF2a-kinase PERK in response to altered expression levels of ETC subunits. PERK activation leads to ATF4 translation, inducing a transcriptional stress response. The *Drosophila* ATF4 response has unique features, as it induces well-known ISR targets, mitochondrial UPR targets and glycolytic enzymes (summarised in Figure D1).

Part Two: General implications for ETC-knockdown and/or ATF4-dependent phenotypes

Within the previous part I have discussed the molecular pathway that connects ETC stress with the activation of ATF4. Here, I want to focus on the phenotypes caused by ETC knockdown in the developing eye and the contribution of ATF4 to these phenotypes. Moreover, I will provide a more general view on possible implications of these phenotypes.

ETC knockdown phenotypes in the eye disc

I have shown that knockdown of most of the ETC subunits I tested disturbed eye development and caused small eye phenotypes with differentiation defects. The phenotypes I discovered can be classified into two broad categories, which I termed "COX7a-like" and "ND75-like" after their founding members. The major difference between the two categories is the severity of the phenotype, as knockdown of COX7a-like subunits cause slight reductions in eye size and minor differentiation defects, whereas knockdown of ND75-like subunits disrupts eye disc development at early stages and primarily causes dead, headless pharates (where no head capsule is formed by the eye-antenna disc). The severity of phenotypes can be in part explained by the fact that ND75-like phenotypes were established at an earlier developmental time point, when eye-antenna discs were already strongly reduced and apoptotic, or completely absent in late L2 / early L3 larvae. At this developmental stage knockdowns that fall into the COX7a-like category still appeared morphologically wildtype and just started to show LDH-GFP expression, suggesting that the phenotype just started developing precisely at that time.

Early experiments suggested that the difference in the two categories could be a consequence of different types of RNAi constructs with different knockdown efficiencies (Ni et al., 2011). Later experiments, however, falsified this hypothesis as even different types of RNAi constructs for the same gene resulted in identical phenotypes. Therefore, the experiments suggested that quantitatively different requirements for each subunit

exist. A mechanistic explanation could be that the weaker COX7a-like subunits are assembled into ETC complexes at a late step, so their loss only causes mild affects. Nijtmans and colleagues have described the step-wise assembly of Complex IV (Nijtmans et al., 1998), but their results do not correlate well with the phenotypic categories: While COX7a is indeed assembled late into the Complex, after a semi-functional S3 sub-complex has been formed, COX5a, which causes very similar phenotypes as COX7a, is assembled at an earlier, more critical step into Complex IV. Similarly, Complex I assembly was shown to require most of the small subunits for assembly of the complex (Stroud et al., 2016), including the subunit ND-PDSW (NDUFB10 in human) that showed COX7a-like phenotypes.

In summary, my experiments showed ETC subunits to be particularly sensitive genes during development of the *Drosophila* eye, as even relatively mild reductions of mRNA expression levels (approximately 6-fold in Microarray analysis) readily induced eye phenotypes and the ATF4 stress response. My results failed to indicate a specific feature of COX7a-like versus ND75-like subunits. Therefore, the conclusion from my work is that ETC subunits are similarly, but quantitatively unequally required for cell survival and development.

The ATF4-response and its involvement in ETC-knockdown phenotypes

Knockdown of ETC subunits generally disrupted eye development and induced LDH-GFP, arguing for a common regulation of LDH through ATF4. With the single exception of COX6a, which is incorporated into Complex IV together with COX7a, small eye phenotypes and LDH-GFP induction co-occurred. From these observations, an important biological question arises that is whether the ATF4 response is a) causing the developmental defects, b) neutral for the development of the phenotype or, c) beneficial for the cells' development.

My results cannot provide a simple answer to this question, as the phenotypic consequence of ATF4 knockdown is changing dependent on nutrition and strength of the COX7a knockdown (knockdown of ATF4 alone has no consequence for eye development). Clearly, mild knockdown of COX7a and ATF4 together (on standard fly

food) rescues most phenotypes caused by COX7a alone, arguing that the ATF4 response is actually causing the small eye phenotype and the differentiation defects in the posterior eye under these conditions. At the same temperature but under nutrient restriction, the ATF4 response (which is stronger under these conditions) appears to be beneficial for survival and differentiation, as the double-knockdown exhibits higher lethality and more severely reduced eyes. At higher temperature, where knockdown of both COX7a and ATF4 should be enhanced, the double-knockdown is lethal and shows headless pharates (similar to ND75-like phenotypes), also suggesting that the ATF4 response is required to maintain cell survival under conditions of stronger COX7a depletion. Overall, the ATF4 response appears to have the expected "cyto-protective" function, especially under conditions of stronger interference with ETC function. Instead, very mild attenuation of COX7a function seems to induce the ATF4 response in the absence of an actual developmental defect of the cells, which in this case acts "over-protective".

The cooperation between COX7a knockdown and Delta over-expression is strictly dependent on ATF4 function. Knockdown of ATF4 rescues the cooperative over-proliferation and causes an eye phenotype that resembles a slightly smaller ey>Dl eye. The rescue is still apparent under nutrient restriction or enhanced knockdown conditions, though a direct comparison with the crosses in the ey-Gal4 setup (mentioned in previous paragraph) is not possible due to differences in the genetic setup of the experiments. The increase in differentiation defects found in "rescued discs" (Delta over-expression, COX7a and ATF4 knockdown) at higher temperature suggest again that the ATF4-mediated adaptation is in principle protecting cellular fitness and in this case the potential of cells to enter a differentiation programme.

The context-dependent role of ATF4 (schematically depicted in Fig. D2) can be explained by (i) the temporal (and spatial) separation between the two main Delta, COX7a-induced cellular phenotypes, over-proliferation in the anterior progenitor compartment and differentiation defects in the posterior compartment, and (ii) a different role of the ATF4-mediated adaptation in the development of these two processes.

Nevertheless, the transcriptional response induced by ATF4 appears to be the molecular element explaining the genetic interaction between ETC knockdown and Notch activation.

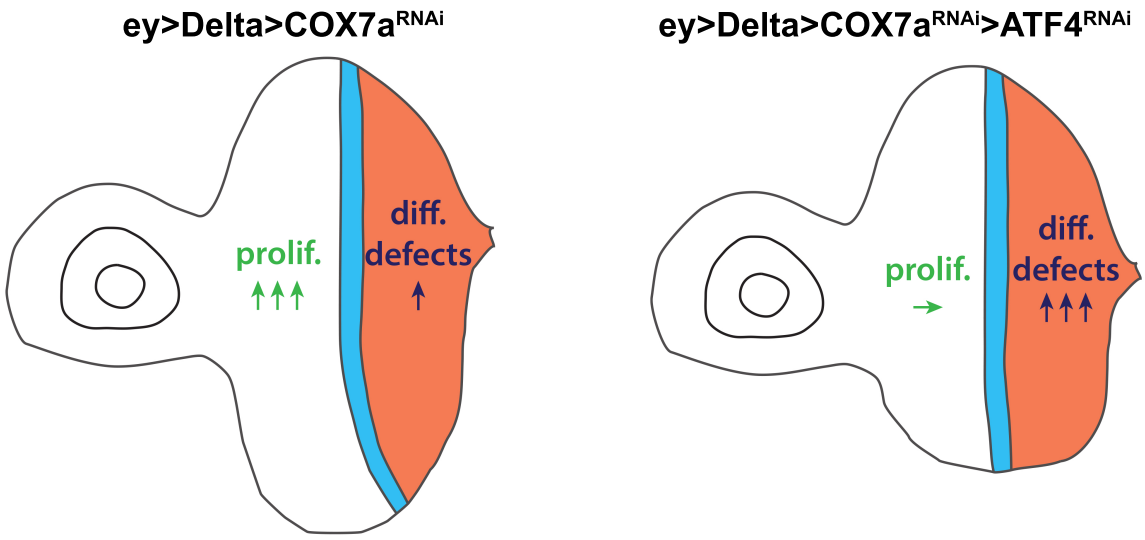

Figure D2: ATF4-dependent modulation of COX7a phenotypes
Schematic representation of indicated mid-L3 discs of the Delta,COX7a (left) or Delta,COX7a,ATF4 (right) genotype. Arrows indicate strength of the phenotypes (proliferation or differentiation defects) in relation to the Delta background.

The ATF4-response in cancer

My results show that the ATF4-mediated adaptation acts pro-proliferative with activated Notch- or EGFR/Ras-pathways in eye progenitor cells. A conceptually similar, but mechanistically different scenario has been described for mutant clones of ETC subunits that express oncogenic Ras^{v12} and drive non-autonomous overgrowth (Ohsawa et al., 2013). Ohsawa and colleagues showed high levels of ROS in ETC^{-}/Ras^{v12}-expressing clones that trigger JNK signalling, which subsequently inactivates the Hippo cascade, leading to Yki-dependent induction of the Wg- and Upd-cytokines. While I detected some residual activation of JNK- and Yki-activity in Delta,COX7a discs, activation of JNK was not required for over-proliferation and clearly not induced by ROS species, as no increase in ROS production could be detected. It is of interest to test, if ATF4 is also activated in these clones and how it contributes to the non-autonomous phenotypes. Apparently, there are several discrepancies between the results from Ohsawa et al. and a previous study using the same ETC mutant clones (Owusu-Ansah et

al., 2008), for example in terms of ROS production. While Owusu-Ansah and colleagues detect high amounts of ROS by DHE staining within Pdsw^{-} clones, Ohsawa and colleagues do not detect any in the same clones (Ohsawa et al., 2013; Owusu-Ansah et al., 2008). In my experiments, live-imaging with DHE showed a clear mitochondrial signal throughout the eye disc (consistent with mitochondrial respiration producing superoxide radicals) and extremely rarely a strong nuclear signal in single cells. I never detected increases in DHE signal intensities.

In regard to existing literature for *Drosophila*, my results are the first to link the ATF4 response to proliferative behaviour. In the mammalian field, GCN2- or PERK-dependent ATF4 activation in cancer tissues has been recognised for several years (Ameri et al., 2004; Bi et al., 2005). More recently, a requirement for ATF4 during oncogenesis has also been described (Horiguchi et al., 2012; Ye et al., 2010) and ATF4 has been considered as an attractive cancer drug target (Singleton and Harris, 2012). At present, the common view from these publications is that several stresses, frequently occurring in tumours, can activate ATF4. The activity of ATF4 in mediating expression of amino acid transporter genes (Kilberg et al., 2009), one-carbon metabolic genes (Bao et al., 2016) or the asparagine synthetase gene (Ye et al., 2010) are adaptations that have been attributed with cancer cell survival or proliferative capacity. Furthermore, an ATF4 response has been shown in several contexts to confer resistance against chemotherapeutic drugs, because chemotherapy-stressed cancer cells induce ATF4 and an ATF4 target gene reverses the effect of the initial treatment (Igarashi et al., 2007; Wang et al., 2011). In accordance with my results on the differential phenotypic contributions of ATF4 to COX7a-induced phenotypes (see above), the multitude of cellular functions regulated by ATF4 explain its very general requirement. However, since tumour cells within different organs suffer from different shortcomings or stresses, different aspects of the ATF4 response can become important. Overall, the broad-spectrum adaptation mediated by ATF4 can confer adaptations to various cells during normal development or oncogenic transformation.

To get insights into a possible general role of ATF4 activation in cancer, I made use of the publicly available RNA-seq data of The Cancer Genome Atlas (TCGA,

http://cancergenome.nih.gov/). In order to browse through the enormous amount of data I used Cancer RNA-seq Nexus (CRN, (Li et al., 2016)) and the human protein pathology atlas (Uhlen et al., 2017) for a general assessment of prognostic correlation of gene expression levels and patient survival. I note that this type of "snapshot analysis" is not statistically tested and simply shows correlation of a small number of up-regulated genes with prognosis (which is statistically tested). CRN indicated a relatively clear trend for ATF4 target genes being up-regulated in later stages of Renal Clear Cell Carcinoma compared to normal kidney tissue. Other types of cancer showed a similar but less pronounced trend (including liver and breast cancer). Even more intriguing than pure expression analysis were the results from the protein pathology atlas, which shows a statistically significant correlation between high expression levels and disease outcome. I have chosen 13 ATF4 target genes (CHOP, TRIB3, ASNS, SLC1A4, SLC1A5, PSAT1, CHAC1, PSPH, SLC7A11, VEGFA, SHMT2, MTFHD2, BCAT1), covering various aspects of the ATF4 adaptation, from the recent literature (Bao et al., 2016; Celardo et al., 2017; Kilberg et al., 2009; Quirós et al., 2017) as well as ATF4 itself. From these 14 genes, 11 scored as unfavourable prognostic markers in renal cancer and 8 as unfavourable prognostic markers in liver cancer. While this analysis just shows correlation for a limited number of ATF4 target genes, it nevertheless strongly suggests ATF4 activation in these cancers and an overall negative contribution of the response to the patients' survival.

Part Three: An assessment of experimental conditions

Throughout this thesis I have presented results of experiments aimed to unravel the molecular mechanisms causing COX7a-knockdown phenotypes. In the last part of this thesis, I want to provide additional information for a readership that is interested in a more general assessment of experimental conditions that a researcher should be aware of. This information is not backed up by statistical analysis, but rather represents a personal opinion after eight years of fly work, given with best intentions.

Effects of larval density on development and phenotypes

Recently, a study identified the underlying mechanism for negative effects of crowding on adult lifespan, which had been recognised almost a century ago (Pearl and Parker, 1922). The mechanism involves "autotoxins" that accumulate depending on larval and adult diet and become toxic for the fly in a concentration-dependent manner (Stefana et al., 2017).

Conceptually, I have made similar observations throughout my studies on COX7a and other eye phenotypes. Importantly, these phenotypes are not limited to COX7a, but I have observed identical dependencies with unrelated genotypes (for example ey>Dl>Pros) and phenotypes. The "metastasis" phenotype, where ectopic eye tissue is detected in the thorax or abdomen of adult flies, due to collective migration of eye disc cells (S. Sorge, unpublished observation), was detected in several genotypes by me or colleagues (Zhai et al., 2012). This phenotype failed to show in my hands without crowding. I noticed that the dependency of COX7a phenotypes on high larval densities could be counteracted by a low-protein diet (see Results Chapter Eight). Experiments with pre-conditioned vials further suggested that it is not the absolute density of larvae in a vial, but a modification of the food that increases COX7a phenotypes (J. Theelke and S. Sorge, unpublished observation). The modification of the food could involve the secretion of molecules with negative consequences for development like autotoxins, could be caused by the change in food texture that occurs through the secretion of amylase into the food ("social digestion", see (Gregg et al., 1990; Sakaguchi and Suzuki, 2013) or could be a dilution of essential nutrients in the food. With our experiments, we cannot properly discriminate between these and other possibilities. The effects of larval crowding and a low-protein diet could still be mechanistically unrelated. At present, the practical implications are therefore more definitive than the explanations:

I propose that defined culture conditions are required for any developmental phenotypes involving the larval stage. These conditions have to include not only the food composition, as has more recently been recognised by many laboratories, but also the larval density within the vial. A practically applicable approach also for screening purposes is to use a defined number of virgins per vial and egg-depositions of one day

length, so that offspring numbers remain within a comfortable window (approximately 10-15 larvae per cm^2 food surface). Limiting the time of egg-deposition also prevents late-born larvae from suffering disproportionately from the altered food.

RNAi phenotypes in the larval eye-antenna disc

The binary Gal4/UAS-system for gene expression (Brand and Perrimon, 1993) uses the yeast transcriptional activator Gal4, whose activity is temperature-dependent. RNAi-mediated knockdown of genes requires the effector molecules of dsRNA- or shRNA-constructs to bind their target mRNAs, leading to their degradation. Knockdown efficiency can be enhanced by expression of Dicer2 with dsRNA-constructs or generally by increasing the temperature for higher Gal4 activity. For my primary RNAi-screen I reared offspring at 27°C without Dicer2 expression. The screen revealed a total of only three bona fide phenotypes amongst 105 candidates, suggesting either poor candidate selection or conditions not favouring phenotype manifestation. Though not explicitly considered at this early phase of the project, larval densities during the screen were relatively low, giving another explanation for the rather low effects compared to similar approaches (T. Reiff, personal communication). All later experiments were generally carried out at 25°C, where Gal4 activity is even lower. Under these conditions, over-expression using UAS-Delta increased *Delta* mRNA by approximately 4- to 6-fold and knockdown of COX7a with UAS-COX7a^{dsRNA} reduced *COX7a* mRNA levels by approximately 4- to 8-fold. *ATF4* mRNA levels were less strongly reduced by UAS-ATF4^{dsRNA} (2- to 4-fold), yet fully impaired ATF4 translation and rescued COX7a phenotypes. Together, these numbers suggest that my experiments operated at a relatively low level of mRNA expression changes. It further suggests that over-expression is not necessarily stronger than RNAi-knockdown and that the correlation between reductions on the mRNA level, protein levels and "function" is not necessarily very high.

Throughout all my RNAi experiments, COX7a and the other ETC subunits tested stand out as particularly sensitive genes. As I have shown (see Results Chapter Ten), other metabolic enzymes appear less sensitive, even when using validated RNAi-

constructs. Though conclusions from negative results ("no phenotype") are generally difficult, the high proportion of ETC subunit knockdowns that caused developmental defects still suggests that these RNAi constructs are functional with high probability, but that the mild reduction in mRNA levels (2- to 8-fold in my experiments) will only uncover functions of particularly sensitive genes.

The only other RNAi constructs I tested that effectively caused phenotypes in a wild-type background, were a member of the retinal determination network, eyes absent, a component of the proteasome, Rpn12, and Glutamine synthase 1 (Gs1). The apparent relative importance of Gs1 might seem surprising, given the relative unimportance of many other metabolic enzymes I tested. It might also hint at an important metabolic function of Gs1 during disc development, where the metabolic properties of progenitors remain completely unknown.

The metabolic status of imaginal discs

I have described some of the important metabolic constraints operating during larval development within the introduction of this thesis. For example, the amino acid transporter Slimfast, which is required in the fat body to maintain Tor signalling (Colombani et al., 2003). However, surprisingly little is known about amino acid transport or carbohydrate metabolism in imaginal progenitors. According to my microarray, Slimfast is not expressed in eye progenitors at all, but several other amino acid transporters, like minidiscs, pathetic, JhI-21 or CG5535 are expressed at intermediate levels. In principle, this could indicate that imaginal progenitor cells simply use different transporters for the same aim - maintaining Tor signalling - but it is also conceivable that alternative mechanisms operate to uncouple Tor activity from intracellular amino acid availability, similar to processes during "brain sparing" (Cheng et al., 2011). Interestingly, the study from Cheng and colleagues also showed that wing discs grow normally in animals with hypomorphic Tor mutations, while Tor mutant clones in the wing disc grow slower (Cheng et al., 2011). These results might therefore suggest that imaginal disc progenitors are sensitive to relative differences in Tor activity, but maintain sufficient Tor

output under conditions where absolute Tor activity is reduced. Given these findings, it is not surprising that a heterozygous mutation in Tor did not alter the Delta,COX7a-induced over-proliferation.

According to GO-annotations, the *Drosophila* genome encodes for 25 proteins in the family of "SLC2 FAMILY OF HEXOSE SUGAR TRANSPORTERS". Of these, my transcriptomic analysis suggests only three to be expressed at low levels and one gene at intermediate levels. These three are the Trehalose-transporter *Tret1-1* and two uncharacterised transporter genes, *CG10960* and *CG4797*. IF staining against Tret1-1 failed to show clear immunoreactivity in progenitors of control discs (see Results Chapter Five), arguing that the low mRNA levels might reflect expression in glia cells, which show clear protein accumulation. The sugar transporter expressed at intermediate levels is called *sugar transporter 1*. Given this data, it is at present unclear how imaginal progenitor cells take up glucose or trehalose from the hemolymph and, given the overall low expression of transporters, and how relevant conventional sugar metabolism through glycolysis and oxidative phosphorylation is.

IV – Conclusions

With the work presented in this thesis I could contribute to our understanding of two aspects of basic biological research. The first aspect is the molecular wiring of an intracellular stress response pathway. The second aspect is the implication this stress response pathway has on organismal development.

Genetic perturbance of mitochondrial protein homeostasis – that is RNAi-mediated knockdown of single subunits of the electron transport chain (ETC) – induced a transcriptional response in the nucleus through ATF4. Activation of ATF4 required the eIF2α-kinase PERK, which has well documented functions as a sensor of protein homeostasis within the endoplasmic reticulum. Through experiments in cultured cells I could show that the *Drosophila* genome encodes a PERK isoform that is targeted to mitochondria, arguing that this isoform acts as a sensor of mitochondrial protein homeostasis.

The PERK-ATF4 response protects cellular fitness during mitochondrial protein folding stress and helps developing cells to properly enter a differentiation programme. At the same time, the modulation of cellular metabolic functions through this adaptation also induces a proliferation-promoting condition within dividing progenitor cells. When combined with a growth-promoting signalling pathway, cells over-proliferate and cause strongly enlarged eye phenotypes.

V – Materials and Methods

1. Fly husbandry

Flies were maintained according to standard procedures (Greenspan, 2004). Homozygous or balanced fly stocks were kept in small vials (2,5cm diameter) on a standard cornmeal-molasses food (see Media and Solutions for formulation) at room-temperature (23°C). Crosses were set up with roughly equal numbers of virgins and males and maintained in a 25°C incubator. Virgins were collected by collecting all eclosed females twice a day with overnight incubation at 18°C, thereby preventing the existence of sexually mature males. Experimental fly crosses (to compare phenotypes or perform IF analysis) were set up from the same batch of virgins and crossed to males of different "tester" stocks (RNAi, etc). To avoid larval crowding (see Results and Discussion), experimental crosses used defined numbers of virgins per vial (10 or 12) and short egg collections (usually one day, maximum two days). Whenever possible, experimental crosses contained the same number of UAS-transgenes (to account for possible dilution of Gal4 activity) and were set up from the same meiotic-recombinant stocks. Stable recombinant stocks (especially ey>COX7a^{RNAi} and ey>Dl>COX7a^{RNAi}) showed progressive silencing of one of the transgenes after many generations.

For crowding experiments, crosses were kept in small cages and eggs were collected on small petri dishes (6cm) with fly food or apple juice-agar and fresh yeast paste. Freshly hatched L1 larvae (24h to 26h after egg-lay) were transferred with a pin to vials.

For the primary RNAi screen (see Results Chapter One), crosses were set up in big fly food vials (bottles; 6cm diameter) with 25 virgins and males from the Vienna KK library maintained in the laboratory of Michael Boutros (DKFZ, Heidelberg). Crosses were incubated at 27°C.

Phenotypic categories scored in RNAi screen and later experiments evolved over time. For some of the quantifications shown in this thesis, some phenotypic categories were grouped together. The main categories that I discriminated are defined as follows:

"wildtype"	– like wildtype in size and morphology (lattice and bristles)
"reduced"	– reduced in size and/or defective in morphology; three graduations of reduced were scored
"reduced and fold"	– eyes at the same time reduced in occupied area of the head but folded outwards; also included cuticle overgrowth; usually represented severe phenot.
"reduced eyDl"	– typical eyDl morphology but reduced in overall eye size
"eyDl"	– typical eyDl, meaning elongated along DV axis and with mild roughness
"mild folding"	– like eyDl but with at least one clear fold in the eye tissue
"strong folding"	– grouped from "intermediate folding" (several clear folds throughout the eye) and "strong folding" (folded and with severe three-dimensional outgrowths)
"metastasis"	– flies exhibiting red pigmented eye tissue in parts of the body distant from the head
"dead pupae"	– pharates that failed to eclose from the pupa case or pupae that died during metamorphosis

For the Microarray analysis, crosses were set up in small cages and flies allowed to lay eggs directly on fly food poured into petri dishes (first Microarray analysis) or protein-restricted fly food in petri dishes (second Microarray analysis).

The main Gal4-line used, eyeless-Gal4, was created by meiotic recombination of the eyeless-Gal4, UAS-Delta stock (from Maria Dominguez, Alicante, Spain; originally created by Uwe Walldorf, Saarbrücken, Germany) and selection against the Delta phenotype and for Gal4-activity in the eye disc. The eyeless-Gal4 stock was homozygous lethal as the original eyeless-Gal4, UAS-Delta stock. Two other Gal4-lines (ey3.5-Gal4 and so-Gal4 from Bloomington Drosophila Stock Center, BDSC) with similar activity in the eye disc were tested and gave near-identical phenotypes. UAS-RNAi stocks were from the Vienna KK library (made available through M. Boutros) or the TRiP-project (available through BDSC). Some UAS-ORF stocks were from FlyORF (Zurich, Switzerland). Most other stocks were distributed by the BDSC or obtained from the Drosophila community. All RNAi lines used in the primary screen are found in the Results part, Table 1 Appendix. All other stocks are found in the following Tables MM1 and MM2.

group	name	genotype	source
Gal4-lines	ey-Gal4	w[*]; P{w[+mC]=ey-GAL4};	Maria Dominguez, Alicante
	ey3.5-Gal4	y[1] w[1118]; P{w[+mC]=ey3.5-GAL4.Exel}2	BDSC (BL-8220)
	so-Gal4	y[1] w[*]; P{w[+mC]=so7-GAL4}A	BDSC (BL-26810)
	GMR-Gal4	w[*]; P{w[+mC]=GAL4-ninaE.GMR}12	BDSC (BL-1104)
UAS-lines	UAS-BskDN	w[*];;P{UAS-Bdsk[DN]}MU#97	Mirka Uhlirova, Köln
	UAS-Xbp1-EGFP	w[*]; P{w[+mC]=UAS-Xbp1.EGFP.LG}2/CyO	BDSC (BL-39720)
	UAS-Delta	w[*];P{w[+mC]=UAS-Dl};	Maria Dominguez, Alicante
	UAS-Notch-intra2	P{ry[+t7.2]=hsFLP}1, y[1] w[*]; P{w[+mC]=UAS-N.intra.GS}2/CyO; MKRS/TM2	BDSC (BL-52008)
	UAS-GFPnls	w[*]; UAS-GFPnls;	Bruce Edgar, Salt Lake City
	UAS-mCD8-GFP	y[1] w[*]; P{w[+mC]=UAS-mCD8::GFP.L}LL5, P{UAS-mCD8::GFP.L}2	BDSC (BL-5137)
	UAS-Flybow1.1	P{UAS-Flybow.1.1}VIE-260B	BDSC (BL-35537)
	UAS-rasv12	w[*]; P{w[+mC]=UAS-ras85D[v12]};	unknown
	UAS-p35	w[*]; P{w[+mC]=UAS-p35.H}BH2	BDSC (BL-5073)
	UAS-AOX	w[*];;P{UAS-AOX[F24]}#54	Deniz Senyilmaz, Heidelberg
	UAS-CycE	w[*]; P{w[+mC]=UAS-CycE.L}ML1	Bruce Edgar, Salt Lake City
	UAS-mitoGFP	w[*]; P{w[+mC]=UAS-mito-HA-GFP.AP}2; P{w[+mW.hs]=GawB}C57/T(2;3)TSTL, CyO: TM6B, Tb[1]	BDSC (BL-52001)
others	LDH-GFP	w[*];;P{LDH-GFP}	Z. Zhai, Lausanne
	TRE-GFP	w[*];P{TRE-GFP}attP16;	M. La Fortezza, München
	TorDP	w[*];FRT40A, Tor[DP]/CyO;	J. Romero, Heidelberg

Table MM1: List 1 of *Drosophila melanogaster* stocks used

group	name	genotype	source
RNAi-lines	COX7a-RNAi	P{KK110870}VIE-260B	VDRC (v106661)
	COX7a-RNAi	y[1] sc[*] v[1]; P{y[+t7.7] v[+t1.8]=TRiP.HMC04889}attP40	BDSC (BL-57572)
	COX5a-RNAi	P{KK115466}VIE-260B	VDRC (v109070)
	COX5a-RNAi	y[1] v[1]; P{y[+t7.7] v[+t1.8]=TRiP.HMJ22367}attP40	BDSC (BL-58282)
	cype-RNAi	y[1] sc[*] v[1]; P{y[+t7.7] v[+t1.8]=TRiP.HMS00815}attP2	BDSC (BL-33878)
	levy-RNAi	y[1] sc[*] v[1]; P{y[+t7.7] v[+t1.8]=TRiP.HMS05703}attP40/CyO	BDSC (BL-67789)
	ND75-RNAi	y[1] sc[*] v[1]; P{y[+t7.7] v[+t1.8]=TRiP.HMS00853}attP2	BDSC (BL-33910)
	ND75-RNAi	y[1] sc[*] v[1]; P{y[+t7.7] v[+t1.8]=TRiP.HMS00854}attP2	BDSC (BL-33911)
	ND75-RNAi	P{KK108222}VIE-260B	VDRC (v100733)
	ND23-RNAi	y[1] v[1]; P{y[+t7.7] v[+t1.8]=TRiP.HMC03353}attP40	BDSC (BL-30487)
	ND-PDSW	y[1] v[1]; P{y[+t7.7] v[+t1.8]=TRiP.JF03271}attP2	BDSC (BL-29592)
	ND-49	y[1] v[1]; P{y[+t7.7] v[+t1.8]=TRiP.HM05059}attP2	BDSC (BL-28573)
	UQCR-Q	y[1] sc[*] v[1]; P{y[+t7.7] v[+t1.8]=TRiP.HMC03242}attP2	BDSC (BL-51357)
	UQCR-11	y[1] sc[*] v[1]; P{y[+t7.7] v[+t1.8]=TRiP.HMC05769}attP40	BDSC (BL-64896)
	UQCR-C1	y[1] sc[*] v[1]; P{y[+t7.7] v[+t1.8]=TRiP.HMC03394}attP2	BDSC (BL-51822)
	ATF4-RNAi	y[1] v[1]; P{y[+t7.7] v[+t1.8]=TRiP.JF02007}attP2	BDSC (BL-25985)
	PERK-RNAi	y[1] v[1]; P{y[+t7.7] v[+t1.8]=TRiP.HMJ02063}attP40	BDSC (BL-42499)
	PERK-RNAi	P{KK100348}VIE-260B	VDRC (v110278)
	GCN2-RNAi	y[1] sc[*] v[1]; P{y[+t7.7] v[+t1.8]=TRiP.HMC06316}attP40	BDSC (BL-67215)
	LDH-RNAi	P{KK102330}VIE-260B	VDRC (v110190)
	Tret1-1-RNAi	y[1] sc[*] v[1]; P{y[+t7.7] v[+t1.8]=TRiP.HMS02573}attP2	BDSC (BL-42880)
	path-RNAi	y[1] sc[*] v[1]; P{y[+t7.7] v[+t1.8]=TRiP.HMS05365}attP40	BDSC (BL-64029)
	mnd-RNAi	y[1] sc[*] v[1]; P{y[+t7.7] v[+t1.8]=TRiP.HMC05214}attP40	BDSC (BL-62207)
	BCAT1-RNAi	y[1] sc[*] v[1]; P{y[+t7.7] v[+t1.8]=TRiP.HMS01832}attP2	BDSC (BL-38363)
	PDH-RNAi	y[1] v[1]; P{y[+t7.7] v[+t1.8]=TRiP.HMS02170}attP40/CyO	BDSC (BL-40922)
	CG5214-RNAi	P{KK109081}VIE-260B	VDRC (v108403)
	Mpc1-RNAi	P{KK102734}VIE-260B	VDRC (v103829)
	PDHB-RNAi	P{KK107865}VIE-260B	VDRC (v104022)
	mCherry-RNAi	y[1] sc[*] v[1]; P{y[+t7.7] v[+t1.8]=VALIUM20-mCherry}attP2	BDSC (BL-35785)
	EGFP-RNAi	y[1] sc[*] v[1]; P{y[+t7.7] v[+t1.8]=VALIUM20-EGFP.shRNA.3}attP2	BDSC (BL-41560)

Table MM2: List 2 of *Drosophila melanogaster* stocks used

2. Immunofluorescence

Immunofluorescence (IF) antibody staining was carried out according to standard protocols (Patel, 1994). Larvae of appropriate age were collected from vials and washed in PBS to remove residual food. Larvae were rough dissected in PBS by holding larvae in their middle third and pulling with the other forcep on the mouth hooks. "Larval heads" (typically containing mouth hooks, cephalopharyngeal skeleton, eye-antenna disc and CNS) were transferred to Eppendorf tubes on ice with PBS containing 0,01% Tween-20. Tissues were fixed with 4% Paraformaldehyde in PBS for 18 minutes on a nutator. Fixation was followed by extensive washes with PBTw (at least 2 times rinse; 3 times wash for at least 10 minutes). One 10 minute wash with PBTx followed to enhance antibody penetration. Blocking was done with 1% blocking reagent (BR, from PerkinElmer) in PBTw for at least 1 hour at RT. Primary antibody incubation was usually done overnight at 4°C in BR. Extensive washes followed as before with PBTw. Secondary antibody incubation was either overnight at 4°C or for 2 hours at RT and was done in BR. After the same washes as before, PBTw was removed and tissue incubated overnight in VectaShield with DAPI (H-1200 from VectorLabs). Fine dissections to release eye-antenna discs from the rest of the larval head were done in VectaShield directly prior to mounting. Discs were oriented on a microscopic glass slide with a "pulled glass needle" in a 10µl drop of fresh VectaShield. Cover slips used were 22x22x0,17mm (#1.5H Marienfeld Superior).

Table MM3 lists all primary and secondary antibodies used.

	name	source	host	dilution
Primary Antibodies	anti-Dachshund	DSHB (mAbdac1-1)	mouse	1:300
	anti-ELAV	DSHB (7E8A10)	rat	1:300
	anti-Wingless	DSHB (4D4)	mouse	1:50
	anti-Armadillo	DSHB (N27A1)	mouse	1:100
	anti-phospho Histone 3	SantaCruz sc-8656	rabbit	1:1000
	anti-ATP5a	Abcam ab14748	mouse	1:500
	anti-Calreticulin	Abcam ab2907	rabbit	1:500
	anti-cleaved Caspase 3	Cell Signaling	rabbit	1:200
	anti-dATF4	Min-Ji Kang, Seoul	guinea pig	1:50
	anti-dPERK	Stefan Marciniak, Cambridge	rabbit	1:1000
	anti-Tret1-1	Stefanie Schirrmeier, Münster	guinea pig	1:50
Secondary Antibodies	anti-rat-488	Jackson ImmunoResearch (112-545-167)	goat	1:300
	anti-rat-Cy3	Jackson ImmunoResearch (112-165-167)	goat	1:300
	anti-mouse-488	Jackson ImmunoResearch (115-545-166)	goat	1:300
	anti-mouse-Cy3	Jackson ImmunoResearch (115-165-166)	goat	1:300
	anti-guinea pig-Cy3	Jackson ImmunoResearch (706-165-148)	donkey	1:300
	anti-guinea pig-647	Jackson ImmunoResearch (706-605-148)	donkey	1:300
	anti-rabbit-488	Jackson ImmunoResearch (711-545-152)	donkey	1:300
	anti-rabbit-Cy3	Jackson ImmunoResearch (111-165-144)	goat	1:300
	anti-rabbit-633	Thermo Fisher Scientific (A-21070)	goat	1:300

Table MM3: List of primary and secondary Antibodies used

3. Microscopy and image analysis

IF stainings of dissected larval tissues were mainly imaged with a Leica TCS SP8 confocal (Ingrid Lohmann laboratory) or a Nikon A1R confocal (Nikon Imaging Center at the University of Heidelberg). Laser lines used were 405nm, 488nm, 552nm and 637nm. In most cases, Z-stacks were acquired covering the whole three-dimensional volume of eye-antenna discs, other tissues or S2R+ cells.

Live-imaging of dissected eye-antenna discs or cultured S2R+ cells was carried out in Schneider's Drosophila Medium (Gibco) in glass-bottom dishes (MatTek) using the same confocal microscopes.

Photographs of adult eyes were taken on a Zeiss Discovery V12 stereomicroscope equipped with Zeiss HR3 camera.

Fly work and larval dissections were carried out on Zeiss Stemi or Nikon SMZ745 stereomicroscopes.

Microscopic images were captured with the manufacturers software. Most image analysis was done with the ImageJ distribution Fiji. As a general rule, brightness was adjusted where necessary, but contrast was not enhanced. For some IF stainings, "rolling ball background subtraction" was used, with the same parameters for all images of an experiment. Measurements of tissue sizes were done by manually marking the relevant areas (using anti-Dachshund IF staining as marker for eye territory where possible). Naturally occurring folding of the ventral or dorsal extremes of the eye disc were accounted for. To normalise for differences in both developmental age and artefacts from mounting (flattening), sizes were expressed as relative to the size of the antenna a2 segment (meaning the a2 plus the inner a3 and aR segments) of the same eye-antenna disc. Apoptotic foci (marked by cleaved Caspase-3 antibody) or mitotic cells (marked by phospho-Histone 3 antibody) were counted with the Fiji plugin "3D Objects Counter" using Otsu-thresholded Z-stacks.

4. RNA-isolation, RT, qPCR and Microarray

Dissected tissues or cell pellets for mRNA expression analysis were lysed and homogenised in TriZol (Invitrogen). Homogenates were stored at -80°C if necessary. Total RNA isolation was carried out using the DirectZol Micro-Prep column-based kit

(ZymoResearch) according to the manufacturers instructions. On-column DNAseI digest was performed to remove genomic DNA.

Total RNA for Microarray was eluted with 8µl H_2O and subsequently delivered to the GeneCore facility of EMBL Heidelberg. The facility carried out subsequent steps of reverse-transcription and in vitro transcription using Affymetrix GeneChip® 3' IVT Express Reagent Kit (for first Microarray analysis) or GeneChip® 3' IVT PLUS Reagent Kit (for second Microarray analysis) with 50ng total RNA as starting material. Finally, cRNA was hybridised to Affymetrix Drosophila Genome2.0 chips. Analysis of intensity files was carried out with Affymetrix Expression Console and Transcriptome Analysis Console software using RMA normalisation. Reported p-Values of fold-changes are based on ANOVA-analysis (One-way Between-Subject ANOVA, unpaired).

Reverse transcription was carried out with RevertAid-RT kit (ThermoScientific) with 500ng or 1µg total RNA starting material. Quantitative PCR was carried out with PlatinumSYBRGreen (Invitrogen) in 20µl reactions in 96-well plates. An Applied Biosystems StepOnePlus cycler was used for qPCR (Thomas Holstein laboratory). Primer pairs for qPCR were designed with Primer3 and are listed in Table MM4.

target name	forward primer	ID forward	reverse primer	ID reverse	product size
Sgs3	GCAAGATCCGTCAATGCGTC	IL02402	AGCGTAGTCAAAGTCCTGGC	IL02403	149
Vglut	CATTGTGGCCAACTTCTGCC	IL02404	AACATGCCGCCAAATGGAAC	IL02405	162
chaoptin	AATTCCTCGTGGAGTGGACG	IL02406	TCAGCGAATTGTAGCCCAGA	IL02407	160
eya	GCTACCGCAAGATCAAGGAC	IL02408	GCTGGGAGATCATGCTCAGG	IL02409	165
elav	ATGTTCTAAACGGCCTGCGA	IL02472	GCAGAATGCGCGATGTGATT	IL02473	180
zfh2	TACAATCGGTGCCTGTTCCG	IL02410	GCCAATTGCATTGGGGACAT	IL02411	158
Dll	GCACTTTGTTCGTGTGCAGT	IL01663	TCACTTAGCTCGACGCAGAA	IL01664	105
COX5a	TGGAGAAGATCACCCCCACA	IL02412	AGCTAGTGTCGCTGTAACGTG	IL02413	163
COX7a	GGGCAAGCTTTTCTACGAGC	IL02414	GTCCAGGTATCCAGGGCAAG	IL02415	158
eyg	TCTCACGTTTCGGTGGACTG	IL02416	TCGCGCTTGTACTGTTCGAT	IL02417	172
Rp49	ACAGGCCCAAGATCGTGAAG	IL02470	TGCGCTTGTTCGATCCGTAA	IL02471	174
LDH	GCCGCCATTAAGGACAGTCT	IL02660	GACATCGATGAGGCACACCT	IL02661	156
Glut1	CTGCTCATTACCAAGCAGTGG	IL02662	ATATGTGGCTCTCGGACTGC	IL02663	133
PyK	TCCGTAAGGTTCTTGGCGAG	IL02664	GGCGGGAATCTCAATACCCA	IL02665	149
CG2964	GCGGGTTCACCAACAATGTC	IL02666	TTCTTATCAGCAGGCTCCCG	IL02667	139
CG7069	GCAAGAAAGAGAAGAAACCACCG	IL02668	AGCTTTTCTGGGCTGTTGGA	IL02669	163
Impl2	TCCAAGGACATCGCCACAGG	IL02989	GGCGGTATCCTTTCCGACGA	IL02990	119
Tret1-1	TCGCGAAACACCATGTTGGA	IL02991	AATGGTGGATCCCGCATCCTT	IL02992	150
Hsc70-2	GAGCGCTTGATTGGCGATCC	IL02993	GAAGGGCCAGAGCTTCAGGT	IL02994	135
Hsc70-5	GAACTGTTTGGACGCCAGCC	IL03275	CCAGCGAGAGGGGAGTAACG	IL03276	128
Pfk	CCAAACGCACACTGCCTGAG	IL03405	ACTGTGGGTAGTTGTCCCGC	IL03406	147
mnd	AAAAACGCCGCACATCTCCC	IL03407	AGCTTTACCCCGGAACCCTG	IL03408	145
Aldolase	CAACCATGGGCAAGCGTCTG	IL03425	GTGCCATCATCGGCCTTCTG	IL03426	163
Atf4	GACGCTGCTTCGCTTCCTTC	IL03508	ACGGGTTTTGGCTGTGCATC	IL03509	140

Table MM4: Primer pairs for qPCR expression analysis of indicated target genes

5. Cell culture

Drosophila S2R+ cells (DGRC, Bloomington) were maintained in Schneider's Drosophila Medium (Gibco) supplemented with 10% heat-inactivated FBS (Gibco) at 25°C without antibiotics.

Qiagen Effectene was used for transient transfections with PERK constructs using 1µg of plasmid DNA with 12µl Enhancer and 4µl Effectene. pAW_mCherry (from Ioanna Koltsaki) was used as transfection control.

RNAi treatments were done with long dsRNA transcribed from PCR products that covered the identical region of the mRNA as the constructs used for *in vivo* RNAi. $1*10^6$ were treated with 14µg dsRNA for 1h in serum-free medium. After this incubation, medium with 20% serum was added to adjust concentration to standard 10%. Cells were allowed to grow for 4 days, then split to the original density ($1*10^6$ cells per well of 6-well plate) and collected at 6 or 7 days after initial treatment. Cells for metabolomics analysis were treated according to this protocol, split after 4d to $1*10^6$ cells per well, counted and collected after 6 days.

TMRM incorporation into S2R+ cells was conducted by incubating cells with 100nM TMRM (SigmaAldrich) in DMSO (ThermoFisherScientific) for 10 minutes, followed by serial dilution with fresh medium to a final concentration of 5nM that was maintained throughout imaging.

6. Metabolomics analysis

The cell culture metabolomics analysis was performed by the Metabolomics Core Technology Platform (MCTP, COS, University of Heidelberg) as follows:

"Free amino acids and thiols were extracted from $1*10^6$ S2R+ cells with 0.3 ml of 0.1 M HCl in an ultrasonic ice-bath for 10 min. The resulting extracts were centrifuged twice for 10 min at 4°C and 16.400 g to remove cell debris. Amino acids were derivatised with AccQ-Tag reagent (Waters) and determined as described in (Weger et al., 2016). Total glutathione was quantified by reducing disulfides with DTT followed by thiol derivatisation with the fluorescent dye monobromobimane (Thiolyte, Calbiochem). For quantification of GSSG, free thiols were first blocked by NEM followed by DTT reduction and monobromobimane derivatisation. GSH equivalents were calculated by subtracting GSSG from total glutathione levels. Derivatisation was performed as described in (Wirtz

et al., 2004). UPLC-FLR analysis was carried out using an Acquity H-class UPLC system. Separation was achieved with a binary gradient of buffer A (100 mM potassium acetate, pH 5.3) and solvent B (acetonitrile) with the following gradient: 0 min 2.3 % buffer B; 0.99 min 2.3 %, 1 min 70 %, 1.45 min 70 %, and re-equilibration to 2.3 % B in 1.05 min at a flow rate of 0.85 ml min^{-1}. The column (Acquity BEH Shield RP18 column, 50 mm x 2.1 mm, 1.7 µm, Waters) was maintained at 45°C and sample temperature was kept constant at 14 °C. Monobromobimane conjugates were detected by fluorescence at 480 nm after excitation at 380 nm and quantified using ultrapure standards (Sigma). Determination of organic acids was adapted from (Uran et al., 2007). In brief, $1*10^6$ S2R+ cells per sample were extracted in 0.2 ml ice-cold methanol with sonication on ice. 50 µl extract was mixed with 25µl 140 mM 3-Nitrophenylhydrazine hydrochloride (Sigma-Aldrich), 25 µl methanol and 100 µl 50 mM Ethyl-3-(3-dimethylaminopropyl) carbodiimide hydrochloride (Sigma-Aldrich) and incubated for 20 min at 60°C. Separation was carried out on the above described UPLC system coupled to a QDa mass detector (Waters) using an Acquity HSS T3 column (100 mm x 2.1 mm, 1.8 µm, Waters) which was heated to 40°C. Separation of derivates was achieved by increasing the concentration of 0.1 % formic acid in acetonitrile (B) in 0.1 % formic acid in water (A) at 0.55 ml min^{-1} as follows: 2 min 15% B, 2.01 min 31% B, 5 min 54% B, 5.01 min 90% B, hold for 2 min, and return to 15% B in 2 min. Mass signals for the following compounds were detected in single ion record (SIR) mode using negative detector polarity and 0.8 kV capillary voltage: Lactate (224.3 m/z; 25 V CV), malate (403.3 m/z; 25 V CV), succinate (387.3 m/z; 25 CV), fumarate (385.3 m/z; 30 V), citrate (443.3 m/z; 10 V), pyruvate (357.3 m/z; 15 V) and ketoglutarate (550.2 m/z; 25 CV). Data acquisition and processing was performed with the Empower3 software suite (Waters). The Metabolomics Core Technology Platform at the University of Heidelberg performed Metabolomic analysis." (this description was provided by Gernot Poschet, MCTP, Heidelberg and is also part of Sorge et al., in preparation).

Analysis of free amino acids, thiols and Adenosines from dissected late third instar eye-antenna discs was carried out using the same methodology.

7. Transmission electron microscopy (TEM)

This experiment was carried out by Christian Altbürger under my supervision and together with Steffi Gold and Stefan Hillmer from the Electron Microscopy Core Facility of University Heidelberg (Altbürger, 2014). For this thesis, I measured mitochondrial diameter with Fiji in images obtained by Christian Altbürger and Stefan Hillmer and me.

8. Molecular biology

Molecular cloning was carried out using standard methods and procedures (Sorge, 2012). Q5-High fidelity polymerase (NEB) was used for PCR. Fusions of PERK N-terminal sequences with EGFP were done using Gibson Assembly (NEB) into pENTR-D-TOPO vector. Assembly design was created using NEBuilder Assembly Tool (https://nebuilder.neb.com/). Entry clones were recombined into pAc5.1_DEST destination vector using LR Clonase II enzyme mix (Invitrogen). Oligos and standard sequencing service was provided by Eurofins Genomics. Table MM5 lists Oligos used to create PERK-N-terminal fusions.

ID	name	sequence
IL04023	pENTR_TGA_f	tgaTGGGCGCGCCGACCCAGC
IL04024	pENTR_r	CCGCGGAGCCTGCTTTTTTG
IL04025	EGFP_r	gggtcggcgcgcccatcaCTTGTACAGCTCGTCCATGC
IL04026	PERK_RA_f	aagcaggctccgcggTTATATGCGCGTACGATGCAGGACGAC
IL04027	PERK_RA_r	ctcaccatTTCGAGCCCGGGGGGACG
IL04028	EGFP_RA_f	ggctcgaaATGGTGAGCAAGGGCGAG
IL04029	PERK_RB_f	aagcaggctccgcggATAATATGAACCCACATGTTTGC
IL04030	PERK_RB_r	ctcaccatATGGATGCTGGACGAGATTAG
IL04031	EGFP_RB_f	gcatccatATGGTGAGCAAGGGCGAG

Table MM5: List of Primers used to clone PERK N-terminal fusions

9. Media and Solutions

Chemicals were primarily obtained from Sigma-Aldrich, Carl Roth or AppliChem and were of analytical grade or similar. Solutions were prepared in accordance with general principles of good laboratory practice with maximum cleanliness in mind.

10X PBS (Phosphate buffered saline)

75.97 g Sodiumchloride (NaCl)

12.46 g Sodiumdihydrogenphosphate (NaH_2PO4)

4.14 g Disodiumhydrogenphosphate (Na_2HPO4)

Ingredients were dissolved in 850 ml of deionised water (Millipore) and the pH adjusted to 7.4 with Sodiumhydroxide (NaOH). The volume was adjusted to 1 l and the solution sterilized by autoclaving and stored at room temperature (RT).

1X PBS (Phosphate buffered saline)

10X PBS solution was diluted 1:10 in dH2O and stored at RT.

1x PBTw

100ml 10x PBS were mixed with 0,9g Tween20 and 899ml H20 to obtain 1xPBS with 0.1% (v/v) Tween20 detergent.

1x PBTx

100ml 10x PBS were mixed with 2,7g Triton X-100 and 899ml H20 to obtain 1xPBS with 0.3% (v/v) Triton X-100 detergent.

4 % PFA (Paraformaldehyde)

4g of paraformaldehyde was dissolved in 80 ml H_20 under gentle heating (50°C) and by drop-wise adding of 0.1 M NaOH. When the powder was fully dissolved, 10ml 10xPBS was added, pH was adjusted to pH 7.2 with concentrated HCl and the volume filled to 100ml. Aliquots of 2 ml were stored at -20 °C.

1% BR (Blocking reagent in PBT)

1g of Blocking reagent powder (PerkinElmer) was dissolved in 100ml PBTw under stirring and gentle heating (40°C). 1% BR was stored in the fridge.

Fly food formulations

The standard fly food of the laboratory ("normal food") was prepared by Bernhard Glass according to a recipe from the DKFZ fly food kitchen (final volume approximately 36l):

2400g	corn meal
2400g	malted wheat
640g	molasses
300g	soy flour
540g	yeast extract
320g	Agar
187ml	propionic acid
18,7ml	phosphoric acid
72g	Nipagin (dissolved in 96% ethanol)
30l	H_20 (tap water)

The "nutrient restriction food" with reduced protein content was adapted from a recipe from (Nowak et al., 2013). 20g fresh yeast per liter was used for "nutrient restriction". 60g fresh yeast per liter was used as "fully fed". I found the 60g food to behave in the same way as our "normal food". The formulation was as follows (for 1l of food):

75g	sugar (Sucrose)
55g	corn meal
10g	wheat flour
8g	Bacto-Agar
20g / 60g	fresh bakers yeast
6ml	propionic acid
900ml	H_2O (Millipore)

10. Consumables

The following Table MM6 lists the main commercial consumables and kits used.

reagent	catalogue number	manufacturer
Schneider's Drosophila Medium	#21720001	Gibco/TFS
Fetal Bovine Serum	#10270	Gibco/TFS
TRIzol	# 15596026	Invitrogen/TFS
DirectZol MicroPrep	R2060	Zymo Research
RevertAid First-strand cDNA Synthes	K1621	ThermoScientific/TFS
Platinum SYBR Green mix	#11744500	Invitrogen/TFS
Gibson Assembly kit	E5510	NEB
Q5 High-fidelitly DNA polymerase	M0491S	NEB
pENTR/D-TOPO Cloning Kit	K240020	Invitrogen/TFS
LR Clonase II Plus enzyme	#12538120	Invitrogen/TFS
Effectene Transfection Reagent	#301427	Qiagen

Table MM6: List of reagents and kits.

VI – References

Acevedo, J.M., Hoermann, B., Schlimbach, T., and Teleman, A.A. (2018). Changes in global translation elongation or initiation rates shape the proteome via the Kozak sequence. Scientific Reports 1–12.

Agrawal, N., Delanoue, R., Mauri, A., Basco, D., Pasco, M., Thorens, B., and Léopold, P. (2016). The Drosophila TNF Eiger Is an Adipokine that Acts on Insulin-Producing Cells to Mediate Nutrient Response. Cell Metabolism *23*, 675–684.

Alexandre, C., Baena-Lopez, A., and Vincent, J.P. (2015). Patterning and growth control by membrane-tethered Wingless. Nature *505*, 180–185.

Altbürger, C. (2014). Cooperation between Notch signaling and mitochondrial dysfunction drives overproliferation in.

Ameri, K., Lewis, C.E., Raida, M., Sowter, H., Hai, T., and Harris, A.L. (2004). Anoxic induction of ATF-4 through HIF-1-independent pathways of protein stabilization in human cancer cells. Blood *103*, 1876–1882.

Ashburner, M., and Bonner, J.J. (1979). The induction of gene activity in drosophila by heat shock. Cell *17*, 241–254.

Baker, N.E. (2001). Cell proliferation, survival, and death in the Drosophila eye. Seminars in Cell & Developmental Biology *12*, 499–507.

Bao, X.R., Ong, S.-E., Goldberger, O., Peng, J., Sharma, R., Thompson, D.A., Vafai, S.B., Cox, A.G., Marutani, E., Ichinose, F., et al. (2016). Mitochondrial dysfunction remodels one-carbon metabolism in human cells. eLife *5*, 1910.

Bi, M., Naczki, C., Koritzinsky, M., Fels, D., Blais, J., Hu, N., Harding, H., Novoa, I., Varia, M., Raleigh, J., et al. (2005). ER stress-regulated translation increases tolerance to extreme hypoxia and promotes tumor growth. Embo J. *24*, 3470–3481.

Birsoy, K., Wang, T., Chen, W.W., Freinkman, E., Abu-Remaileh, M., and Sabatini, D.M. (2015). An Essential Role of the Mitochondrial Electron Transport Chain in Cell Proliferation Is to Enable Aspartate Synthesis. Cell *162*, 540–551.

Bosch, P.S., Ziukaite, R., Alexandre, C., Basler, K., and Vincent, J.P. (2017). Dpp controls

growth and patterning in Drosophila wing precursors through distinct modes of action. eLife *6*, 375.

Brand, A.H., and Perrimon, N. (1993). Targeted gene expression as a means of altering cell fates and generating dominant phenotypes. Development *118*, 401–415.

Britton, J.S., Lockwood, W.K., Li, L., Cohen, S.M., and Edgar, B.A. (2002). Drosophila's insulin/PI3-kinase pathway coordinates cellular metabolism with nutritional conditions. Developmental Cell *2*, 239–249.

Brogiolo, W., Stocker, H., Ikeya, T., Rintelen, F., Fernandez, R., and Hafen, E. (2001). An evolutionarily conserved function of the Drosophila insulin receptor and insulin-like peptides in growth control. Curbio *11*, 213–221.

Bryant, P.J., and Levinson, P. (1985). Intrinsic growth control in the imaginal primordia of Drosophila, and the autonomous action of a lethal mutation causing overgrowth. Developmental Biology *107*, 355–363.

Cai, L., and Tu, B.P. (2012). Driving the Cell Cycle Through Metabolism. Annu. Rev. Cell Dev. Biol. *28*, 59–87.

Celardo, I., Costa, A.C., Lehmann, S., Jones, C., Wood, N., Mencacci, N.E., Mallucci, G.R., Loh, S.H.Y., and Martins, L.M. (2016). Mitofusin-mediated ER stress triggers neurodegeneration in pink1/parkin models of Parkinson's disease. Cell Death Dis *7*, e2271–e2271.

Celardo, I., Lehmann, S., Costa, A.C., Loh, S.H., and Martins, L.M. (2017). dATF4 regulation of mitochondrial folate-mediated one-carbon metabolism is neuroprotective. *24*, 638–648.

Chao, J.-L., Tsai, Y.-C., Chiu, S.-J., and Sun, Y.H. (2004). Localized Notch signal acts through eyg and upd to promote global growth in Drosophila eye. Development *131*, 3839–3847.

Cheng, L.Y., Bailey, A.P., Leevers, S.J., Ragan, T.J., Driscoll, P.C., and Gould, A.P. (2011). Anaplastic Lymphoma Kinase Spares Organ Growth during Nutrient Restriction in Drosophila. Cell *146*, 435–447.

Claros, M.G., and Vincens, P. (1996). Computational method to predict mitochondrially imported proteins and their targeting sequences. Eur. J. Biochem. *241*, 779–786.

Colombani, J., Raisin, S., Pantalacci, S., Radimerski, T., Montagne, J., and Leopold, P. (2003). A nutrient sensor mechanism controls Drosophila growth. Cell *114*, 739–749.

Colombani, J., Andersen, D.S., and Léopold, P. (2012). Secreted peptide Dilp8 coordinates Drosophila tissue growth with developmental timing. Science *336*, 582–585.

Colombani, J., Andersen, D.S., Boulan, L., Boone, E., Romero, N., Virolle, V., Texada, M.,

and Léopold, P. (2015). Drosophila Lgr3 Couples Organ Growth with Maturation and Ensures Developmental Stability. Curbio *25*, 2723–2729.

Cox, J.S., Shamu, C.E., and Walter, P. (1993). Transcriptional Induction of Genes Encoding Endoplasmic-Reticulum Resident Proteins Requires a Transmembrane Protein-Kinase. Cell *73*, 1197–1206.

Delanoue, R., Meschi, E., Agrawal, N., Mauri, A., Tsatskis, Y., McNeill, H., and Leopold, P. (2016). Drosophila insulin release is triggered by adipose Stunted ligand to brain Methuselah receptor. Science *353*, 1553–1556.

Demay, Y., Perochon, J., Szuplewski, S., Mignotte, B., and Gaumer, S. (2014). The PERK pathway independently triggers apoptosis and a Rac1/Slpr/JNK/Dilp8 signaling favoring tissue homeostasis in a chronic ER stress Drosophila model. Cell Death Dis *5*, e1452.

DeNicola, G.M., and Cantley, L.C. (2015). Cancer's Fuel Choice: New Flavors for a Picky Eater. Molecular Cell *60*, 514–523.

Dever, T.E., Feng, L., Wek, R.C., Cigan, A.M., Donahue, T.F., and Hinnebusch, A.G. (1992). Phosphorylation of Initiation Factor-2-Alpha by Protein-Kinase Gcn2 Mediates Gene-Specific Translational Control of Gcn4 in Yeast. Cell *68*, 585–596.

Dobbing, J., and Sands, J. (1971). Vulnerability of developing brain. IX. The effect of nutritional growth retardation on the timing of the brain growth-spurt. Biology of the Neonate *19*, 363–378.

Dominguez, M., and de Celis, J.F. (1998). A dorsal/ventral boundary established by Notch controls growth and polarity in the Drosophila eye. Nature.

Dominguez, M., Ferres-Marco, D., Gutierrez-Aviño, F.J., Speicher, S.A., and Beneyto, M. (2003). Growth and specification of the eye are controlled independently by Eyegone and Eyeless in Drosophila melanogaster. Nature Genetics *36*, 31–39.

Edgar, B.A. (2006). How flies get their size: genetics meets physiology. Nat Rev Genet *7*, 907–916.

Efeyan, A., Zoncu, R., and Sabatini, D.M. (2012). Amino acids and mTORC1: from lysosomes to disease. Trends in Molecular Medicine *18*, 524–533.

Estella, C., and Baonza, A. (2015). Cell proliferation control by Notch signalling during imaginal discs development in Drosophila. AIMS Genetics *2*, 70–96.

Faubert, B., Li, K.Y., Cai, L., Hensley, C.T., Kim, J., Zacharias, L.G., Yang, C., Do, Q.N., Doucette, S., Burguete, D., et al. (2017). Lactate Metabolism in Human Lung Tumors. Cell *171*, 358–367.e359.

Fiorese, C.J., Schulz, A.M., Lin, Y.-F., Rosin, N., Pellegrino, M.W., and Haynes, C.M. (2016). The Transcription Factor ATF5 Mediates a Mammalian Mitochondrial UPR. Curbio

26, 2037–2043.

Fried, P., Sánchez-Aragón, M., Aguilar-Hidalgo, D., Lehtinen, B., Casares, F., and Iber, D. (2016). A Model of the Spatio-temporal Dynamics of Drosophila Eye Disc Development. PLoS Comput Biol *12*, e1005052–23.

Garelli, A., Gontijo, A.M., Miguela, V., Caparros, E., and Dominguez, M. (2012). Imaginal Discs Secrete Insulin-Like Peptide 8 to Mediate Plasticity of Growth and Maturation. Science *336*, 579–582.

Green, E.W., Fedele, G., Giorgini, F., and Kyriacou, C.P. (2014). correspondence. Nat Meth *11*, 222–223.

Greenspan, R.J. (2004). Fly Pushing (CSHL Press).

Gregg, T.G., McCrate, A., Reveal, G., Hall, S., and Rypstra, A.L. (1990). Insectivory and social digestion in Drosophila. Biochem. Genet. *28*, 197–207.

Gutierrez-Aviño, F.J., Ferres-Marco, D., and Dominguez, M. (2009). The position and function of the Notch-mediated eye growth organizer: the roles of JAK/STAT and four-jointed. EMBO Reports *10*, 1051–1058.

Hadorn, E. (1963). Differenzierungsleistungen Wiederholt Fragmentierter Teilstucke Mannlicher Genitalscheiben Von Drosophila Melanogaster Nach Kultur in Vivo. Developmental Biology *7*, 617–&.

Hara, K., Yonezawa, K., Weng, Q.P., Kozlowski, M.T., Belham, C., and Avruch, J. (1998). Amino acid sufficiency and mTOR regulate p70 S6 kinase and eIF-4E BP1 through a common effector mechanism. Journal of Biological Chemistry *273*, 14484–14494.

Harding, H.P., Novoa, I., Zhang, Y.H., Zeng, H.Q., Wek, R., Schapira, M., and Ron, D. (2000). Regulated translation initiation controls stress-induced gene expression in mammalian cells. Molecular Cell *6*, 1099–1108.

Harding, H.P., Zhang, Y.H., and Ron, D. (1999). Protein translation and folding are coupled by an endoplasmic-reticulum-resident kinase. Nature *397*, 271–274.

Harding, H.P., Zhang, Y., Zeng, H., Novoa, I., Lu, P.D., Calfon, M., Sadri, N., Yun, C., Popko, B., Paules, R., et al. (2003). An Integrated Stress Response Regulates Amino Acid Metabolism and Resistance to Oxidative Stress. Molecular Cell *11*, 619–633.

Hariharan, I.K. (2015). Organ Size Control: Lessons from Drosophila. Developmental Cell *34*, 255–265.

Harrison, R.G. (1924). Some unexpected results of the heteroplastic transplantation of limbs. Proceedings of the National Academy of Sciences *10*, 69–74.

Harvey, K.F., Pfleger, C.M., and Hariharan, I.K. (2003). The Drosophila Mst Ortholog,

hippo, Restricts Growth and Cell Proliferation and Promotes Apoptosis. Cell *114*, 457–467.

Hay, B.A., Wolff, T., and Rubin, G.M. (1994). Expression of Baculovirus P35 Prevents Cell-Death in Drosophila. Development *120*, 2121–2129.

Haynes, C.M., Yang, Y., Blais, S.P., Neubert, T.A., and Ron, D. (2010). The Matrix Peptide Exporter HAF-1 Signals a Mitochondrial UPR by Activating the Transcription Factor ZC376.7 in C. elegans. Molecular Cell *37*, 529–540.

Haze, K., Yoshida, H., Yanagi, H., Yura, T., and Mori, K. (1999). Mammalian transcription factor ATF6 is synthesized as a transmembrane protein and activated by proteolysis in response to endoplasmic reticulum stress. Mol. Biol. Cell *10*, 3787–3799.

Hinnebusch, A.G. (1997). Translational Regulation of Yeast GCN4. Journal of Biological Chemistry *272*, 21661–21664.

Homem, C.C.F., Steinmann, V., Burkard, T.R., Jais, A., Esterbauer, H., and Knoblich, J.A. (2014). Ecdysone and Mediator Change Energy Metabolism to Terminate Proliferation in Drosophila Neural Stem Cells. Cell *158*, 874–888.

Horiguchi, M., Koyanagi, S., Okamoto, A., Suzuki, S.O., Matsunaga, N., and Ohdo, S. (2012). Stress-regulated transcription factor ATF4 promotes neoplastic transformation by suppressing expression of the INK4a/ARF cell senescence factors. Cancer Research *72*, 395–401.

Huang, D.W., Sherman, B.T., and Lempicki, R.A. (2009). Systematic and integrative analysis of large gene lists using DAVID bioinformatics resources. Nat Protoc *4*, 44–57.

Hwang, C., Sinskey, A.J., and Lodish, H.F. (1992). Oxidized redox state of glutathione in the endoplasmic reticulum. Science *257*, 1496–1502.

Igarashi, T., Izumi, H., Uchiumi, T., Nishio, K., Arao, T., Tanabe, M., Uramoto, H., Sugio, K., Yasumoto, K., Sasaguri, Y., et al. (2007). Clock and ATF4 transcription system regulates drug resistance in human cancer cell lines. Oncogene *26*, 4749–4760.

Janky, R., Verfaillie, A., Imrichová, H., Van de Sande, B., Standaert, L., Christiaens, V., Hulselmans, G., Herten, K., Naval Sanchez, M., Potier, D., et al. (2014). iRegulon: From a Gene List to a Gene Regulatory Network Using Large Motif and Track Collections. PLoS Comput Biol *10*, e1003731–19.

Jennings, B., Preiss, A., Delidakis, C., and Bray, S. (1994). The Notch signalling pathway is required for Enhancer of split bHLH protein expression during neurogenesis in the Drosophila embryo. Development *120*, 3537–3548.

Jensen, M.B., and Jasper, H. (2014). Mitochondrial Proteostasis in the Control of Aging and Longevity. Cell Metabolism *20*, 214–225.

Johnston, L.A., Prober, D.A., Edgar, B.A., Eisenman, R.N., and Gallant, P. (1999). Drosophila myc regulates cellular growth during development. Cell *98*, 779–790.

Justice, R.W., Zilian, O., Woods, D.F., Noll, M., and Bryant, P.J. (1995). The Drosophila Tumor-Suppressor Gene Warts Encodes a Homolog of Human Myotonic-Dystrophy Kinase and Is Required for the Control of Cell-Shape and Proliferation. Genes & Development *9*, 534–546.

Kang, K., Ryoo, H.D., Park, J.-E., Yoon, J.-H., and Kang, M.-J. (2015). A Drosophila Reporter for the Translational Activation of ATF4 Marks Stressed Cells during Development. PLoS ONE *10*, e0126795–15.

Kang, M.-J., Vasudevan, D., Kang, K., Kim, K., Park, J.-E., Zhang, N., Zeng, X., Neubert, T.A., Marr, M.T., II, and Ryoo, H.D. (2017). 4E-BP is a target of the GCN2–ATF4 pathway during Drosophiladevelopment and aging. The Journal of Cell Biology *216*, 115–129.

Kemppainen, K.K., Rinne, J., Sriram, A., Lakanmaa, M., Zeb, A., Tuomela, T., Popplestone, A., Singh, S., Sanz, A., Rustin, P., et al. (2013). Expression of alternative oxidase in Drosophila ameliorates diverse phenotypes due to cytochrome oxidase deficiency. Human Molecular Genetics *23*, 2078–2093.

Khan, N.A., Nikkanen, J., Yatsuga, S., Jackson, C., Wang, L., Pradhan, S., Kivelä, R., Pessia, A., Velagapudi, V., and Suomalainen, A. (2017). mTORC1 Regulates Mitochondrial Integrated Stress Response and Mitochondrial Myopathy Progression. Cell Metabolism *26*, 419–428.e5.

Kilberg, M.S., Shan, J., and Su, N. (2009). ATF4-dependent transcription mediates signaling of amino acid limitation. Trends in Endocrinology & Metabolism *20*, 436–443.

Koppenol, W.H., Bounds, P.L., and Dang, C.V. (2011). Otto Warburg's contributions to current concepts of cancer metabolism. Nat Rev Cancer *11*, 325–337.

Korennykh, A., and Walter, P. (2012). Structural Basis of the Unfolded Protein Response. Annu. Rev. Cell Dev. Biol. *28*, 251–277.

Kozak, M. (1986). Point mutations define a sequence flanking the AUG initiator codon that modulates translation by eukaryotic ribosomes. Cell *44*, 283–292.

Kumar, J.P. (2010). Retinal determination the beginning of eye development. Curr. Top. Dev. Biol. *93*, 1–28.

Kumar, J.P. (2011). Building an ommatidium one cell at a time. Dev. Dyn. *241*, 136–149.

Kurucz, E., Zettervall, C.-J., Sinka, R., Vilmos, P., Pivarcsi, A., Ekengren, S., Hegedüs, Z., Ando, I., and Hultmark, D. (2003). Hemese, a hemocyte-specific transmembrane protein, affects the cellular immune response in Drosophila. Proceedings of the National Academy of Sciences *100*, 2622–2627.

Lazarou, M., Smith, S.M., Thorburn, D.R., Ryan, M.T., and McKenzie, M. (2009). Assembly of nuclear DNA-encoded subunits into mitochondrial complex IV, and their preferential integration into supercomplex forms in patient mitochondria. FEBS Journal *276*, 6701–6713.

Lee, J.E., Oney, M., Frizzell, K., Phadnis, N., and Hollien, J. (2015a). Drosophila melanogaster activating transcription factor 4 regulates glycolysis during endoplasmic reticulum stress. G3 (Bethesda) *5*, 667–675.

Lee, J.E., Oney, M., Frizzell, K., Phadnis, N., and Hollien, J. (2015b). Drosophila melanogaster activating transcription factor 4 regulates glycolysis during endoplasmic reticulum stress. G3 (Bethesda) *5*, 667–675.

Li, J.-R., Sun, C.-H., Li, W., Chao, R.-F., Huang, C.-C., Zhou, X.J., and Liu, C.-C. (2016). Cancer RNA-Seq Nexus: a database of phenotype-specific transcriptome profiling in cancer cells. Nucleic Acids Res. *44*, D944–D951.

Lolo, F.-N., Casas-Tintó, S., and Moreno, E. (2012). Cell Competition Time Line: Winners Kill Losers, which Are Extruded and Engulfed by Hemocytes. CellReports *2*, 526–539.

Lynch, M., and Force, A. (2000). The probability of duplicate gene preservation by subfunctionalization. Genetics *154*, 459–473.

Ma, K., Vattem, K.M., and Wek, R.C. (2002). Dimerization and release of molecular chaperone inhibition facilitate activation of eukaryotic initiation factor-2 kinase in response to endoplasmic reticulum stress. Journal of Biological Chemistry *277*, 18728–18735.

Malzer, E., Dominicus, C.S., Chambers, J.E., Dickens, J.A., Mookerjee, S., and Marciniak, S.J. (2018). The integrated stress response regulates BMP signalling through effects on translation. 1–15.

Mandal, S., Guptan, P., Owusu-Ansah, E., and Banerjee, U. (2005). Mitochondrial Regulation of Cell Cycle Progression during Development as Revealed by the tenured Mutation in Drosophila. Developmental Cell *9*, 843–854.

Martin, F.A., Herrera, S.C., and Morata, G. (2009). Cell competition, growth and size control in the Drosophila wing imaginal disc. Development *136*, 3747–3756.

Martinus, R.D., Garth, G.P., Webster, T.L., Cartwright, P., Naylor, D.J., Høj, P.B., and Hoogenraad, N.J. (1996). Selective Induction of Mitochondrial Chaperones in Response to Loss of the Mitochondrial Genome. Eur. J. Biochem. *240*, 98–103.

Mashimo, T., Pichumani, K., Vemireddy, V., Hatanpaa, K.J., Singh, D.K., Sirasanagandla, S., Nannepaga, S., Piccirillo, S.G., Kovacs, Z., Foong, C., et al. (2014). Acetate Is a Bioenergetic Substrate for Human Glioblastoma and Brain Metastases. Cell *159*, 1603–1614.

Morata, G., and Ripoll, P. (1975). Minutes: mutants of drosophila autonomously affecting cell division rate. Developmental Biology *42*, 211–221.

Mori, K. (2009). Signalling pathways in the unfolded protein response: development from yeast to mammals. J. Biochem. *146*, 743–750.

Münch, C., and Harper, J.W. (2016). Mitochondrial unfolded protein response controls matrix pre-RNA processing and translation. Nature Publishing Group *534*, 710–713.

Nargund, A.M., Pellegrino, M.W., Fiorese, C.J., Baker, B.M., and Haynes, C.M. (2012). Mitochondrial Import Efficiency of ATFS-1 Regulates Mitochondrial UPR Activation. Science *337*, 587–590.

Neufeld, T.P., la Cruz, de, A.F., Johnston, L.A., and Edgar, B.A. (1998). Coordination of growth and cell division in the Drosophila wing. Cell *93*, 1183–1193.

Ni, J.-Q., Zhou, R., Czech, B., Liu, L.-P., Holderbaum, L., Yang-Zhou, D., Shim, H.-S., Tao, R., Handler, D., Karpowicz, P., et al. (2011). a genome-scale shrna resource for transgenic rnai in. Nat Meth 1–5.

Nijtmans, L., Taanman, J.W., Muijsers, A.O., Speijer, D., and Van den Bogert, C. (1998). Assembly of cytochrome-c oxidase in cultured human cells. Eur. J. Biochem. *254*, 389–394.

Nowak, K., Seisenbacher, G., Hafen, E., and Stocker, H. (2013). Nutrient restriction enhances the proliferative potential of cells lacking the tumor suppressor PTEN in mitotic tissues. eLife *2*, e00380–21.

Ohsawa, S., Sato, Y., Enomoto, M., Nakamura, M., Betsumiya, A., and Igaki, T. (2013). Mitochondrial defect drives non-autonomous tumour progression through Hippo signalling in Drosophila. Nature *490*, 547–551.

Owusu-Ansah, E., Yavari, A., Mandal, S., and Banerjee, U. (2008). Distinct mitochondrial retrograde signals control the G1-S cell cycle checkpoint. Nature Genetics *40*, 356–361.

Palmer, A.R., and Strobeck, C. (1986). Fluctuating Asymmetry - Measurement, Analysis, Patterns. Annual Review of Ecology and Systematics *17*, 391–421.

Pan, Y.-X., Chen, H., Thiaville, M.M., and Kilberg, M.S. (2007). Activation of theATF3gene through a co-ordinated amino acid-sensing response programme that controls transcriptional regulation of responsive genes following amino acid limitation. Biochem. J. *401*, 299–307.

Papayannopoulos, V., Tomlinson, A., Panin, V.M., Rauskolb, C., and Irvine, K.D. (1998). Dorsal-ventral signaling in the Drosophila eye. Science *281*, 2031–2034.

Patel, N.H. (1994). Chapter 24 Imaging Neuronal Subsets and Other Cell Types in Whole-Mount Drosophila Embryos and Larvae Using Antibody Probes (Elsevier).

Pearl, R., and Parker, S.L. (1922). Experimental Studies on the Duration of Life. IV. Data on the Influence of Density of Population on Duration of Life in Drosophila. The American Naturalist *56*, 312–321.

Quirós, P.M., Prado, M.A., Zamboni, N., D'Amico, D., Williams, R.W., Finley, D., Gygi, S.P., and Auwerx, J. (2017). Multi-omics analysis identifies ATF4 as a key regulator of the mitochondrial stress response in mammals. The Journal of Cell Biology *216*, 2027–2045.

Reinke, A.W., Baek, J., Ashenberg, O., and Keating, A.E. (2013). Networks of bZIP Protein-Protein Interactions Diversified Over a Billion Years of Evolution. Science *340*, 730–734.

Richter, K., Haslbeck, M., and Buchner, J. (2010). The Heat Shock Response: Life on the Verge of Death. Molecular Cell *40*, 253–266.

Rizki, T.M., Rizki, R.M., and Bellotti, R.A. (1985). Genetics of a Drosophila phenoloxidase. Mol. Gen. Genet. *201*, 7–13.

Ryoo, H.D., Domingos, P.M., Kang, M.-J., and Steller, H. (2007). Unfolded protein response in a Drosophila model for retinal degeneration. Embo J. *26*, 242–252.

Sakaguchi, H., and Suzuki, M.G. (2013). Drosophila melanogaster larvae control amylase secretion according to the hardness of food. Front Physiol *4*, 200.

Scaduto, R.C., Jr, and Grotyohann, L.W. (1999). Measurement of Mitochondrial Membrane Potential Using Fluorescent Rhodamine Derivatives. Biophysical Journal *76*, 469–477.

Senyilmaz, D., and Teleman, A.A. (2015). Chicken or the egg: Warburg effect and mitochondrial dysfunction. 1–13.

Simpson, P., and Schneidermann, H.A. (1975). Isolation of Temperature Sensitive Mutations Blocking Clone Development in Drosophila-Melanogaster, and Effects of a Temperature Sensitive Cell Lethal Mutation on Pattern Formation in Imaginal Disks. Wilhelm Rouxs Archives of Developmental Biology *178*, 247–275.

Simpson, P., Berreur, P., and Berreur-Bonnenfant, J. (1980). The Initiation of Pupariation in Drosophila - Dependence on Growth of the Imaginal Disks. J Embryol Exp Morphol *57*, 155–165.

Singleton, D.C., and Harris, A.L. (2012). Targeting the ATF4 pathway in cancer therapy. Expert Opinion on Therapeutic Targets *16*, 1189–1202.

Sorge, S. (2012). Deformed co-factor and collaborator analysis in Drosophila melanogaster.

Stefana, M.I., Driscoll, P.C., Obata, F., Pengelly, A.R., Newell, C.L., MacRae, J.I., and Gould, A.P. (2017). Developmental diet regulates Drosophila lifespan via lipid autotoxins.

Nature Communications 1–13.

Stroud, D.A., Surgenor, E.E., Formosa, L.E., Reljic, B., Frazier, A.E., Dibley, M.G., Osellame, L.D., Stait, T., Beilharz, T.H., Thorburn, D.R., et al. (2016). Accessory subunits are integral for assembly and function of human mitochondrial complex I. Nature Publishing Group *538*, 123–126.

Sullivan, L.B., Gui, D.Y., Hosios, A.M., Bush, L.N., Freinkman, E., and Vander Heiden, M.G. (2015). Supporting Aspartate Biosynthesis Is an Essential Function of Respiration in Proliferating Cells. Cell *162*, 552–563.

Tapon, N., Harvey, K.F., Bell, D.W., Wahrer, D.C.R., Schiripo, T.A., Haber, D.A., and Hariharan, I.K. (2002). salvador Promotes Both Cell Cycle Exit and Apoptosis in Drosophila and Is Mutated in Human Cancer Cell Lines. Cell *110*, 467–478.

Teleman, A.A. (2010). Molecular mechanisms of metabolic regulation by insulin in Drosophila. Biochem. J. *425*, 13–26.

Thiaville, M.M., Dudenhausen, E.E., Zhong, C., Pan, Y.-X., and Kilberg, M.S. (2008). Deprivation of protein or amino acid induces C/EBPβ synthesis and binding to amino acid response elements, but its action is not an absolute requirement for enhanced transcription. Biochem. J. *410*, 473–484.

Twitty, V.C., and Schwind, J.L. (1931). The growth of eyes and limbs transplanted heteroplastically between two species of Amblystoma. Journal of Experimental Zoology *59*, 61–86.

Udan, R.S., Kango-Singh, M., Nolo, R., Tao, C., and Halder, G. (2003). Hippo promotes proliferation arrest and apoptosis in the Salvador/Warts pathway. Nat Cell Biol *5*, 914–920.

Uhlen, M., Zhang, C., Lee, S., Sjöstedt, E., Fagerberg, L., Bidkhori, G., Benfeitas, R., Arif, M., Liu, Z., Edfors, F., et al. (2017). A pathology atlas of the human cancer transcriptome. Science *357*, eaan2507–eaan2513.

Uran, S., Landmark, K.E., Hjellum, G., and Skotland, T. (2007). Quantification of 13C pyruvate and 13C lactate in dog blood by reversed-phase liquid chromatography–electrospray ionization mass spectrometry after derivatization with 3-nitrophenylhydrazine. Journal of Pharmaceutical and Biomedical Analysis *44*, 947–954.

Vallejo, D.M., Juarez-Carreño, S., Bolivar, J., Morante, J., and Dominguez, M. (2015). A brain circuit that synchronizes growth and maturation revealed through Dilp8 binding to Lgr3. Science *350*, aac6767–aac6767.

Vander Heiden, M.G., and DeBerardinis, R.J. (2017). Understanding the Intersections between Metabolism and Cancer Biology. Cell *168*, 657–669.

Vander Heiden, M.G., Cantley, L.C., and Thompson, C.B. (2009). Understanding the

Warburg effect: the metabolic requirements of cell proliferation. Science *324*, 1029–1033.

Vattem, K.M., and Wek, R.C. (2004). Reinitiation involving upstream ORFs regulates ATF4 mRNA translation in mammalian cells. Proceedings of the National Academy of Sciences *101*, 11269–11274.

Villegas, S.N., Gombos, R., García-López, L., Gutierrez-Perez, I., García-Castillo, J., Vallejo, D.M., Da Ros, V.G., Ballesta-Illán, E., Mihály, J., and Dominguez, M. (2018). PI3K/Akt Cooperates with Oncogenic Notch by Inducing Nitric Oxide-Dependent Inflammation. CellReports *22*, 2541–2549.

Vollmer, J., Fried, P., Aguilar-Hidalgo, D., Sánchez-Aragón, M., Iannini, A., Casares, F., and Iber, D. (2017). Growth control in the Drosophila eye disc by the cytokine Unpaired. Development *144*, 837–843.

Walter, P., and Ron, D. (2011). The unfolded protein response: from stress pathway to homeostatic regulation. Science *334*, 1081–1086.

Wang, C.W., Purkayastha, A., Jones, K.T., Thaker, S.K., and Banerjee, U. (2016). In vivo genetic dissection of tumor growth and the Warburg effect. eLife *5*.

Wang, L.-H., Chiu, S.-J., and Sun, Y.H. (2008). Temporal switching of regulation and function of eye gone (eyg) in Drosophila eye development. Developmental Biology *321*, 515–527.

Wang, Q., Bailey, C.G., Ng, C., Tiffen, J., Thoeng, A., Minhas, V., Lehman, M.L., Hendy, S.C., Buchanan, G., Nelson, C.C., et al. (2011). Androgen receptor and nutrient signaling pathways coordinate the demand for increased amino acid transport during prostate cancer progression. Cancer Research *71*, 7525–7536.

Wang, Y.-H., and Huang, M.-L. (2009). Reduction of Lobe leads to TORC1 hypoactivation that induces ectopic Jak/STAT signaling to impair Drosophila eye development. Mechanisms of Development *126*, 781–790.

Warburg, O., Posener, K., and Negelein, E. (1924). On the metabolism of carcinoma cells. Biochemische Zeitschrift *152*, 309–344.

Wartlick, O., Jülicher, F., and Gonzalez-Gaitan, M. (2014). Growth control by a moving morphogen gradient during Drosophila eye development. Development *141*, 1884–1893.

Weger, B.D., Weger, M., Görling, B., Schink, A., Gobet, C., Keime, C., Poschet, G., Jost, B., Krone, N., Hell, R., et al. (2016). Extensive Regulation of Diurnal Transcription and Metabolism by Glucocorticoids. PLoS Genet. *12*, e1006512–e1006524.

Wirtz, M., Droux, M., and Hell, R. (2004). O-acetylserine (thiol) lyase: an enigmatic enzyme of plant cysteine biosynthesis revisited in Arabidopsis thaliana. J. Exp. Bot. *55*,

1785–1798.

Wu, S., Huang, J., Dong, J., and Pan, D. (2003). hippo Encodes a Ste-20 Family Protein Kinase that Restricts Cell Proliferation and Promotes Apoptosis in Conjunction with salvador and warts. Cell *114*, 445–456.

Yamamoto, K., Sato, T., Matsui, T., Sato, M., Okada, T., Yoshida, H., Harada, A., and Mori, K. (2007). Transcriptional Induction of Mammalian ER Quality Control Proteins Is Mediated by Single or Combined Action of ATF6α and XBP1. Developmental Cell *13*, 365–376.

Ye, J., Rawson, R.B., Komuro, R., Chen, X., Dave, U.P., Prywes, R., Brown, M.S., and Goldstein, J.L. (2000). ER stress induces cleavage of membrane-bound ATF6 by the same proteases that process SREBPs. Molecular Cell *6*, 1355–1364.

Ye, J., Kumanova, M., Hart, L.S., Sloane, K., Zhang, H., De Panis, D.N., Bobrovnikova-Marjon, E., Diehl, J.A., Ron, D., and Koumenis, C. (2010). The GCN2-ATF4 pathway is critical for tumour cell survival and proliferation in response to nutrient deprivation. Embo J. *29*, 2082–2096.

Yoneda, T., Benedetti, C., Urano, F., Clark, S.G., Harding, H.P., and Ron, D. (2004). Compartment-specific perturbation of protein handling activates genes encoding mitochondrial chaperones. J Cell Sci *117*, 4055–4066.

Zhai, Z., Ha, N., Papagiannouli, F., Hamacher-Brady, A., Brady, N., Sorge, S., Bezdan, D., and Lohmann, I. (2012). Antagonistic Regulation of Apoptosis and Differentiation by the Cut Transcription Factor Represents a Tumor-Suppressing Mechanism in Drosophila. PLoS Genet. *8*, e1002582.

Zhao, Q., Wang, J.H., Levichkin, I.V., Stasinopoulos, S., Ryan, M.T., and Hoogenraad, N.J. (2002). A mitochondrial specific stress response in mammalian cells. Embo J. *21*, 4411–4419.